

ALMA MATER STUDIORUM · UNIVERSITÀ DI BOLOGNA

Scuola di Scienze
Dipartimento di Fisica e Astronomia
Corso di Laurea Magistrale in Fisica

The cosmological moduli problem in multi-field string inflationary models

Relatore:
Prof. Michele Cicoli

Presentata da:
Alessandro Barone

Anno Accademico 2017/2018

Abstract

The 4D low-energy limit of string compactifications is characterised by the ubiquitous presence of string moduli which are new gravitationally coupled scalar fields which develop mass via supersymmetry breaking effects. During inflation it is generically expected that these fields receive large contributions to their mass of order the Hubble constant. They are therefore shifted from their minimum and after the end of inflation start oscillating around it behaving as non-relativistic matter. Given that matter redshifts slower than radiation, the moduli quickly come to dominate the energy density of the universe. Hence, when they decay, they would dilute anything that has been produced before. It is thus crucial to require that the moduli decay before Big-bang nucleosynthesis in order to preserve the successful prediction for the abundances of the light elements. This condition sets a lower bound on their masses of order 50 TeV. This potential problem goes under the name of “cosmological moduli problem”. In this thesis, we shall study this problem in promising multi-field inflationary models which naturally emerge in type IIB compactifications. In particular, we will explore if the presence of a large number of spectator fields during inflation can reduce the initial misalignment of the moduli. We shall also explore if the dynamics of the system can forbid a period of moduli domination after the end of inflation.

Sommario

Il limite di bassa energia della compattificazione delle stringhe è caratterizzato dalla presenza di moduli, ovvero campi scalari accoppiati con il campo gravitazionale che sviluppano massa tramite effetti di rottura di supersimmetria. Durante l'inflazione si prevede che questi campi ricevano grandi contributi alla loro massa dell'ordine della costante di Hubble. Di conseguenza, vengono spostati rispetto al loro minimo e durante l'inflazione iniziano ad oscillare intorno a questo, comportandosi come materia non relativistica. Considerando poi che in un universo in espansione la materia si diluisce più lentamente della radiazione, i moduli possono dominare rapidamente la densità di energia dell'universo. In questo caso, quando decadono diluiscono tutto ciò che era stato prodotto precedentemente. Risulta quindi cruciale imporre che i moduli decadano prima della nucleosintesi degli elementi, così da preservare le ottime previsioni per l'abbondanza degli elementi leggeri nell'universo. Questa richiesta fissa un limite inferiore per le loro masse dell'ordine dei 50 TeV; questo potenziale problema va sotto il nome di "cosmological moduli problem". In questa tesi ci proponiamo di studiare questo problema in modelli inflazionari a più campi, che emergono naturalmente dalla compattificazione delle stringhe di tipo IIB. In particolare, indagheremo se la presenza di un grande numero di campi spettatori durante l'inflazione è in grado di ridurre lo spostamento iniziale dei moduli. Inoltre, ci proponiamo di studiare se la dinamica del sistema può proibire un periodo in cui l'energia dell'universo è dominata dai moduli dopo la fine dell'inflazione.

Introduction	1
1 A brief review of supersymmetry and supergravity	3
1.1 Why supersymmetry?	3
1.2 Supersymmetry algebra	5
1.3 Superspace and superfields	7
1.4 General scalar superfield	9
1.4.1 Chiral superfield	9
1.4.2 Vector superfield	10
1.5 Supersymmetric Lagrangians	11
1.6 Supersymmetry breaking	13
1.7 $\mathcal{N} = 1, \mathbf{D} = 4$ supergravity Lagrangian	14
2 4D LVS string models	15
2.1 Why string theory?	15
2.2 Compactification and dimensional reduction	16
2.2.1 Moduli	17
2.3 Moduli stabilization	18
2.3.1 Perturbative corrections	20
2.3.2 Non-perturbative corrections	20
2.4 The Large Volume Scenario	21
2.4.1 Uplift	23

3	The cosmological moduli problem	25
3.1	Inflation	25
3.1.1	Cosmological perturbations	28
3.1.2	Slow-roll model	29
3.2	Cosmological moduli problem	31
3.2.1	Moduli cosmological evolution	32
3.2.2	Reheating from moduli decay	33
4	Kähler moduli inflation and moduli domination	35
4.1	Kähler moduli inflation: effective action	35
4.1.1	The scalar potential	35
4.1.2	Large Volume Limit and constraints	37
4.1.3	Preliminary considerations on stability	38
4.2	Kähler moduli inflation: inflationary analysis	40
4.2.1	Single-field potential	41
4.2.2	Slow-roll parameters	44
4.3	Post-inflationary scenario	45
4.3.1	Inflaton domination	45
4.3.2	Modulus domination	46
4.3.3	Number of efoldings	48
4.4	Numerical analysis	48
4.4.1	Example 1	50
4.4.2	Example 2	54
4.4.3	Example 3	63
4.4.4	Remarks on numerical analysis	68
	Conclusions	69
A	Computational details	73
A.1	Preliminary considerations on mass terms	73
A.2	Kähler metric	74
A.3	Potential calculations	76
A.4	Masses computation	78
A.4.1	$n=3$	79

A.4.2	n=4	81
A.4.3	Generic n	82
B	Generic uplift	85
B.1	Constraints for a generic uplift	85
B.2	Multi-field consequences	86
	Bibliography	i
	List of Tables	iii
	List of Figures	vi

INTRODUCTION

Cosmic inflation is a theory of accelerated cosmological expansion following the conjectured Big Bang singularity. It was first elaborated in 1979 by Alan Guth and further developed over the following years. Since then, this theory has been the object of great interest among physicists, as it has proven to be extremely successful: it is able to explain, among other aspects, the origin of the large scale structure of the universe.

Despite this, the mechanism to describe this cosmic expansion is still unknown; it is commonly believed that the dynamics of a scalar particle called *inflaton* is responsible for inflation. In particular, a great deal of attention has been attracted to the so called *slow-roll models*.

Recently, string theory has been an important source of inspiration for the development of effective theories for inflation. Indeed, string theory is a candidate for the fundamental theory of Nature and thus it should be able to describe every single aspect of our universe. In particular, the four-dimensional low energy limit of string compactifications gives origin to supergravity models with many moduli, i.e. gravitationally coupled scalar fields. Recent developments in moduli stabilization techniques have opened the way to string phenomenology, as moduli VEVs determine such basic quantities as the string scale and the gauge coupling constants. Given the moduli potential, one possible application is precisely to inflation theory.

In this thesis we focus on the study of promising inflationary models with Kähler moduli derived from the low energy limit of type IIB string theory compactifications.

The first chapter is dedicated to a brief discussion of supersymmetry and supergravity. The focus is on the mathematical structure of generic theories in order to present the procedure for building supersymmetric models. Particular attention is given to models with $\mathcal{N} = 1$ supersymmetric charges and to the derivation of the scalar potential of the theory.

The second chapter is meant to bring to light some of the features of string theory which allow one to obtain low energies effective supersymmetric theories. We provide the main concepts of string compactifications for type IIB string theory with emphasis on the scalar fields that arise from this procedure, i.e. the moduli. The large volume scenario of moduli stabilization is then reviewed in a simple case.

In the third chapter we introduce the very basis of cosmology and inflation, underlying the problems of the hot Big Bang model and the necessity of introducing the inflationary scenario. We then give a first insight on string inflation using a toy model effective potential for the moduli in order to discuss the standard assumptions of the inflationary epoch. Finally, we introduce the *cosmological moduli problem* of the post-inflationary epoch, as this problem is present in lots of

inflationary models.

The fourth chapter contains the original part of this work. After a general review of Kähler moduli inflation, we first derive general strong constraints necessary to obtain phenomenological acceptable models, which could correctly reproduce the properties of the present universe. The calculations aim to account for the most general case, and we do not assume any specific values for the various parameters until the end. We then analyze the multi-field case, on the assumption that almost all the particles behave in the same way, and gather the expected output of the system. In particular, we derive an expression for the shift between the volume modulus during inflation and the volume after inflation, together with an expression for the ratio between its mass and the inflationary Hubble constant. These are fundamental parameters for understanding the physics of these models. After that, we discuss the post inflationary scenario and we derive an expression based on fundamental parameters useful to estimate whether a post-inflationary period of matter domination is present. Finally, we numerically solve the complete system of differential equations freely choosing some parameters and exploiting the previously derived relations in order to assign the remaining ones.

The appendix is also an important integrating part of this thesis, as we perform detailed calculations of the masses of the moduli in the multi-field case, showing the dependence on the number of fields n , and we clarify how the specific uplift term of the potential affects the connection between n and the parameters of the model.

CHAPTER 1

A BRIEF REVIEW OF SUPERSYMMETRY AND SUPERGRAVITY

1.1 Why supersymmetry?

During the last decades, the Standard Model of particle physics has proven to provide a wonderful description of some properties of the subatomic world, explaining a wide spectrum of phenomena. It represents a concrete example of application of QFT, as it is a gauge theory based on the internal symmetry

$$G_{SM} = SU(3)_c \otimes SU(2)_L \otimes U(1)_Y ,$$

which accounts for strong and electroweak forces. In particular, it describes all known particles and interactions in four-dimensional spacetime:

- matter particles, i.e. quarks and leptons, which are organized in three families differing only by their mass;
- interaction particles, arising from the gauge group G_{SM} , namely the photon γ , the gluons g and the electroweak bosons Z^0 and W^\pm ;
- Higgs boson, the scalar particle responsible for the breaking of SM gauge symmetry and for the mass of all the particles.

Despite its success, SM is not the end of the story as it cannot answer many questions. Hence, it cannot be a fundamental theory of the universe, but only an effective theory valid at low energies. Indeed, SM is not able to address some of the modern physics puzzles:

- quantum gravity: SM describes three of the four fundamental interactions at quantum level, but it does not include gravity, which has to be treated at classical level;
- hierarchy problem: it is not clear why there are totally different energy scales, namely $M_{EW} \sim 10^2$ GeV (the electroweak scale) and $M_P \sim 10^{18}$ GeV (the reduced Planck scale, $M_P = \sqrt{\frac{1}{8\pi G}}$ in natural units);

- cosmological constant: the vacuum energy predicted by SM is much smaller than the observed cosmological constant of the universe.

These are only few of the serious problems we face; other issues concern for example the strong CP problem, the treatment of strong coupling field theories (as for instance QCD, due to the asymptotic freedom property), the origin of the parameters of the SM, the mass of the Higgs boson,...etc.

There are several different ways to try to extend the Standard Model, from *ad hoc* addition of new physics guided by experiments to theoretical extensions suggested by first principles. In this last procedure, the idea is to look for more general symmetries of Nature, which could be both internal symmetries (as for example the GUTs) or spacetime symmetries. The former case relies on the assumption that these new symmetries are broken at some scale $M_{GUT} > M_{EW}$ and give origin to SM at lower energies, the latter exploits higher dimensional spaces or more general symmetries (such as supersymmetry) for the standard four-dimensional spacetime.

Supersymmetry is one of the candidate theory for an extension of the Standard Model, even though it does not solve all the problems we cited before. Indeed, it addresses somehow the hierarchy problem, in the sense that it affects the sensitivity of the Higgs potential to the new physics. In addition, supersymmetry really seems to be a fundamental symmetry of Nature: in 1975, Haag, Lopuszanski and Sohnius generalized the Coleman-Mandula theorem, discovering that the most general superalgebras admitted in quantum field theory are the supersymmetry algebras, which extend the Poincaré algebra.

The problem linked to the Higgs boson consists in the fact that its mass receives enormous quantum corrections from the virtual effects of every particle which couples (directly or indirectly) with the Higgs field H . For instance, if we write the Higgs potential as

$$V_H = m_H^2 |H|^2 + \lambda |H|^4,$$

for a Dirac fermion f which couples with H with the term $-\lambda_f H \bar{f} f$, a loop diagram gives the correction

$$\Delta_f m_H^2 = -\frac{|\lambda_f|^2}{8\pi^2} \Lambda_{UV}^2, \tag{1.1}$$

whereas for a scalar particle S with a Lagrangian term $-\lambda_S |H|^2 |S|^2$ it gives

$$\Delta_S m_H^2 = -\frac{\lambda_S}{16\pi^2} \left[\Lambda_{UV}^2 - 2m_S^2 \ln \left(\frac{\Lambda_{UV}}{m_S} \right) \right]. \tag{1.2}$$

These corrections depend on the ultraviolet momentum cutoff Λ_{UV} , i.e. the energy scale at which new physics is expected. We do not know the value of Λ_{UV} , but for a large value, for example $\Lambda_{UV} \sim M_P$, the Higgs mass receives enormous quantum corrections, which are not compatible with the experimental measurements. Furthermore, even if the other SM particles do not have direct quadratic sensitivity to Λ_{UV} , they are indirectly affected due to their coupling with the Higgs boson.

A possible solution to avoid such effect is to look for cancellations between the various contributions to Δm_H^2 : looking at (1.1) and (1.2), from the relative minus sign between the two corrections we can imagine that we need a symmetry that relates fermions and bosons. This is precisely the idea behind supersymmetry: each particle of the Standard Model has to be accompanied by a supersymmetric partner (or *sparticle*) with a spin differing by 1/2 unit and

with $\lambda_s = |\lambda_f|^2$. For example, an electron is expected to come with two scalar fields called *selectrons*, one for each chirality state of the fermion. Then, their combined contribution to the Higgs mass looks like

$$\Delta m_H^2 \sim \lambda \ln \left(\frac{\Lambda_{UV}}{m} \right). \quad (1.3)$$

Hence, the quadratic dependence on Λ_{UV} is “substituted” by a logarithmic behavior, which is much less dangerous.

The above discussion is of course exactly valid if supersymmetry is unbroken. However, since no supersymmetric particle has ever been observed, it is clear that supersymmetry (if it really exists) must be a broken symmetry. Thus in a realistic theory we must account for a term \mathcal{L}_{break} in the Lagrangian which does not spoil the cancellation between scalar and fermionic contributions to the Higgs mass.

Supersymmetric particles are also of interest in theoretical physics as they may be related to dark matter. In particular, one of the neutral scalar particles that arise in the Minimal Supersymmetric Standard Model (MSSM) is the so called WIMP (Weakly Interacting Massive Particle), which constitutes a promising candidate for dark matter.

Despite the benefits that supersymmetry would bring to fundamental physics, it does not address the cosmological constant problem, which still remains one of the greatest mysteries of present physics.

In this chapter we shall provide a brief description of the main tools necessary to construct a supersymmetric theory. The goal is to show how to build a generic supersymmetric Lagrangian and how to derive from it an expression for a scalar potential. In particular, this discussion is meant to give an idea on how to derive a scalar potential from a supergravity theory, as such potential is a fundamental ingredient for the inflationary models we are studying in this thesis.

1.2 Supersymmetry algebra

We introduce here the supersymmetry algebra. Before giving the properties of this algebra, we briefly recall a few definitions.

Def. (Graded algebra). Let Δ be a commutative group. An algebra \mathfrak{g} over a field \mathbb{K} is said to be *graded* if it can be written as a direct sum

$$\mathfrak{g} = \bigoplus_{i \in \Delta} \mathfrak{g}_i$$

of vector spaces \mathfrak{g}_i over \mathbb{K} with a bilinear map

$$\star : \mathfrak{g} \times \mathfrak{g} \rightarrow \mathfrak{g}.$$

such that

$$\star(\mathfrak{g}_i, \mathfrak{g}_j) \subseteq \mathfrak{g}_{i+j}.$$

If $\Delta = \mathbb{Z}_2$ the algebra is called a *superalgebra*.

Def. (Graded Lie algebra). A graded Lie algebra \mathfrak{K} over a field is a graded algebra where the map

$$\star : \mathfrak{g} \times \mathfrak{g} \rightarrow \mathfrak{g}, \quad \star(g_i, g_j) \rightarrow [g_i, g_j], \quad \forall g_i \in \mathfrak{g}_i, g_j \in \mathfrak{g}_j$$

generalizes the Lie product and satisfies

- $[\mathfrak{g}_i, \mathfrak{g}_j] \subset \mathfrak{g}_{i+j}, \forall i, j \in \Delta;$
- $[g_i, g_j] = -(-1)^{ij}[g_j, g_i], \quad \forall g_i \in \mathfrak{g}_i, g_j \in \mathfrak{g}_j;$
- $(-1)^{ik}[g_i, [g_j, g_k]] + (-1)^{ij}[g_j, [g_k, g_i]] + (-1)^{jk}[g_k, [g_i, g_j]] = 0,$
 $\forall g_i \in \mathfrak{g}_i, g_j \in \mathfrak{g}_j, g_k \in \mathfrak{g}_k.$

Def. (Lie superalgebra). A Lie superalgebra is a graded Lie algebra where $\Delta = \mathbb{Z}_2$. It contains a set of generators $\{G_a\}$ which satisfy

$$G_a G_b - (-1)^{\eta_a \eta_b} G_b G_a = i C_{ab}^e G_e$$

where the gradings η_a take the values

$$\eta_a = \begin{cases} 0 & \text{for bosonic generators} \\ 1 & \text{for fermionic generators} \end{cases}.$$

If we call B_a the bosonic generators and F_α the fermionic generators, the generalized Lie product satisfies

$$\begin{aligned} [B_a, B_b] &= i f_{ab}^c B_c, \\ [B_a, F_\alpha] &= i g_{a\alpha}^\beta F_\beta, \\ \{F_\alpha, F_\beta\} &= h_{\alpha\beta}^a B_a, \end{aligned}$$

and the Jacobi identity can be written as

$$[G_a, [G_b, G_c]] + \text{cyclic graded perm.} = 0,$$

where we used the notation

$$[\cdot, \cdot] = \begin{cases} \{\cdot, \cdot\} & \text{if they are both fermionic,} \\ [\cdot, \cdot] & \text{otherwise.} \end{cases}$$

We point out that these definitions are not “standard”, as some authors refer to a *graded Lie algebra* as an ordinary Lie algebra endowed with a gradation compatible with the Lie product and use the above properties to define a *graded Lie superalgebra*. We will refer to [1] for our convention.

Finally, after these definitions we come to the *supersymmetry algebra*, which is a Lie superalgebra that extends the Poincaré algebra. For this reason it is also called *super Poincaré algebra*. First of all we recall the Poincaré algebra

$$\begin{aligned} [P^\mu, P^\nu] &= 0, \\ [M^{\mu\nu}, P^\rho] &= i(P^\mu \eta^{\nu\rho} - P^\nu \eta^{\mu\rho}) \\ [M^{\mu\nu}, M^{\rho\sigma}] &= i(M^{\mu\sigma} \eta^{\nu\rho} + M^{\nu\rho} \eta^{\mu\sigma} - M^{\mu\rho} \eta^{\nu\sigma} - M^{\nu\sigma} \eta^{\mu\rho}), \end{aligned} \tag{1.4}$$

where P^μ are the generators linked to translations and $M^{\mu\nu}$ are the ones related to rotations. We can now add the fermionic generators Q_α^A , where $A = 1, 2, \dots, \mathcal{N}$ for generic extended SUSY, to enlarge our algebra. We will focus on the case of simple SUSY with $\mathcal{N} = 1$, since it is the interesting case for us.

We already know the commutation relations of the Poincaré algebra, so we just need to find the relations with Q_α and Q_β^\dagger . We will not derive them here, but we indicate two different strategies to do it.

The first idea, followed in [2], is to use the index structure to make an ansatz and use some known results to find the correct relations. It also use the fact that fermionic generators are both spinors and operators, and they should transform following both ways.

The second idea, more physical, is to start building a minimal Lagrangian with a single left-handed Weyl fermion and its supersymmetric partner (i.e. a complex scalar field). After having defined the transformation rules of the fields and added a scalar auxiliary field (in order to make the algebra closed off-shell), the Noether supercurrent and the conserved charges can be found. The latter are the generators of supersymmetry transformations and their commutation relations can be worked out using their quantum mechanical properties and the transformation rules of the fields. For more details see [3].

The relations are then

$$[Q_\alpha, M^{\mu\nu}] = (\sigma^{\mu\nu})_\alpha{}^\beta Q_\beta \quad (1.5)$$

$$[Q_\alpha, P^\mu] = [Q^{\dagger\dot{\alpha}}, P^\mu] = 0 \quad (1.6)$$

$$\{Q_\alpha, Q_\beta\} = \{Q_\alpha^\dagger, Q_\beta^\dagger\} = 0 \quad (1.7)$$

$$\{Q_\alpha, Q_\beta^\dagger\} = 2(\sigma^\mu)_{\alpha\dot{\beta}} P_\mu. \quad (1.8)$$

It is really important to note that the relation (1.8) implies that supersymmetry is a spacetime symmetry and not an internal one, as the combination of two supersymmetry charges is linked to a spacetime translation.

1.3 Superspace and superfields

In this section we define some very important mathematical tools useful to understand the structure of supersymmetric theories.

We first recall that in non supersymmetric theories particles are described by fields defined on Minkowski space

$$\phi : \mathcal{M}^4 \rightarrow \mathbb{R},$$

which transform under the Lorentz group.

The idea for supersymmetric theories is to extend these fields into some objects Φ acting on a *superspace*, whose coordinates are identified by X , and which transform under the super Poincaré group.

Let us start by defining the superspace coordinates

$$X = (x^\mu, \theta^\alpha, \theta_\alpha^\dagger), \quad (1.9)$$

where θ^α and θ_α^\dagger are spinors of Grassman variables (also known as anticommuting numbers or fermionic variables). Grassman variables are objects g_i which generate a *Grassman algebra* \mathcal{G}_n and satisfy the relations

$$\{g_i, g_j\} = 0 \quad \forall i, j = 1, 2, \dots, n.$$

If we consider a single variable g it is easy to see that a generic function $f : \mathcal{G}_1 \rightarrow \mathbb{R}$ can be written as

$$f(g) = \sum_{k=0}^{\infty} f_k g^k = f_0 + f_1 g,$$

which tells us that the most general function is linear. Its derivative is simply

$$\frac{df}{dg} = f_1,$$

and requiring that the integral of a Grassman valued function is invariant under translation, i.e. $\int dg f(g) = \int dg f(g+h)$, we found that

$$\int dg g = 1, \quad \int dg 1 = 0. \quad (1.10)$$

These properties define the Berezin integral

$$\int dg f(g) = \int dg (f_0 + f_1 g) = f_1 = \frac{df}{dg}. \quad (1.11)$$

It is important to specify that the derivatives act on the left: for example, with two Grassman variables g, h we have

$$\frac{\partial}{\partial g}(gh) = h, \quad \frac{\partial}{\partial g}(hg) = \frac{\partial}{\partial g}(-gh) = -h.$$

Let us come back to our spinors and give some definitions

$$\theta\theta := \theta^\alpha \theta_\alpha, \quad \theta^\dagger \theta^\dagger := \theta_{\dot{\alpha}}^\dagger \theta^{\dot{\alpha}}, \quad (1.12)$$

which imply

$$\theta^\alpha \theta^\beta = -\frac{1}{2} \epsilon^{\alpha\beta} \theta\theta, \quad \theta^{\dot{\alpha}} \theta^{\dot{\beta}} = \frac{1}{2} \epsilon^{\dot{\alpha}\dot{\beta}} \theta^\dagger \theta^\dagger. \quad (1.13)$$

For the derivatives we have

$$\frac{\partial}{\partial \theta^\alpha} (\theta^\beta) = \delta_\alpha^\beta, \quad \frac{\partial}{\partial \theta^\alpha} (\theta_{\dot{\beta}}^\dagger) = 0, \quad \frac{\partial}{\partial \theta_{\dot{\alpha}}^\dagger} (\theta_{\dot{\beta}}^\dagger) = \delta_{\dot{\beta}}^{\dot{\alpha}}, \quad \frac{\partial}{\partial \theta_{\dot{\alpha}}^\dagger} (\theta^\beta) = 0, \quad (1.14)$$

whereas for multi integrals

$$\int d\theta^1 \int d\theta^2 \theta^2 \theta^1 = \frac{1}{2} \int d\theta^1 \int d\theta^2 \theta\theta = 1. \quad (1.15)$$

This last leads to the definition

$$\frac{1}{2} \int d\theta^1 \int d\theta^2 = \int d^2\theta, \quad (1.16)$$

and to integrate over a superspace we use

$$d^2\theta = -\frac{1}{4} d\theta^\alpha d\theta^\beta \epsilon_{\alpha\beta}, \quad d^2\theta^\dagger = -\frac{1}{4} d\theta_{\dot{\alpha}}^\dagger d\theta_{\dot{\beta}}^\dagger \epsilon_{\dot{\alpha}\dot{\beta}}. \quad (1.17)$$

1.4 General scalar superfield

To write the general scalar superfield in a superspace with coordinates $x^\mu, \theta^\alpha, \theta^\dagger_{\dot{\alpha}}$ we expand the field in power series in the anti-commuting variables

$$S(x, \theta, \theta^\dagger) = \varphi(x) + \theta\psi(x) + \theta^\dagger\chi^\dagger(x) + \theta\theta M(x) + \theta^\dagger\theta^\dagger N(x) + (\theta\sigma^\mu\theta^\dagger)V_\mu(x) \\ + (\theta\theta)\theta^\dagger\lambda^\dagger(x) + (\theta^\dagger\theta^\dagger)\theta\rho(x) + (\theta\theta)(\theta^\dagger\theta^\dagger)D(x). \quad (1.18)$$

Geometrically, a SUSY transformation is a translation in the superspace along the θ and θ^\dagger directions, but, as we pointed out before, (1.8) states that supersymmetry transformations also generate spacetime translations. Hence a SUSY transformation can be written as

$$S(x, \theta, \theta^\dagger) \mapsto \exp\left(i(\epsilon Q + \epsilon^\dagger Q^\dagger)\right)S(x, \theta, \theta^\dagger) = S(x^\mu - i(\epsilon\sigma^\mu\theta^\dagger) + i(\theta\sigma^\mu\epsilon^\dagger), \theta + \epsilon, \theta^\dagger + \epsilon^\dagger). \quad (1.19)$$

From these translation arguments we can define the differential operators acting on superfields:

$$Q_\alpha = -i\frac{\partial}{\partial\theta^\alpha} - (\sigma^\mu\theta^\dagger)_\alpha\partial_\mu, \quad (1.20)$$

$$Q^\dagger_{\dot{\alpha}} = +i\frac{\partial}{\partial\theta^\dagger_{\dot{\alpha}}} + (\theta\sigma^\mu)_{\dot{\alpha}}\partial_\mu, \quad (1.21)$$

$$P_\mu = -i\partial_\mu. \quad (1.22)$$

It is easy to show that these operators satisfy the super Poincaré algebra. From an infinitesimal SUSY transformation

$$\delta S = i(\epsilon Q + \epsilon^\dagger Q^\dagger)S \quad (1.23)$$

we can get explicit terms for the transformations of the different fields of $S(x, \theta, \theta^\dagger)$. We will not do that here (see [2]), as we are more interested in the chiral superfields, which are the basic fields we need in order to build a Lagrangian.

It is enough for our purposes to give the transformation of the D-term

$$\delta D = \frac{i}{2}\partial_\mu(\epsilon\sigma^\mu\lambda^\dagger - \rho\sigma^\mu\epsilon^\dagger), \quad (1.24)$$

since it is the only term which transforms as a total derivative and for this reason it will play a crucial role to build a generic Lagrangian.

1.4.1 Chiral superfield

If we want to construct generic supersymmetric Lagrangians in superspace, we need derivatives respect to the Grassman variables which are invariant under SUSY global transformations. But

$$\delta\left(\frac{\partial S}{\partial\theta^\alpha}\right) \neq \frac{\partial}{\partial\theta^\alpha}(\delta S),$$

i.e. derivatives respect to θ^α (and $\theta^\dagger_{\dot{\alpha}}$) are not superfields.

To fix this problem we define the covariant derivatives

$$D_\alpha = \frac{\partial}{\partial\theta^\alpha} + i(\sigma^\mu\theta^\dagger)_\alpha\partial_\mu, \quad \bar{D}_{\dot{\alpha}} = -\frac{\partial}{\partial\theta^\dagger_{\dot{\alpha}}} - i(\theta\sigma^\mu)_{\dot{\alpha}}\partial_\mu, \quad (1.25)$$

which satisfy

$$\begin{aligned}\{D_\alpha, Q_\beta\} &= \{D_\alpha, Q_\beta^\dagger\} = \{\bar{D}_{\dot{\alpha}}, Q_\beta\} = \{\bar{D}_{\dot{\alpha}}, Q_\beta^\dagger\} = 0, \\ \{D_\alpha, D_\beta\} &= \{\bar{D}_{\dot{\alpha}}, \bar{D}_{\dot{\beta}}\} = 0, \\ \{D_\alpha, \bar{D}_{\dot{\beta}}\} &= -2i(\sigma^\mu)_{\alpha\dot{\beta}}\partial_\mu.\end{aligned}\tag{1.26}$$

In this way it is straightforward to verify that $D_\alpha S$ is a superfield and finally transforms as $D_\alpha(\delta S) = (\delta D_\alpha S)$, as required for a supersymmetry transformation.

Since $S(x, \theta, \theta^\dagger)$ is not an irreducible representation of supersymmetry we are free to eliminate some components: this allows us to find an irreducible representation of the supersymmetry algebra.

One of the very important fields is the *chiral field*, as it contains matter particles (quarks and leptons) and the Higgs boson, together with their supersymmetric partners. It is defined by the condition

$$\bar{D}_{\dot{\alpha}}\Phi = 0,$$

and it can be explicitly written in term of its components as

$$\begin{aligned}\Phi(x, \theta, \theta^\dagger) &= \varphi(x) + \sqrt{2}\theta\psi(x) + \theta\theta F(x) + i\theta\sigma^\mu\theta^\dagger\partial_\mu\varphi(x) \\ &\quad - \frac{i}{\sqrt{2}}(\theta\theta)\partial_\mu\psi(x)\sigma^\mu\theta^\dagger + \frac{1}{4}(\theta\theta)(\theta^\dagger\theta^\dagger)\partial_\mu\partial^\mu\varphi(x),\end{aligned}\tag{1.27}$$

where φ represents the scalar part, ψ the fermionic one and F is an auxiliary field necessary to close the supersymmetry algebra off-shell.

Under a SUSY transformation (1.23) we find for the change in components

$$\delta\varphi = \sqrt{2}\epsilon\psi, \tag{1.28}$$

$$\delta\psi = i\sqrt{2}\sigma^\mu\epsilon^\dagger\partial_\mu\varphi + \sqrt{2}\epsilon F, \tag{1.29}$$

$$\delta F = i\sqrt{2}\epsilon^\dagger\bar{\sigma}^\mu\partial_\mu\psi. \tag{1.30}$$

Similarly, an *antichiral field* is defined by the condition $D_\alpha\Phi^\dagger = 0$. It is important to notice that the product $\Phi^\dagger\Phi$ and the sum $\Phi^\dagger + \Phi$ are both real superfields but neither chiral nor antichiral.

1.4.2 Vector superfield

The most general real field $V(x, \theta, \theta^\dagger) = V^\dagger(x, \theta, \theta^\dagger)$ is

$$\begin{aligned}V(x, \theta, \theta^\dagger) &= C(x) + i\theta\chi(x) - i\theta^\dagger\chi^\dagger(x) + \frac{i}{2}\theta\theta(M(x) + iN(x)) - \frac{i}{2}\theta^\dagger\theta^\dagger(M(x) - iN(x)) \\ &\quad + \theta\sigma^\mu\theta^\dagger V_\mu(x) + i(\theta\theta)\theta^\dagger\left(-i\lambda^\dagger(x) + \frac{i}{2}\bar{\sigma}^\mu\partial_\mu\chi(x)\right) \\ &\quad - i(\theta^\dagger\theta^\dagger)\theta\left(i\lambda(x) - \frac{i}{2}\sigma^\mu\partial_\mu\chi^\dagger(x)\right) + \frac{1}{2}(\theta\theta)(\theta^\dagger\theta^\dagger)\left(D - \frac{1}{2}\partial_\mu\partial^\mu C\right).\end{aligned}\tag{1.31}$$

To enlighten its physical meaning we note that if Λ is a chiral field, then the combination $i(\Lambda - \Lambda^\dagger)$ is a vector superfield. We can then define a gauge transformation

$$V \mapsto V - \frac{i}{2}(\Lambda - \Lambda^\dagger),$$

and we can freely choose the components of Λ . A very important choice is the *Wess-Zumino gauge*, in which the superfield takes the form

$$V_{WZ}(x, \theta, \theta^\dagger) = (\theta\sigma^\mu\theta^\dagger)V_\mu(x) + (\theta\theta)(\theta^\dagger\lambda^\dagger(x)) + (\theta^\dagger\theta^\dagger)(\theta\lambda(x)) + \frac{1}{2}(\theta\theta)(\theta^\dagger\theta^\dagger)D(x). \quad (1.32)$$

From (1.32) is clear that such superfield contains the gauge particles V_μ (photons, gluons, W^\pm , Z^0) and the gauginos λ and λ^\dagger , plus an auxiliary field $D(x)$.

1.5 Supersymmetric Lagrangians

Now that we have all the mathematical tools we need, we can try to define a general supersymmetric Lagrangian. We will consider few simple cases as the main goal of this chapter is to find the general structure of the supergravity potential without gauge fields.

We start considering the general *chiral superfield Lagrangian*. In order to build a Lagrangian invariant under global supersymmetry we recall the supersymmetry transformations (1.24) and (1.30): we can exploit these properties in order to ensure that $\delta\mathcal{L}$ is a total derivative under SUSY transformations. The most general Lagrangian for chiral fields Φ_i is then

$$\mathcal{L} = K(\Phi_i, \Phi^{j\dagger}) \Big|_D + \left(W(\Phi_i) \Big|_F + \text{h.c.} \right), \quad (1.33)$$

where $K(\Phi_i, \Phi^{j\dagger})$, known as *Kähler potential*, is a real function and $W(\Phi_i)$, called *superpotential*, is a holomorphic function of the chiral superfields and thus it is a chiral superfield itself. With these properties, we can give general form of such functions ([3], [4])

$$K(\Phi_i, \Phi^{j\dagger}) = \Phi^{\dagger i}\Phi_i, \quad (1.34)$$

$$W(\Phi_i) = L^i\Phi_i + \frac{1}{2}M^{ij}\Phi_i\Phi_j + \frac{1}{6}y^{ijk}\Phi_i\Phi_j\Phi_k, \quad (1.35)$$

where $L^i \neq 0$ only if Φ_i is a gauge singlet, M^{ij} is a symmetric mass matrix for fermion fields and y^{ijk} is a Yukawa coupling of a scalar and two fermions that must be totally symmetric under interchange of i, j, k .

To obtain the expression of the Lagrangian in terms of the components of the superfields we can expand around $\Phi_i = \varphi_i$; in particular, the superpotential is

$$W(\Phi_i) = W(\varphi_i) + \frac{\partial W}{\partial \Phi_i} \Big|_{\Phi_i=\varphi_i} (\Phi_i - \varphi_i) + \frac{1}{2} \frac{\partial^2 W}{\partial \Phi_i \partial \Phi_j} \Big|_{\Phi_i=\varphi_i} (\Phi_i - \varphi_i)(\Phi_j - \varphi_j), \quad (1.36)$$

and defining $\frac{\partial W}{\partial \Phi_i} \Big|_{\Phi_i=\varphi_i} \equiv \frac{\partial W}{\partial \varphi_i}$ the F-term of W are

$$W(\Phi_i) \Big|_F = \frac{\partial W}{\partial \varphi_i} [(\Phi_i - \varphi_i)] \Big|_F + \frac{1}{2} \frac{\partial^2 W}{\partial \varphi_i \partial \varphi_j} [(\Phi_i - \varphi_i)(\Phi_j - \varphi_j)] \Big|_F. \quad (1.37)$$

With the same reasoning for the Kähler potential we finally come to the full Lagrangian

$$\mathcal{L} = \partial^\mu \varphi^{*i} \partial_\mu \varphi_i + i\psi^{\dagger i} \bar{\sigma}^\mu \partial_\mu \psi_i - \frac{1}{2} \left(\frac{\partial^2 W}{\partial \varphi_i \partial \varphi_j} \psi_i \psi_j + \text{h.c.} \right) + \mathcal{L}_F, \quad (1.38)$$

where

$$\mathcal{L}_F = F_i F^{*i} + \frac{\partial W}{\partial \varphi_i} F_i + \frac{\partial W}{\partial \varphi^{*i}} F^{*i} \quad (1.39)$$

is the part of the Lagrangian containing the F fields, which are not physical. Indeed, from \mathcal{L}_F it is evident that the fields F_i do not propagate due to the absence of derivatives.

We can now eliminate these auxiliary fields using the equations of motion

$$\begin{cases} F^{*i} &= -\frac{\partial W}{\partial \varphi_i} \\ F_i &= -\frac{\partial W}{\partial \varphi^{*i}} \end{cases} ; \quad (1.40)$$

these define the scalar potential

$$V_F = -\mathcal{L}_F = \frac{\partial W}{\partial \varphi_i} \frac{\partial W}{\partial \varphi^{*i}}. \quad (1.41)$$

Let us now give the framework of a more general theory. If we want to introduce interactions, we also need vector superfields with their kinetic terms. We can build a supergauge theory, in analogy with what we do in non supersymmetric cases. In this case, the Lagrangian takes the form

$$\mathcal{L} = K(\Phi_i, \tilde{\Phi}^{\dagger j}) \Big|_D + \left(\left(\frac{1}{4} f_{ab}(\Phi_i) \mathcal{W}^{a\mu} \mathcal{W}_\mu^b + W(\Phi_i) \right) \Big|_F + \text{h.c.} \right), \quad (1.42)$$

where $f_{ab}(\Phi_i)$ are the *gauge kinetic functions*, \mathcal{W}_α are the field-strength superfields and

$$\begin{aligned} \tilde{\Phi}^{\dagger j} &= (\Phi^* e^V)^j, \\ V &= 2g_a T^a V^a, \end{aligned}$$

where T^a are the generators of the gauge symmetry, V^a are vector superfields (one for each Lie algebra generator) and g_a are the gauge couplings.

In this case, if we want to find the scalar potential, we have to take into account that in the Lagrangian are also present D-terms; therefore, eliminating all the auxiliary fields through their equations of motion, we find a scalar potential of the form $V_s = V_F + V_D$.

In such general cases the F-term scalar potential V_F takes the form

$$V_F = K^{i\bar{j}} \frac{\partial W}{\partial \varphi_i} \frac{\partial W}{\partial \varphi_{\bar{j}}^*}, \quad (1.43)$$

where $K^{i\bar{j}}$ is the inverse of the *Kähler metric*

$$K_{i\bar{j}} = \left(\frac{\partial^2 K}{\partial \varphi^i \partial \varphi^{*\bar{j}}} \right), \quad (1.44)$$

which is the metric over a complex Kähler manifold whose coordinates are the scalar fields φ^i .

In summary, a general supersymmetric Lagrangian depends on three functions of superfields:

- the Kähler potential K , a real function of both chiral and anti-chiral superfields, which could include vector superfields in order to be supergauge invariant;
- the superpotential W , an arbitrary holomorphic function of the chiral superfields, which must be invariant under the gauge symmetries of the theory;
- the gauge kinetic function f_{ab} , a dimensionless holomorphic function, symmetric under interchange of its two indices a, b , which run over the gauge group.

1.6 Supersymmetry breaking

As we outlined in the introduction of this chapter, supersymmetry must be a broken symmetry. For what concerns the symmetry breaking, we remind that a symmetry is said to be spontaneously broken if the Lagrangian is invariant under such transformations but the vacuum state is not. We then speak of broken SUSY if the vacuum state satisfies

$$Q_\alpha |\text{vac}\rangle \neq 0. \quad (1.45)$$

Let us consider (1.8) contracted with $(\bar{\sigma}^0)^{\dot{\beta}\alpha}$

$$(\bar{\sigma}^0)^{\dot{\beta}\alpha} \{Q_\alpha, Q_\beta^\dagger\} = \sum_{\alpha=1}^2 (Q_\alpha Q_\alpha^\dagger + Q_\alpha^\dagger Q_\alpha) = 4P^0 = E; \quad (1.46)$$

since for a generic state $|\Psi\rangle$

$$\langle\Psi|Q_\alpha Q_\alpha^\dagger + Q_\alpha^\dagger Q_\alpha|\Psi\rangle = |Q_\alpha|\Psi\rangle|^2 + |Q_\alpha^\dagger|\Psi\rangle|^2 > 0, \quad (1.47)$$

it follows that $E \geq 0$ always. This also implies that if the state $|\Psi_0\rangle$ has $E = 0$ it must be a ground state; however, not every ground state has zero energy and from (1.45) it is clear that SUSY is broken if

$$\langle\text{vac}|Q_\alpha Q_\alpha^\dagger + Q_\alpha^\dagger Q_\alpha|\text{vac}\rangle > 0, \quad (1.48)$$

i.e. the vacuum has positive energy. If we now look at the chiral field transformation laws (1.28), (1.29) and (1.30), it is evident that if one among $\delta\varphi$, $\delta\psi$, $\delta F \neq 0$ then supersymmetry is broken. Actually, to preserve Lorentz invariance we need $\langle\psi\rangle = \langle\partial_\mu\varphi\rangle = 0$ which implies $\delta\psi = \delta F = 0$; hence supersymmetry is broken if and only if $\delta\varphi \neq 0$ or

$$\langle F\rangle \neq 0.$$

If we look at the equations of motion (1.40) for the auxiliary fields F_i , from (1.41) it is evident that in terms of F_i the scalar potential is

$$V_F = F_i F^{*i}, \quad (1.49)$$

and the SUSY breaking conditions are equivalent to

$$\langle V_F\rangle > 0. \quad (1.50)$$

If we consider a vector field $V(\lambda, A_\mu, D)$, given that (see [3] and [4])

$$\delta\lambda = \epsilon D + \frac{i}{2}(\sigma^\mu \bar{\sigma}^\nu)(\partial_\mu V_\nu - \partial_\nu V_\mu),$$

with the same reasoning as before it is evident that if

$$\langle D\rangle \neq 0,$$

then supersymmetry is broken.

In conclusion, in a general model with both F-fields and D-fields supersymmetry is broken if at least one of the auxiliary fields acquires a non-vanishing vacuum expectation value.

1.7 $\mathcal{N} = 1$, $D = 4$ supergravity Lagrangian

Supergravity is the gauge theory that arises when we extend SUSY to a local symmetry; intuitively, this is similar to General Relativity invariance under general coordinate transformations. This operation introduces a gravity supermultiplet with two more particles, the graviton (a spin 2 particle) and the gravitino (a spin $\frac{3}{2}$ particle).

Supergravity is a quantum theory of gravity, and the case $\mathcal{N} = 1$ is the most interesting one as it includes gravity in a natural way and it is the only one phenomenologically acceptable. Anyway, this theory is not renormalizable, and supergravity Lagrangian has to be considered an effective phenomenological Lagrangian which comes from a more complex framework.

We present here some useful results that we will use in the following chapters. A $D = 4$, $\mathcal{N} = 1$ supergravity Lagrangian depends only on two functions, the *Kähler function*

$$G(\Phi, \Phi^\dagger) = K(\Phi, \Phi^\dagger) + \ln |W(\Phi)|^2, \quad (1.51)$$

and the gauge kinetic function

$$f_{ab}(\Phi). \quad (1.52)$$

We see that for supergravity the Kähler potential and superpotential are not independent; however, it is still useful to work with them instead of G . In this case, the action exhibits an extra symmetry, the so called *Kähler invariance*

$$\begin{aligned} K &\rightarrow K + h(\Phi) + h^*(\Phi^\dagger), \\ W &\rightarrow e^{-h(\Phi)} W \end{aligned} \quad (1.53)$$

where $h(\Phi)$ is an arbitrary function.

Let us concentrate on the *chiral supergravity Lagrangian*: we are not interested in the gauge fields coupled to supergravity, as these fields do not arise from compactifications of the extra dimensions of string theory we will consider in the next chapters. In particular, from this procedure lots of scalar fields are originated. Hence, we do not write the full Lagrangian explicitly, which can be found in [5], but we give the general form of the Lagrangian for a scalar field, which is

$$\mathcal{L}_\varphi = K_{i\bar{j}} \partial_\mu \varphi^i \partial^\mu \varphi^{*\bar{j}} - V_F. \quad (1.54)$$

The scalar potential, which can be derived as in section 1.5, is now

$$V_F = e^{\frac{K}{M_P^2}} \left(K^{i\bar{j}} D_i W \overline{D_j W} - 3 \frac{|W|^2}{M_P^2} \right), \quad (1.55)$$

where

$$D_i W := \partial_i W + \frac{1}{M_P^2} (\partial_i K) W. \quad (1.56)$$

In this case, the F-terms are given by

$$F^i = e^{\frac{K}{2M_P^2}} K^{i\bar{j}} \overline{D_j W}, \quad F^{\bar{j}} = e^{\frac{K}{2M_P^2}} K^{i\bar{j}} D_i W. \quad (1.57)$$

Note that in the limit $M_P \rightarrow \infty$ the potential (1.55) becomes equal to the standard supersymmetric case of (1.43), as we expect.

2.1 Why string theory?

Nowadays string theory is one of the most promising fundamental theories which may be able to describe all the known interactions in an elegant unified framework. It is built on a rich mathematical structure where the point-like objects of particle physics are replaced by one-dimensional objects, namely the strings. Such theory requires the existence of six extra dimensions for internal consistency, introduced with the help of a six-dimensional manifold.

It seems there exist only five different string theories: type I string theory (closed and open strings), type IIA and IIB string theory (closed strings), heterotic $E_8 \times E_8$ and $SO(32)$ string theory. These theories are related by a number of dualities and are believed to correspond to different limits of an underlying theory known as M-theory.

In order to make contact with our four-dimensional world, it is necessary to find a way to “hide” the extra dimensions making them invisible at our present instrumentation. This technique is called *compactification* and it corresponds to the low energy limit of string theory. This limit (some orders of magnitude below the Planck scale) leads in general to a supersymmetric low energy effective theory. Hence, it is particularly interesting as it can provide an extension of the Standard Model, naturally accounting for supersymmetric particles, and cosmological models useful to describe some features of the universe evolution.

Despite being a candidate to describe Nature in all its aspects, string theory lacks any kind of experimental evidence. However, even if a direct confirmation seems at present impossible, it is worth to look for phenomenological implications of the theory, which could produce realistic models of some natural phenomena.

In particular, in this thesis we are interested in cosmological models for inflation, i.e. the period of accelerated cosmological expansion soon after the Big Bang. In this chapter we will focus on some results of type IIB string theory necessary to build suitable model for this purpose; the goal of this discussion is to give an idea of the underlying theory and its low energy limit without any claim of completeness. More exhaustive treatments can be found for example in [6], [7] and [8].

2.2 Compactification and dimensional reduction

In this section we present the most important features of the low energy limit of string compactifications for type IIB string theory. This procedure allows us to get rid of the extra dimensions, providing a connection with our four-dimensional world and obtaining an effective theory we can work with. In particular, we are interested in supersymmetric compactifications in order to find a $\mathcal{N} = 1$ supergravity potential, which is the most interesting one from a phenomenological point of view. Indeed, in general the low energy limit gives origin to supersymmetric theories in which supersymmetry is broken, for instance supergravity with $\mathcal{N} = 8$, $\mathcal{N} = 2$ or $\mathcal{N} = 1$.

In relevant models for cosmology, the ten-dimensional space is assumed to be factorized as

$$\mathcal{M}_{10} = \mathcal{M}_4 \times Y_6, \quad (2.1)$$

where \mathcal{M}_4 is the Minkowski space-time and Y_6 is a compact Calabi-Yau three-fold, which is typically compactified at low energies. This specific choice is justified by the fact that with this manifold we can recover a 4D $\mathcal{N} = 2$ supergravity, which can be further reduced to $\mathcal{N} = 1$. In this case the line element (ignoring possible warping) can be written as

$$ds^2 = G_{MN}dX^M dX^N = g_{\mu\nu}dx^\mu dx^\nu + \hat{g}_{mn}dy^m dy^n, \quad (2.2)$$

where y^m , $m = 1, 2, \dots, 6$ are coordinates on Y_6 and \hat{g}_{mn} is a metric on it. In general, the theory does not provide a specific choice for the internal space Y_6 . Its form has to be determined in order to match observations and we can be guided by cosmology and particle physics to gather an ansatz for the structure of the manifold.

We sketch here the idea of dimensional reduction, following [6]. To compute the four-dimensional effective action we begin with the ten-dimensional Einstein-Hilbert action

$$S_{EH}^{10} = \frac{M_s^8}{2} \int d^{10}X \sqrt{G} \mathcal{R}_{10}, \quad (2.3)$$

where M_s is the string scale, G is the modulus of the determinant of the metric G_{MN} and \mathcal{R}_{10} is the ten-dimensional Ricci scalar constructed from G_{MN} . The next step consists into performing a Kaluza-Klein reduction (i.e. considering the low energy limit below the Kaluza-Klein scale M_{KK}), noting that in this case the integral can be factorized as

$$S_{EH}^{10} = \frac{M_s^8}{2} \int d^6y \sqrt{\hat{g}} \int d^4x \sqrt{g} \mathcal{R}_4, \quad (2.4)$$

where $g = |\det g_{\mu\nu}|$, $\hat{g} = |\det \hat{g}_{mn}|$ and \mathcal{R}_4 is the usual Ricci scalar in four dimensions. The volume of the internal space is given by

$$\text{Vol}(Y_6) = \int_{Y_6} d^6y \sqrt{\hat{g}} \equiv \mathcal{V} l_s^6, \quad (2.5)$$

where $l_s = 2\pi\sqrt{\alpha'}$ is the string length and $\frac{1}{2\pi\alpha'}$ is the string tension. The string length is linked to the string mass scale M_s by $l_s = \frac{1}{M_s}$.

To recover the Einstein-Hilbert action in four dimension

$$S_{EH}^4 = \frac{M_P^2}{2} \int d^4x \sqrt{g} \mathcal{R}_4, \quad (2.6)$$

is immediate to make the identification

$$M_s \sim \frac{M_P}{\sqrt{\mathcal{V}}}. \quad (2.7)$$

where the volume is intended in string length units ($l_s = 1$). The value of M_s is smaller than M_P and we need $\mathcal{V} \gg 1$. Beside this, we can also put an upper bound given the fact that up to now LHC did not find any hint of new physics above 1 TeV; thus, the volume should be $\mathcal{V} \ll 10^{30}$ [9].

We can now also estimate the Kaluza-Klein scale considering that it has to be the scale for which lengths are bigger than the Calabi-Yau characteristic dimension

$$M_{KK} \sim \frac{1}{(\text{Vol}(Y_6)^{1/6})} \sim \frac{1}{\mathcal{V}^{1/6} l_s} \sim \frac{M_s}{\mathcal{V}^{1/6}} \sim \frac{M_P}{\mathcal{V}^{2/3}}. \quad (2.8)$$

Referring to M_s , the low energy limit gives rise to a ten-dimensional type IIB supergravity with $\mathcal{N} = 2$ whose field content is given by the massless degrees of freedom of string theory. To compactify the extra dimensions is necessary to go below M_{KK} , as we did in the above example. For the sake of simplicity, from now on we will work in Planck units $M_P = 1$, unless otherwise specified.

2.2.1 Moduli

After Calabi-Yau compactifications, we are left with lots of different type of moduli, which are neutral scalar fields gravitationally coupled to matter fields through Planck-suppressed interactions. In this section we will show the connection of these fields with the geometry of the considered manifold.

We have already mentioned that the simplest compactification with Calabi-Yau manifold leads to a $\mathcal{N} = 2$ supergravity theory. We then exploit this feature in order to outline where the moduli come from; we will focus exclusively on them, as the other forms and additional scalar fields of the theory do not directly appear in this thesis.

Once we get a 4D effective theory, we can basically distinguish three kind of moduli fields:

- *axio-dilaton* $S = e^{-\Phi} + iC_0$, where C_0 is an axion-like field and Φ is a field called *dilaton*, whose VEV fixes the string coupling $e^{-\langle \Phi \rangle} = 1/g_s$;
- *complex structure moduli* ζ^A , which parametrize the shape of internal space and arise from deformations of the complex structure on Y_6 , which may be written as

$$\delta g_{ij} = \frac{i}{\|\Omega\|^2} \zeta^A(x) (\chi_A)_{i\bar{j}\bar{k}} \Omega^{\bar{j}\bar{k}}_j \quad (2.9)$$

where χ_A represents a set of harmonic (1,2)-forms, $A = 1, 2, \dots, h^{1,2}$ ($h^{1,2}$ is a Hodge number, thus in this case the dimension of the Dolbeault cohomology group $H^{1,2}$) and $\Omega = \Omega_{ijk} dz^i \wedge dz^j \wedge dz^k$ is the holomorphic (3,0)-form of Y_6 , $\|\Omega\|^2 = \frac{1}{3!} \Omega_{ijk} \bar{\Omega}^{ijk}$;

- *Kähler moduli* t^I , which are deformations of the Kähler form

$$J = i g_{i\bar{j}} dz^i \wedge \bar{z}^{\bar{j}}, \quad (2.10)$$

which can be parametrized by a set of harmonic (1,1)-forms \hat{D}^I , $I = 1, 2, \dots, h^{1,1}$ ($h^{1,1}$ is a Hodge number, thus in this case the dimension of the Dolbeault cohomology group $H^{1,1}$), as

$$J = t^I(x) \hat{D}_I. \quad (2.11)$$

Let us now turn to the most interesting case. In order to finally obtain an acceptable phenomenological model, it is possible to introduce an *orientifold projection* \mathcal{O} which breaks the $\mathcal{N} = 2$ supersymmetry into a $\mathcal{N} = 1$ supersymmetry. These type of compactifications typically include non-trivial background fluxes and local sources such as D-branes.

Under the orientifold action the cohomology groups split into

$$H^{p,q} = H_+^{p,q} \oplus H_-^{p,q}, \quad (2.12)$$

where the subscripts denote the parity of the forms under orientifold action. Consequently, also the basis for $H^{1,1}$ and $H^{1,2}$ decompose into basis for an even and an odd space.

The Kähler form can be written as

$$J = t^i(x) \hat{D}_i, \quad i = 1, 2, \dots, h_+^{1,1}, \quad (2.13)$$

where as before t^i are the Kähler moduli, which measure the volume of two-cycles that are even under the involution \mathcal{O} . In the same way, the complex structure moduli are ζ^α , $\alpha = 1, 2, \dots, h_-^{1,2}$, whereas Φ and C_0 are automatically invariant under the orientifold action.

Now we can further discuss this last framework. We begin noticing that the compactification volume can now be written with the help of the Kähler form as

$$\mathcal{V} = \frac{1}{3!} \int_{Y_6} J \wedge J \wedge J = \frac{1}{3!} t^i t^j t^k \int_{Y_6} \hat{D}_i \wedge \hat{D}_j \wedge \hat{D}_k \equiv \frac{1}{3!} c_{ijk} t^i t^j t^k, \quad (2.14)$$

where c_{ijk} are the triple intersection numbers of Y_6 .

The fields entering the $\mathcal{N} = 1$ chiral multiplets are the complexified Kähler moduli

$$T_i = \tau_i + i\theta_i, \quad (2.15)$$

where τ_i is a four-cycle and θ_i is its axion-like partner, i.e. a pseudoscalar field with Peccei-Quinn shift symmetries of the form $\theta_i \mapsto \theta_i + \text{const.}$

The four-cycle volumes are related to the two-cycle volumes by

$$\tau_i = \frac{\partial \mathcal{V}}{\partial t^i} = \frac{1}{2} \int_{Y_6} \hat{D}^i \wedge J \wedge J = \frac{1}{2} c_{ijk} t^j t^k. \quad (2.16)$$

2.3 Moduli stabilization

As we have seen, moduli are zero-energy deformations arising from the geometrical properties of the Calabi-Yau manifold. All of them are characterized by a vanishing potential at some level of approximation; some of them have exactly vanishing potential before supersymmetry breaking, while others have vanishing classical potential but acquire mass thanks to quantum effects. In order to describe cosmological evolution it is fundamental to understand the dynamics of these scalar fields.

A first task is then to find vacua in which all moduli have positive mass-squared. This operation is extremely important, as moduli VEVs determine fundamental quantities such as coupling constants, and allows us to build realistic models. Furthermore, we know that moduli cannot be massless, otherwise they would originate a fifth force and we would have already observed them. This technique goes under the name of *moduli stabilization*.

Let us now list the fundamental functions of the supersymmetric effective theory. After having compactified the Calabi-Yau manifold in order to obtain a 4D $\mathcal{N} = 1$ supergravity, we can write the corresponding Kähler potential and superpotential. At leading order in the α' and string loop expansions, the Kähler potential is

$$K_0 = -2 \log(\mathcal{V}) - \log(S + \bar{S}) - \log \left(-i \int \Omega \wedge \bar{\Omega} \right), \quad (2.17)$$

where the holomorphic three-form Ω of the Calabi-Yau manifold depends on the complex structure moduli ζ_α and the volume depends on the Kähler moduli T_i .

The tree level (flux-induced) superpotential is

$$W_0 = \frac{c}{\alpha'} \int G_3 \wedge \Omega, \quad (2.18)$$

where c is a constant and G_3 is a three-form flux. The superpotential is independent from the Kähler moduli since $G_3 \equiv G_3(S)$ depends only on the axio-dilaton and $\Omega \equiv \Omega(\zeta)$; thus we can write $W_0 = W_0(S, \zeta)$.

The scalar potential associated with K_0 and W_0 is then

$$V_F^0 = e^{K_0} \left[K_0^{I\bar{J}} D_I W_0 \overline{D_{\bar{J}} W_0} - 3|W_0|^2 \right], \quad (2.19)$$

where the indexes I, J run over all the moduli $(T_i, \zeta_\alpha, \tau)$. The Kähler potential in (2.17) satisfies the *no-scale condition*

$$\sum_{I, J=T_i} K_0^{I\bar{J}} D_I W_0 \overline{D_{\bar{J}} W_0} = 3 \quad (2.20)$$

and the scalar potential (2.19) reduces to

$$V_F^0 = e^{K_0} \sum_{I, J \neq T_i} K_0^{I\bar{J}} D_I W_0 \overline{D_{\bar{J}} W_0}; \quad (2.21)$$

this property is the so called *no-scale structure*. Since the superpotential (2.18) is independent of the Kähler moduli, the scalar potential is now independent from the F-terms of the Kähler moduli.

At tree level the potential is positive semi-definite and the minimum is then $V_{F, min}^0 = 0$, which implies

$$D_S W_0 = 0, \quad D_{\zeta_\alpha} W_0 = 0. \quad (2.22)$$

Hence, the axio-dilaton and the complex structure moduli can be stabilized at tree level solving these equations. In particular, as mentioned before, we obtain $Re(\langle S \rangle) = e^{-\langle \Phi \rangle} = 1/g_s$; it is fundamental to stabilize the dilaton in order to have $g_s \ll 1$. In this case, from (1.57) it is immediate to recognize that the global minimum is supersymmetric as long as $D_{T_i} W_0 = 0$.

In order to stabilize Kähler moduli we then need to consider perturbative and non-perturbative corrections to the tree level potential, which break the no-scale symmetry, lifting or destabilizing the flat directions and altering the vacuum energy.

2.3.1 Perturbative corrections

The Kähler potential receives corrections order by order in α' and string loop expansions

$$K = \delta K_{\alpha'} + \delta K_{g_s}; \quad (2.23)$$

there are also non-perturbative effects that we can safely ignore as they are subdominant compared to above corrections.

If we neglect string loop contributions (see [10] and [11] for discussions on these terms), we are left with $\delta K_{\alpha'}$, where α' corrections descend from an $(\alpha')^3$ curvature correction in ten dimensions. If we stabilized at tree level the dilaton and the complex structure moduli with the help of (2.22) we get

$$K = K_{cs} - 2 \ln \left[\mathcal{V} + \frac{\xi}{2} \right], \quad K_{cs} = \left\langle \log \left(-i \int \Omega \wedge \bar{\Omega} \right) \right\rangle \quad (2.24)$$

where

$$\xi = - \frac{\chi(Y_6) \zeta(3)}{2(2\pi)^3 g_s^{3/2}}, \quad (2.25)$$

$\chi(Y_6)$ is the Euler characteristic of the manifold Y_6 and $\zeta(3) \approx 1.202$ is Apéry's constant. The α' -corrected Kähler potential no more satisfy the no-scale condition (2.20) unless $\chi(Y_6) = 0$.

It is important to notice that α' -correction is an expansion in inverse volume which can be controlled only at large volume.

The leading contribution to the potential is

$$\delta V_{\alpha'} = 3\xi e^K \frac{(\xi^2 + 7\xi\mathcal{V} + \mathcal{V}^2)}{(\mathcal{V} - \xi)(2\mathcal{V} + \xi)^2} W_0^2 \simeq \frac{3}{4} e^K \frac{\xi W_0^2}{\mathcal{V}} \simeq \frac{3}{4} \frac{\xi W_0^2}{\mathcal{V}^3}, \quad (2.26)$$

where we assumed $K_{cs} \simeq 0$.

2.3.2 Non-perturbative corrections

Unlike the Kähler potential, the superpotential receives no corrections in α' or g_s . Due to the non-renormalization theorem its first corrections arise non-perturbatively and the general form of the corrected superpotential is

$$W = W_0 + W_{np} = W_0 + \sum_{i=1}^{h_+^{1,1}} A_i e^{-a_i T_i}, \quad (2.27)$$

where the coefficients A_i are independent from all the Kähler moduli, but generally depends on the complex structure moduli and on D-brane positions. In particular, such terms can be generated from gaugino condensation in supersymmetric gauge theories located on D7-branes wrapping 4-cycles or from Euclidean D3-branes (also wrapping 4-cycles). In particular, in the first case $a_i = \frac{2\pi}{N}$ (for a $SU(N)$ gauge theory), whereas in the second $a_i = 2\pi$.

Let us now compute the non-perturbative contribution to the scalar potential. For an arbitrary Kähler potential, from (1.55) and (2.27) we get

$$V_{np} = e^K K^{i\bar{j}} \left[a_i A_i a_{\bar{j}} \bar{A}_{\bar{j}} e^{-(a_i T_i + a_{\bar{j}} \bar{T}_{\bar{j}})} - \left(a_i A_i e^{-a_i T_i} \bar{W} \partial_{\bar{j}} K + a_{\bar{j}} \bar{A}_{\bar{j}} e^{-a_{\bar{j}} \bar{T}_{\bar{j}}} W \partial_i K \right) \right]. \quad (2.28)$$

2.4 The Large Volume Scenario

We now turn to investigate whether the new potential corrected with (2.24) and (2.27) presents metastable vacua even though the classical theory has unstabilized Kähler moduli.

In general, leading-order corrections create an instability in the potential, which drives the theory either towards extremely large or extremely small values of the volume, depending on the situation. A metastable vacuum can arise only considering higher-order corrections which can counterbalance the instability generated by leading corrections. Unfortunately, such corrections are in general not known and stabilization may not be an easy task.

However, there exist (at least) two mechanisms which can achieve moduli stabilization exploiting competition among known correction terms; these are known as Large Volume Scenario (LVS) and KKLT scenario. In this section we briefly discuss the LVS as it provides the framework in which the model we will study in chapter 4 is embedded. For a more general discussion see [12].

The LVS allows to obtain Kähler moduli stabilization by balancing the leading α' correction of the corrected Kähler potential (2.24) against the non-perturbative superpotential (2.27). This approach is particularly useful as it allows to stabilize the volume modulus \mathcal{V} at large values; this assures us that we can neglect the unknown α' and g_s corrections, which are subleading compared to (2.24). In particular, this procedure originate a non-supersymmetric AdS minimum at exponentially large volume.

The first thing to do, in analogy with the KKLT scenario, is to integrate out the complex structure moduli: we stabilize the dilaton and complex structure moduli by solving (2.22), as was already suggested. We now can put together the α' -corrected Kähler potential (2.24) and the superpotential (2.27) in order to find the full scalar potential, which depends only on the Kähler moduli

$$V_F = V_{np} + \delta V_{\alpha'} \simeq e^K \left\{ K^{i\bar{j}} [(\partial_i W)(\overline{\partial_j W}) + (\overline{W}(\partial_i W)(\partial_{\bar{j}} K) + W(\overline{\partial_j W})(\partial_i K))] + \frac{3}{4} \frac{\xi W_0^2}{\mathcal{V}} \right\}, \quad (2.29)$$

where we used the large volume limit $\mathcal{V} \gg 1$. Actually, these perturbations generate also a small shift in the minimum of the other fields, namely $D_S W \sim D_{\zeta\alpha} W \sim \mathcal{O}(\mathcal{V}^{-1})$, whose role is analyzed for example in [13]. However, this shift is small and we can regard their values as fixed.

In the following discussion we consider cases with $\xi > 0$ ($\chi(Y_6) < 0$), which is equivalent to have more complex structure moduli than Kähler moduli, as $\chi(Y_6) = 2(h^{1,1} - h^{2,1})$.

In order to distinguish different terms whose combination can generate a metastable vacuum, we first note that the non-perturbative contribution to the potential (2.28) can be splitted into $V_{np} = V_{np1} + V_{np2}$, where

$$V_{np1} = e^K K^{i\bar{j}} ((\partial_i W)(\overline{\partial_j W})), \quad (2.30)$$

$$V_{np2} = e^K K^{i\bar{j}} (\overline{W}(\partial_i W)(\partial_{\bar{j}} K) + W(\overline{\partial_j W})(\partial_i K)). \quad (2.31)$$

In order to achieve stabilization, the authors of [12] assume the presence of several real moduli $\tau_i = Re(T_i)$ which satisfy

$$\tau_i \rightarrow \infty \quad \text{for} \quad \mathcal{V} \rightarrow \infty, \quad (2.32)$$

which is the decompactification limit (in which the corrections to the tree level potential must vanish), and of small modulus τ_s for which this condition does not hold. They also argue that the first limit must be well-defined and that τ_s must appear non-perturbatively in W , whereas this is not necessary for “big” moduli. In order to achieve competition between $\delta K_{\alpha'}$, V_{np1} and V_{np2} the small modulus has to behave like

$$a_s \tau_s = \ln \mathcal{V} \quad \text{for} \quad \mathcal{V} \rightarrow \infty. \quad (2.33)$$

Indeed, with this requirement all the three terms are of the same order in $1/\mathcal{V}$. At large volume the dominant one is the negative contribution of V_{np2} , as we will see in a moment, and thus the potential approaches zero from below. Hence, if such assumptions are suitable to achieve stabilization, the minimum they generate must be AdS.

A more general analysis [14] shows that we can choose a Calabi-Yau with several “big” and “small” moduli such that at the large volume limit

$$\begin{cases} \tau_i \text{ remains small } \forall i = 1, 2, \dots, N_{small} \\ \tau_j \rightarrow \infty, \forall j = N_{small} + 1, \dots, h_{1,1}, \end{cases} \quad (2.34)$$

with a superpotential whose non-perturbative corrections depend only on the small moduli

$$W = W_0 + \sum_{i=1}^{N_{small}} A_i e^{-a_i T_i}. \quad (2.35)$$

In this case the scalar potential admits a set of a AdS non-supersymmetric minima at exponentially large volume located at $\mathcal{V} \sim e^{a_i \tau_i}$, $\forall i = 1, 2, \dots, N_{small}$ if and only if $\xi > 0$ and τ_i is a local blow-up mode resolving a given point-like singularity $\forall i = 1, 2, \dots, N_{small}$.

It can also be shown that τ_i is the only blow-up mode resolving a point-like singularity if and only if $K^{ii} \sim \mathcal{V} \sqrt{\tau_i}$. If the singularity is resolved by more than one blow-ups the structure of K^{ii} is more general, see again [14].

Let us now study a very simple case which enlightens the above idea in a straightforward way and clarifies some of the statements we made. We can assume the simplest possible form for the Calabi-Yau which satisfies the requirements (2.34)

$$\mathcal{V} = \tau_b^{3/2} - \tau_s^{3/2}. \quad (2.36)$$

Using the results of appendix A.2, we can compute the non-perturbative contributions in the large volume limit $\mathcal{V} \sim \tau_b^{3/2} \gg 1$ using the superpotential $W = W_0 + A_s e^{-a_s T_s}$ as in (2.35). For simplicity we assume that both W_0 and A_s are real. For V_{np1} we find

$$V_{np1} = e^K K^{ss} ((\partial_i W)(\bar{\partial}_j \bar{W})) \simeq \frac{8}{3} \frac{e^{K_{cs}}}{\mathcal{V}} \sqrt{\tau_s} a_s^2 A_s^2 e^{-2a_s \tau_2}. \quad (2.37)$$

To compute V_{np2} we need to be more careful. Recalling $\frac{\partial}{\partial T_s} = \frac{1}{2} \frac{\partial}{\partial \tau_s}$ we have

$$\begin{aligned}
V_{np2} &= + e^K K^{ss} (\overline{W}(\partial_s W)(\partial_s K) + W(\overline{\partial_s W})(\partial_s K)) \\
&\quad + e^K K^{sb} (\overline{W}(\partial_s W)(\partial_b K) + W(\overline{\partial_b W})(\partial_s K)) \\
&\quad + e^K K^{bs} (\overline{W}(\partial_b W)(\partial_s K) + W(\overline{\partial_s W})(\partial_b K)) \\
&\simeq - \frac{e^{K_{cs}}}{\mathcal{V}^2} K^{ss} \frac{3}{2\mathcal{V}} \sqrt{\tau_s} \left(a_s A_s W_0 (e^{-a_s T_s} + e^{-a_s \overline{T}_s}) \right) \\
&\quad + e^K K^{sb} (\partial_b K) (\overline{W}(\partial_s W) + W(\overline{\partial_s W})) \\
&\simeq - 8 \frac{e^{K_{cs}}}{\mathcal{V}^2} \tau_s a_s A_s W_0 e^{-a_s \tau_s} \cos(a_s \theta_s) \\
&\quad + 12 \frac{e^{K_{cs}}}{\mathcal{V}^2} \tau_s a_s A_s W_0 e^{-a_s \tau_s} \cos(a_s \theta_s) \\
&\simeq + 4 \frac{e^{K_{cs}}}{\mathcal{V}^2} \tau_s a_s A_s W_0 e^{-a_s \tau_s} \cos(a_s \theta_s),
\end{aligned}$$

where we discarded the terms $e^{-2a_s \tau_s}$. Finally, the total potential looks like

$$V_F \simeq e^{K_{cs}} \left[\frac{8}{3} \frac{1}{\mathcal{V}} a_s^2 A_s^2 \sqrt{\tau_s} e^{-2a_s \tau_2} + 4 \frac{1}{\mathcal{V}^2} A_s W_0 a_s \tau_s e^{-a_s \tau_s} \cos(a_s \theta_s) + \frac{3}{4} \frac{\xi W_0^2}{\mathcal{V}^3} \right]. \quad (2.38)$$

In order to approach zero from below and generate a minimum we can act on axion fields, minimizing them setting $\theta_s = n \frac{2\pi}{a_s}$; we obtain

$$V_F \simeq e^{K_{cs}} \left[\frac{8}{3} \frac{1}{\mathcal{V}} a_s^2 A_s^2 \sqrt{\tau_s} e^{-2a_s \tau_2} - 4 \frac{1}{\mathcal{V}^2} A_s W_0 a_s \tau_s e^{-a_s \tau_s} + \frac{3}{4} \frac{\xi W_0^2}{\mathcal{V}^3} \right]. \quad (2.39)$$

From this final expression it is evident that $V > 0$ for small values of \mathcal{V} ; on the contrary, using (2.33) we then see that at large volume the potential is negative

$$\begin{aligned}
V &\sim e^{K_{cs}} \left[\frac{8}{3} \frac{1}{\mathcal{V}^3} a_s^{3/2} A_s^2 \sqrt{\ln \mathcal{V}} - 4 \frac{1}{\mathcal{V}^3} A_s W_0 \ln \mathcal{V} + \frac{3}{4} \frac{\xi W_0^2}{\mathcal{V}^3} \right] \\
&\sim - 4 \frac{1}{\mathcal{V}^3} A_s W_0 \ln \mathcal{V},
\end{aligned} \quad (2.40)$$

and thus $V < 0$ for $\mathcal{V} \rightarrow \infty$. It is then immediate to gather that it must exist at large volume an AdS minimum, as we stated previously. The form of the potential is sketched in figure 2.1.

We point out that this example explains correctly the idea of the article [12], where the authors assume more in general the presence of several big moduli and just one small modulus, deriving the most general potential

$$V_F \sim \left[\frac{1}{\mathcal{V}} a_s^2 |A_s|^2 (-c_{ssk} t^k) e^{-2a_s \tau_s} - \frac{1}{\mathcal{V}^2} a_s \tau_s e^{-a_s \tau_s} |A_s W| + \frac{\xi}{\mathcal{V}^3} |W|^2 \right]. \quad (2.41)$$

2.4.1 Uplift

Now that we have found a global AdS stable minimum, it is necessary to uplift it to account for a dS vacuum, in order to give a realistic description of our universe. Indeed, to describe inflation

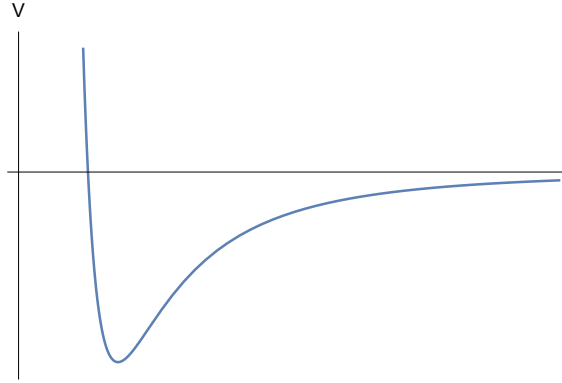


Figure 2.1: Typical behavior of the potential after LVS stabilization.

in the early universe and dark energy in the late universe we need vacua with positive energy. In particular, in order to reproduce the vacuum of our present epoch the global minimum of the potential has to be approximately Minkowskian. This is not always an easy task in string theory, as dS vacua are more susceptible to instabilities.

Common mechanisms to generate such term rely on addition of anti-D3 branes or on the presence of magnetic fluxes on D7-branes. In general, the uplift can be parametrized by

$$V_{up} = \frac{D}{\mathcal{V}^\gamma}, \quad (2.42)$$

where $D > 0$ and γ depends on the specific mechanism generating this term and typically takes values in the range $1 \leq \gamma \leq 3$. The new behavior of the total potential

$$V^{tot} = V + V_{up}$$

is represented in figure 2.2.

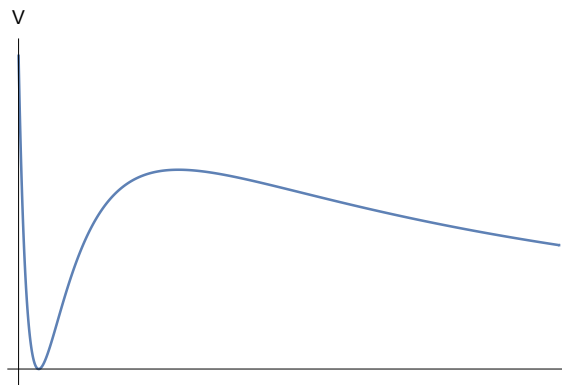


Figure 2.2: Plot of the potential with inclusion of the uplift term V_{up} and with a nearly Minkowskian minimum.

3.1 Inflation

After the development of Einstein's General Relativity, lots of scientists tried to apply this theory to the study of the dynamical structure of the entire universe. In order to study the large scale structure, it is convenient to think about the universe as a fluid where galaxies constitute its particles.

Apart from this assumption, cosmology is based on three principles:

- General Relativity alone is sufficient to describe the large scale features of the universe;
- the motion of the galaxies is governed only by gravitational forces generated by the galaxies themselves; this is the *Weyl's principle*, which in other words states that the world lines of galaxies form a spacetime-filling family of non-intersecting geodesics (which we can consider as “fluid lines”) converging towards the past;
- the universe is the same in any point of the space (homogeneous) and symmetric in any point of the space (isotropic); this is the so called *cosmological principle*.

In particular, the last hypothesis implies that there is no privileged observation point and that the universe appears the same in every place. In addition, it also tells us that the universe must be described by a constant curvature space. From these assumptions we can work out the line element ds^2 for an expanding universe, finding the famous Friedmann-Robertson-Walker (FRW) metric

$$ds^2 = dt^2 - a^2(t) \left[\frac{dr^2}{1 - kr^2} + r^2(d\theta^2 + \sin^2\theta d\phi^2) \right], \quad (3.1)$$

where (r, θ, ϕ) are radial coordinates, k takes into account the geometry for a constant curvature space ($k = 0$ flat, $k = 1$ spherical and $k = -1$ hyperbolic) and $a(t)$ is the scale factor.

Solving Einstein equations we can find the dynamics of the scale factor, which contains all the information on the universe expansion thanks to the homogeneity and isotropy assumptions. In

particular, we obtain the system of equations

$$\begin{cases} 3\ddot{a} = -4\pi G(\rho + 3p)a \\ a\ddot{a} + 2\dot{a}^2 + 2k = 4\pi G(\rho - p)a^2 \end{cases}, \quad (3.2)$$

and combining them we are lead to the Friedmann equation

$$\dot{a}^2 + k = \frac{8\pi G}{3}\rho a^2, \quad (3.3)$$

where p is a pressure term and ρ is the energy density as usual.

Fundamental observational facts strongly suggest that our universe is spatially flat on large scale and that it is then well described by FRW metric with $k = 0$. To better discuss the causal structure of the FRW spacetime it is convenient to write the metric in term of the conformal time τ

$$ds^2 = a^2(\tau) [d\tau^2 - d\mathbf{x}^2], \quad (3.4)$$

such that the distance that a particle can travel in $\Delta\tau$ is simply $|\Delta\mathbf{x}| = \Delta\tau$ (*comoving distance*).

Let us now discuss some features of standard Big Bang cosmology. We begin introducing the concept of *cosmological horizon*. Imagine a signal emitted at the moment of Big Bang ($t = 0$) which travels at the speed of light since then: we can ask what is the distance $l_H(t)$ that such signal covers from the point of its emission after a time $t > 0$. $l_H(t)$ represents the size of the region causally connected by the time t . This means that an observer living at time t cannot know in principle what has happened outside the sphere of radius $l_H(t)$ and therefore this sphere represents the observable part of the universe at time t . This sphere is the so called *cosmological horizon*; $l_H(t)$ increases in time and the horizon opens up.

If we choose the coordinates in order to have the initial singularity at $t = 0$, then the maximum comoving distance that a particle can travel at $t > 0$ since that moment is given by

$$\Delta\tau = \int_0^t \frac{dt'}{a(t')} = \int_0^t \frac{1}{\dot{a}} \frac{\dot{a}}{a} dt' = \int_0^a \frac{1}{aH} d \ln a, \quad H \equiv \frac{\dot{a}}{a}. \quad (3.5)$$

and the physical size is

$$l_H(t) = a(t)\Delta\tau = a(t) \int_0^t \frac{dt'}{a(t')}. \quad (3.6)$$

For example, if the universe was matter dominated, we would have $a(t) \propto t^{2/3}$, $H(t) = 2/(3t)$ and then $l_H(t) = 3t = 2/H(t)$ and the size of the horizon today would be $l_{H_0} = 2/H_0 \simeq 2.6 \times 10^{28}$ cm. Hence, in model with cosmological horizon the observable region has a finite size even if the universe is infinite. For further details and discussion see for example [15].

In standard Big Bang cosmology the expansion of the universe is driven by the energy density of radiation; from (3.2) it is evident that $\ddot{a} < 0$ and that at sufficient early times $a \rightarrow 0$ and the metric becomes singular. Therefore, during standard Big Bang evolution the comoving radius $(aH)^{-1} = (\dot{a})^{-1}$ grows with time and the integral (3.5) is dominated by the contributions from late times. This fact implies that the amount of conformal time between singularity and the formation of the cosmic microwave background (CMB) is much smaller than the time between CMB formation and today. This generates a serious problem: CMB is experimentally found to be the same in every direction (to one part in 10^4), but according to standard Big Bang evolution photons coming from different regions of the universe were never in causal contact.

More precisely, it can be calculated that CMB separated by more than one degree were never in causal contact. This is the so called *horizon problem*.

This situation is illustrated in figure (3.1), from which it is clear that in standard Big Bang theory the light cones of CMB do not overlap.

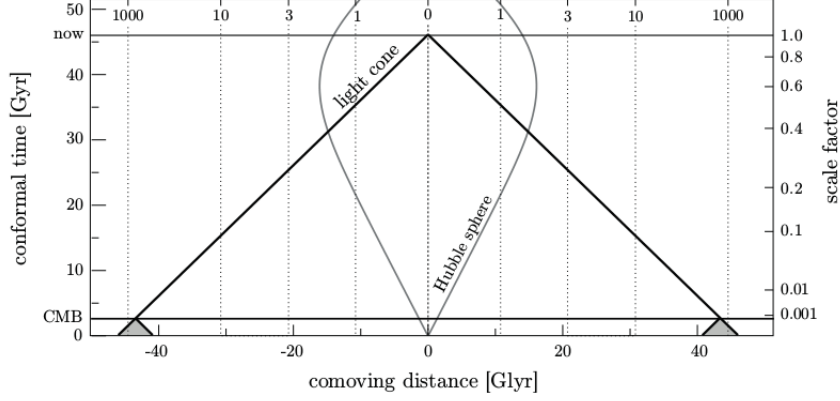


Figure 3.1: Illustration of the horizon problem in comoving coordinates. All the events that we observe (we are the central dotted worldline) are in our past light cone. At time of CMB formation it can be seen that photons coming from opposite regions were never in causal contact, as their light cones (shaded in gray) never cross.

In other words, we can say that the horizon problem is due to the fact that universe expands slowly, so an observer see more and more regions that have never been in causal contact. We can perform some simple calculations exploiting this consideration. At time t_1 the size of a causally connected region is given by

$$l_{H_1} = a(t_1)\Delta\tau = a(t_1) \int_0^{t_1} \frac{dt'}{a(t')}, \quad (3.7)$$

and due to cosmological expansion this very same region at time t_0 is stretched to

$$l_{H_1}(t_0) = \frac{a(t_0)}{a(t_1)}l_{H_1} = a(t_0)\Delta\tau = a(t_0) \int_0^{t_1} \frac{dt'}{a(t')}. \quad (3.8)$$

We can now compare this last expression with the present horizon size l_{H_0}

$$\frac{l_{H_0}}{l_{H_1}(t_0)} = \frac{\int_0^{t_0} \frac{dt'}{a(t')}}{\int_0^{t_1} \frac{dt'}{a(t')}} = \frac{\int_0^{a_0} \frac{da}{a^2 H}}{\int_0^{a_1} \frac{da}{a^2 H}} \simeq \frac{a(t_1)H(t_1)}{a(t_0)H(t_0)}; \quad (3.9)$$

since with matter domination we have $a \propto t^{2/3}$ and $H \propto t^{-1}$, then $aH \propto a^{-1/2}$ and we can rewrite

$$\frac{l_{H_0}}{l_{H_1}(t_0)} = \sqrt{\frac{a(t_0)}{a(t_1)}} = \sqrt{1+z(t_1)}, \quad (3.10)$$

where $z(t_1)$ is the redshift parameter. If we take $t_1 = t_r$, which is the time of recombination, $z(t_r) = 1100$ and

$$\frac{l_{H_0}}{l_{H_1}(t_0)} \simeq 35, \quad (3.11)$$

which implies that the size of the region linked to recombination is around 35 times smaller than the present horizon size. In other words, in Hot Big Bang theory the universe visible at present contain about 35^3 regions that were causally disconnected by recombination.

In order to address the horizon problem, we may imagine that the comoving Hubble radius $(aH)^{-1}$ was decreasing in early universe, so that (3.5) is dominated by the contributions from times very close to the moment of the Big Bang. This add an extra time between the singularity and the CMB formation (and conformal time extends to negative values) and if this period of decreasing comoving Hubble radius is sufficiently long all the points in the CMB originate from a causally connected region of space.

Therefore, to solve this problem we can postulate a period of expansion called *inflation*. According to the inflationary theory, the Hot Big Bang epoch is preceded by an inflationary epoch of accelerated cosmological expansion. At the end of that, the energy density varies slowly in time and the universe expands and becomes homogeneous, isotropic and spatially flat.

We can mathematically translate the requirement of decreasing comoving Hubble radius as

$$\frac{d}{dt}(aH)^{-1} = -\frac{1}{a} \left[\frac{\dot{H}}{H^2} + 1 \right] < 0 \quad (3.12)$$

and introducing the Hubble slow-roll parameters

$$\epsilon \equiv -\frac{\dot{H}}{H^2}, \quad \tilde{\eta} = \frac{\dot{\epsilon}}{H\epsilon} \quad (3.13)$$

we can equivalently require $\epsilon < 1$; this last will be our definition of inflation. In the limit $\epsilon \rightarrow 0$ we found a de Sitter solution

$$a(t) \propto e^{Ht}, \quad (3.14)$$

with $H \simeq \text{const}$, which tell us that the space grows exponentially.

Using H and M_P , we can rewrite the Friedmann equations from (3.2) and (3.3) as

$$\begin{cases} 3M_P^2 H^2 = \rho \\ 6M_P^2 (\dot{H} + H^2) = -(\rho + 3P) \end{cases} \quad (3.15)$$

Working out the above system of equations, we obtain

$$\epsilon = \frac{3}{2} \left(1 + \frac{P}{\rho} \right); \quad (3.16)$$

hence, during inflation $P < -\frac{1}{3}\rho$ and a possible energy source is a positive potential energy density of a scalar field with negligible kinetic energy.

3.1.1 Cosmological perturbations

Inflationary theory is very promising as it not only explains the homogeneity of the universe, but also take into account the primordial inhomogeneities necessary to explain the structure formation.

In this section we will briefly recall some expressions of observables (derived from the treatment

of primordial fluctuations) that will be present in the model we will study in the next chapter; we refer to [6] for further details.

The power spectrum of primordial curvature perturbations is given by

$$\mathcal{P}_{\mathcal{R}}(k) \equiv |\mathcal{R}_k|^2 = \frac{1}{4} \frac{H^4}{M_P^2 |\dot{H}| c_s k^3}, \quad (3.17)$$

together with the dimensionless power spectrum

$$\Delta_{\mathcal{R}}^2 \equiv \frac{k^3}{2\pi^2} \mathcal{P}_{\mathcal{R}}(k) = \frac{1}{8\pi^2} \frac{H^4}{M_P^2 |\dot{H}| c_s}. \quad (3.18)$$

The right-hand side is supposed to be evaluated at horizon crossing, where $c_s k = aH$. In standard model of cosmology, the power spectrum is assumed to behave as

$$\Delta_{\mathcal{R}}^2(k) = A_s \left(\frac{k}{k_*} \right)^{n_s - 1}, \quad (3.19)$$

where n_s is the spectral index that can be found from

$$n_s = 1 + \frac{d \ln \Delta_{\mathcal{R}}^2}{d \ln k} = -2\epsilon - \tilde{\eta} - \kappa, \quad (3.20)$$

where

$$\kappa \equiv \frac{\dot{c}_s}{H c_s}. \quad (3.21)$$

One of the cleanest predictions of inflation is a (dimensionless) spectrum of primordial gravitational waves, which is given by

$$\Delta_h^2(k) \equiv \frac{k^3}{2\pi^2} P_h(k) = \frac{2}{\pi^2} \frac{H^2}{M_P^2}, \quad (3.22)$$

where the right-hand side is evaluated at horizon crossing $k = aH$.

For observational purposes it is useful to define tensor modes with the help of the tensor-to-scalar ratio

$$r = \frac{\Delta_h^2}{\Delta_{\mathcal{R}}^2}, \quad (3.23)$$

as the amplitude of scalar fluctuations can be easily measured.

3.1.2 Slow-roll model

We give here a brief overview of a general *slow-roll model*, which can be used to describe inflation. We are presenting a very simple toy model in order to enlighten the physical idea behind this; in chapter 4 we will study in detail a realistic model arising from the low-energy limit of string compactifications.

In order to describe inflation, we can imagine that there exists a scalar field, the *inflaton*, minimally coupled to gravity whose dynamics leads to inflation. For a single scalar field ϕ , the action is

$$S = \int d^4x \sqrt{-g} \left[\frac{M_P^2}{2} R - \frac{1}{2} (\partial\phi)^2 - V(\phi) \right], \quad (3.24)$$

where $V(\phi)$ is an arbitrary inflaton potential.

In particular, we can imagine to use an exponentially flat potential of the form

$$V(\phi) = V_0 - c\phi e^{-k\phi},$$

as the one in figure (3.2). Inflation occurs in the “plateau” region, for large value of ϕ ; here, the field expectation value is large (and slightly constant for all the duration of inflation) and can account for a large vacuum energy which drives the accelerated expansion of the universe. Inflation ends when the field rolls down towards the minimum and start oscillating around it; here the value of the potential must be zero, in order to account for the vacuum energy of the post-inflationary epoch.

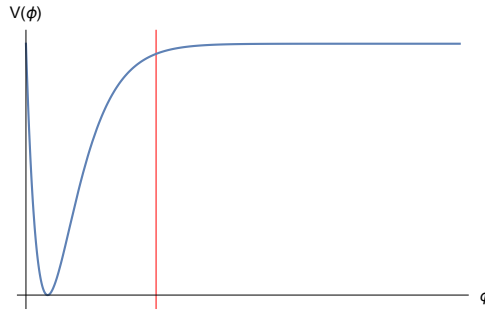


Figure 3.2: Example of an exponentially flat potential. Inflation occurs in the “plateau” region, and ends at the vertical red line, which represents the point where the slow-roll regime ends. After that the field rolls down towards the minimum, oscillating around it.

In presence of a homogeneous scalar field $\phi(t)$ the Friedmann equation and the Klein-Gordon equation respectively have the form

$$3M_P^2 H^2 = \frac{1}{2} \dot{\phi}^2 + V, \quad (3.25)$$

$$\ddot{\phi} + 3H\dot{\phi} + \frac{\partial V}{\partial \phi} = 0. \quad (3.26)$$

If we apply the time derivative $\frac{d}{dt}$ to the Friedmann equation and substitute this expression in the Klein-Gordon equation we obtain

$$\frac{\partial V}{\partial \phi} = \frac{6}{\phi} M_P^2 H \dot{H} - \ddot{\phi} \quad \Rightarrow \quad \dot{H} = -\frac{\dot{\phi}^2}{2M_P^2}.$$

Then the ϵ parameter is now

$$\epsilon = -\frac{\dot{H}}{H^2} = \frac{\frac{1}{2} \dot{\phi}^2}{M_P^2 H^2}; \quad (3.27)$$

inflation therefore occurs when the potential energy of the field dominates over the kinetic energy, $V \gg \frac{1}{2} \dot{\phi}^2$. The kinetic energy remains small and slow-roll persists if the acceleration of the field

is small, $|\ddot{\phi}| \ll 3H|\dot{\phi}|$. From these two conditions and from (3.25) and (3.26) we get

$$\begin{cases} 3M_P^2 H^2 \simeq V \\ 3H\dot{\phi} = -\frac{\partial V}{\partial \phi} \end{cases}, \quad (3.28)$$

and the conditions for prolonged slow-roll inflation can be expressed as conditions on the shape of the potential

$$\epsilon_s = \frac{M_P^2}{2} \left(\frac{1}{V} \frac{\partial V}{\partial \phi} \right)^2 \ll 1, \quad |\eta| = M_P^2 \frac{1}{V} \left| \frac{\partial^2 V}{\partial \phi^2} \right|, \quad (3.29)$$

where $\epsilon_s \ll 1$ and $\eta \ll 1$ are slow-roll parameters. In this model, inflation ends when $\epsilon_s = 1$ (and $\eta \sim \mathcal{O}(1)$).

During a slow-roll period, the ‘‘potential slow-roll parameters’’ ϵ_s and η are related to the ‘‘Hubble slow-roll parameters’’ ϵ and $\tilde{\eta}$ via

$$\begin{cases} \epsilon_s \approx \epsilon \\ \eta \approx \tilde{\eta} + \epsilon \end{cases}. \quad (3.30)$$

For the spectra of scalar and tensor fluctuations we get

$$P_s = \frac{1}{24\pi^2 M_P^2 \epsilon_s} V, \quad P_h = \frac{2}{3\pi^2 M_P^2} V, \quad (3.31)$$

and the scalar spectral index and the tensor-to-scalar ratio are

$$n_s - 1 = 2\eta - 6\epsilon_s, \quad r = 16\epsilon_s. \quad (3.32)$$

The observables have to be evaluated at the time of the horizon exit. This time can be calculated using the number of efoldings $dN_e = H dt$

$$N_e^{tot} = \int H dt = \int \frac{H}{\dot{\phi}} d\phi; \quad (3.33)$$

if $\phi_{exit} > \phi_{end}$ are respectively the value of the field at the horizon exit and at the end of inflation, using (3.28) we find

$$N_e^{tot} = \int_{\phi_{exit}}^{\phi_{end}} \frac{H}{\dot{\phi}} d\phi = \int_{\phi_{end}}^{\phi_{exit}} \frac{1}{M_P^2 \sqrt{2\epsilon_s}} d\phi. \quad (3.34)$$

The value of N_e^{tot} depends on the inflationary model and on the details of reheating and typically takes values in the range $40 \lesssim N_e^{tot} \lesssim 60$.

3.2 Cosmological moduli problem

In this thesis we are interested in inflationary models derived from the low energy limit of string compactifications in type IIB string theory. This procedure is characterized by the presence of gravitationally coupled scalar fields called moduli with Planck-suppressed couplings to Standard Model fields, as we already discussed in chapter 2. For this reason, from now on we will speak about ‘‘moduli’’ and ‘‘scalar fields’’ without distinction.

3.2.1 Moduli cosmological evolution

In general, slow-roll models come with lots of scalar fields. In this section we will consider a simple case with only one field in order to discuss the standard assumptions of inflation and to describe the post-inflationary scenario and its problems. We refer in particular to [16] and [17] for this discussion.

The simplest effective potential we can consider is

$$V = \frac{1}{2}m_\phi^2(\phi - \phi_*)^2 + \frac{C^2}{2}H^2(\phi - \phi_{in})^2, \quad (3.35)$$

where C is some constant factor which could arise from radiative corrections. From (3.26) we then find

$$\ddot{\phi} + 3H\dot{\phi} + m_\phi^2(\phi - \phi_*) + C^2H^2(\phi - \phi_{in}) = 0, \quad (3.36)$$

where we have neglected the decay rate Γ_ϕ of the particle.

Standard assumptions of the cosmological evolution state that at the beginning of inflation $H \gg m_\phi$ and that the field is kept fixed in its inflationary minimum ϕ_{in} , as the friction term $3H\dot{\phi}$ in the equation (3.36) dominates.

When $H \lesssim m_\phi$ the field is no more pinned in ϕ_{in} and it can start to oscillate around its post-inflationary minimum ϕ_* with amplitude roughly $\delta\phi = \phi_{in} - \phi_*$. Hence, at the end of inflation the energy density associated with this field is of order $\rho_\phi \sim m_\phi^2(\delta\phi)^2$.

If we take $H(t) = \frac{2}{3t}$ (for matter domination), we can give an approximate analytic expression of the solution for time $t \gg \frac{1}{m_\phi}$ (which means for $H \ll m_\phi$), which for $C \sim 1$ is

$$\phi \sim \frac{4}{3}(\delta\phi) \left(\frac{2}{3m_\phi t} \right) \sin(m_\phi t). \quad (3.37)$$

The numerical solution can be found in figure (3.3).

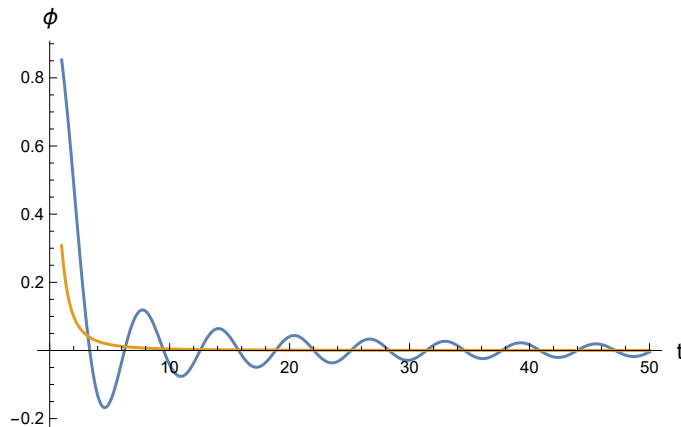


Figure 3.3: Numerical solution with $C = 1$, $m_\phi = 1$, $\phi_* = 0$ and $\phi_{in} = 1$. The yellow line represents the line of the mean value of the field at each time.

The factor $\frac{H(t)}{m_\phi} = \frac{2}{3m_\phi t}$ accounts for the decrease of the amplitude of the oscillations due to the expansion of the universe.

In the above expression the solution has a weak dependence on C ; however, if one takes $C \gg 1$

the behavior of the solution changes dramatically. In fact, the field follows the position of the time-dependent minimum of the effective potential, and its oscillations around it are rather small. In this case the solution looks like

$$\phi \sim \sqrt{\frac{4\pi}{3}} C^{3/2} (\delta\phi) e^{-\frac{C\pi}{3}} \left(\frac{2}{3m_\phi t} \right) \sin(m_\phi t); \quad (3.38)$$

the plot for the numerical solution can be found in figure (3.4).

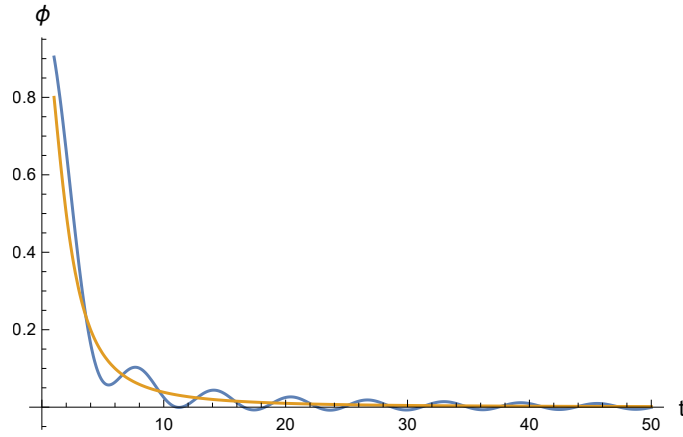


Figure 3.4: Numerical solution with $C = 3$, $m_\phi = 1$, $\phi_* = 0$ and $\phi_{in} = 1$. The yellow line represents the line of the mean value of the field each time.

If we compare (3.38) with (3.37) we can see that the amplitude when $C \gg 1$ reduced by a factor

$$\frac{3}{4} \sqrt{\frac{4\pi}{3}} C^{3/2} e^{-\frac{C\pi}{3}}. \quad (3.39)$$

This has also the effect to reduce the energy density stored in the oscillations of this field; as we will see in the following section and in the next chapter, this could have a significant impact on the post-inflationary scenario.

3.2.2 Reheating from moduli decay

It is now important to consider the post inflationary scenario and the moduli decay. In particular, since they are unstable, we need to consider their decay rate Γ_ϕ and modify the Klein-Gordon equation (3.26) for a single field into

$$\ddot{\phi} + (3H + \Gamma_\phi)\dot{\phi} + \frac{\partial V}{\partial \phi} = 0, \quad (3.40)$$

where $\Gamma_\phi \sim \frac{m_\phi^3}{M_P^2}$. As previously discussed, the energy density associated with this modulus is $\rho_\phi \sim m_\phi^2 (\delta\phi)^2$. Since moduli behave as non relativistic matter, their energy density redshifts as $\rho_m \propto a^{-3}$ and they could come to dominate the energy density of the universe, as it increases with respect standard radiation density $\rho_{rad} \propto a^{-4}$.

If we consider that $\rho_{rad} \sim T^4$, from the Friedmann equation (3.15) we get $H \sim T^2/M_P$ and

since the field starts to oscillate when $H \sim m_\phi$ the initial temperature of this period can be estimated as $T_{in} \sim \sqrt{m_\phi M_P}$. Therefore we can write

$$\rho_\phi(T) = \rho_\phi(T_{in}) \left(\frac{T}{T_{in}} \right)^3 \sim m_\phi^2 (\delta\phi)^2 \left(\frac{T}{\sqrt{m_\phi M_P}} \right)^3. \quad (3.41)$$

If the field ϕ is stable, these oscillations will surely dominate the energy density of the universe. Imposing that the energy density at the temperature T_0 today is

$$\rho_\phi(T_0) < \rho_{critical} = 3H_0^2 M_P^2 \sim (10^{-3} \text{ eV})^4,$$

where T_0 and H_0 are respectively the temperature and the Hubble constant today, we find a constraint on $\delta\phi$

$$\delta\phi < 10^{-10} \left(\frac{m_\phi}{100 \text{ GeV}} \right)^{-1/4} M_P.$$

Hence, if $\delta\phi \sim M_P$ a stable scalar field with $m_\phi > 10^{-26}$ eV would have a large energy density that would be incompatible with our observations.

If the field is unstable, its decay could happen very late in the history of the universe and could spoil the nucleosynthesis process. In particular, the field is expected to decay at a temperature T_D for which $H(T_D) \sim \Gamma_\phi$. Then, using the expressions we found before and (3.15),

$$\begin{cases} \Gamma_\phi \sim \left(\frac{m_\phi^3}{M_P^2} \right) \\ \rho_\phi(T_D) = \rho_\phi(T_{in}) \left(\frac{T_D}{T_{in}} \right)^3 \end{cases} \Rightarrow T_D \sim \frac{m_\phi^{11/6}}{M_P^{1/6} (\delta\phi)^{2/3}}. \quad (3.42)$$

If we assume that at temperature T_D the energy density $\rho_\phi(T_D)$ is promptly converted into radiation we can estimate the reheat temperature as

$$T_{RH} \simeq (\rho_\phi(T_D))^{1/4} \sim (M_P \Gamma_\phi)^{1/2} \sim \left(\frac{m_\phi^3}{M_P} \right)^{1/2}. \quad (3.43)$$

In order not to spoil the successful predictions of the Big Bang nucleosynthesis (BBN) process we need to require that $T_{RH} \geq 10$ MeV, which assures that moduli decay *before* the BBN, as $T_{BBN} \sim \mathcal{O}(1)$ MeV. This puts a bound on the mass $m_\phi \gtrsim 100$ TeV; this is the so called *cosmological moduli problem*. It is therefore important for a successful inflationary model to generate moduli with large masses.

4.1 Kähler moduli inflation: effective action

The theory of inflation has proven to be very successful in explaining lots of phenomena in early universe cosmology. However, it is still not clear what could actually produce a mechanism of accelerating expansion.

One idea is to look for possible ways to explain this period of cosmic evolution within the framework provided by a fundamental theory. Today, one of the most promising fundamental theory is string theory, and the moduli stabilization mechanism discussed in section 2.3 has opened the way to application to inflation. Stabilization techniques represent the first step towards string phenomenology, as moduli VEVs are connected to important basic quantities such as the string scale and the gauge coupling constants.

The idea developed in [18] is to construct a model, called “Kähler moduli inflation”, within the LVS framework for moduli stabilization in IIB flux compactifications with a blow-up Kähler modulus playing the role of the inflaton.

4.1.1 The scalar potential

The structure of the potential of Kahler moduli inflation is such that inflation is obtained naturally and almost inevitably. In particular, the authors of [18] noted that with non-perturbative correction to the superpotential (2.27), in the non-perturbative contribution to the scalar potential of supergravity (2.28)

$$V_{np} = e^K K^{i\bar{j}} \left[a_i A_i a_{\bar{j}} \bar{A}_{\bar{j}} e^{-(a_i T_i + a_j \bar{T}_j)} - (W(\partial_i K) a_{\bar{j}} \bar{A}_{\bar{j}} e^{-a_j \bar{T}_j} + c.c.) \right]$$

T_i only appear non-perturbatively along exponentially flat directions. Such features naturally suggest possible applications to inflation. Indeed, slow-roll inflation precisely requires the presence of almost flat directions in the scalar potential.

In order to build a suitable model, the authors of [18] chose the simplest LVS realisations,

which are provided by Calabi-Yau manifolds whose volume takes the Swiss-cheese form

$$\mathcal{V} = \frac{\alpha}{2\sqrt{2}} \left[(T_1 + \bar{T}_1)^{3/2} - \sum_{i=2}^n \lambda_i (T_i + \bar{T}_i)^{3/2} \right] = \alpha \left(\tau_1^{3/2} - \sum_{i=2}^n \lambda_i \tau_i^{3/2} \right), \quad (4.1)$$

where as before $T_i = \tau_i + i\theta_i$ are the Kähler moduli, τ_i are four-cycles volumes (called blow-ups) and θ_i are the associated axions.

Using the α' -corrected Kähler potential (2.24) and keeping in mind that $\frac{\partial}{\partial T_i} = \frac{1}{2} \frac{\partial}{\partial \tau_i}$ we can now build the Kähler metric for an arbitrary number of moduli

$$\begin{aligned} K_{1\bar{1}} &= \frac{3\alpha^{4/3}(4\mathcal{V} - \xi + 6\alpha \sum_{k=2}^n \lambda_k \tau_k^{3/2})}{4(2\mathcal{V} + \xi)^2 (\mathcal{V} + \alpha \sum_{k=2}^n \lambda_k \tau_k^{3/2})^{1/3}}, & K_{i\bar{i}} &= \frac{3\alpha \lambda_i (2\mathcal{V} + \xi + 6\alpha \lambda_i \tau_i^{3/2})}{4(2\mathcal{V} + \xi)^2 \sqrt{\tau_i}} \\ K_{1\bar{j}} &= -\frac{9\alpha^2 \lambda_j \sqrt{\tau_1} \sqrt{\tau_j}}{2(2\mathcal{V} + \xi)^2}, & K_{i\bar{j}} &= \frac{9\alpha^2 \lambda_i \lambda_j \sqrt{\tau_i} \sqrt{\tau_j}}{2(2\mathcal{V} + \xi)^2}, \end{aligned} \quad (4.2)$$

together with its inverse

$$K^{1\bar{1}} = \frac{4(2\mathcal{V} + \xi) \sqrt{\tau_1} (2\mathcal{V} + \xi + 6\alpha \sum_{k=2}^n \lambda_k \tau_k^{3/2})}{3\alpha(4\mathcal{V} - \xi)}, \quad K^{i\bar{i}} = \frac{4(2\mathcal{V} + \xi) \sqrt{\tau_i} (4\mathcal{V} - \xi + 6\alpha \lambda_i \tau_i^{3/2})}{3\alpha(4\mathcal{V} - \xi) \lambda_i}, \quad (4.3)$$

$$K^{1\bar{j}} = \frac{8(2\mathcal{V} + \xi) \tau_1 \tau_j}{(4\mathcal{V} - \xi)}, \quad K^{i\bar{j}} = \frac{8(2\mathcal{V} + \xi) \tau_i \tau_j}{(4\mathcal{V} - \xi)}.$$

Finally, using the superpotential (2.35)

$$W = W_0 + \sum_{i=2}^n A_i e^{-a_i \tau_i} \quad (4.4)$$

from the expression (1.55) we can work out the explicit form of the potential

$$\begin{aligned} V &= \sum_{i=2}^n \sum_{j=i+1}^n \frac{A_i A_j \cos(a_i \theta_i - a_j \theta_j)}{(4\mathcal{V} - \xi)(2\mathcal{V} + \xi)^2} e^{-(a_i \tau_i + a_j \tau_j)} [32(2\mathcal{V} + \xi)(a_i \tau_i + a_j \tau_j + 2a_i a_j \tau_i \tau_j) + 24\xi] + \\ &\quad (4.5) \\ &\quad \sum_{i=2}^n \left(\frac{16(a_i A_i)^2 \sqrt{\tau_i} e^{-2a_i \tau_i}}{3\alpha \lambda_i (2\mathcal{V} + \xi)} + \frac{32a_i A_i^2 \tau_i (1 + a_i \tau_i) e^{-2a_i \tau_i}}{(4\mathcal{V} - \xi)(2\mathcal{V} + \xi)} + \frac{12\xi A_i^2 e^{-2a_i \tau_i}}{(4\mathcal{V} - \xi)(2\mathcal{V} + \xi)^2} \right) + \\ &\quad \sum_{i=2}^n \frac{8W_0 A_i \cos(a_i \theta_i)}{(4\mathcal{V} - \xi)(2\mathcal{V} + \xi)} e^{-a_i \tau_i} \left(4a_i \tau_i + \frac{3\xi}{2\mathcal{V} + \xi} \right) + \\ &\quad + \frac{12\xi W_0^2}{(4\mathcal{V} - \xi)(2\mathcal{V} + \xi)^2} + V_{up}, \end{aligned}$$

where V_{up} is the uplift term. The chosen form of this term could lead to different dependencies on the internal volume, as shown in appendix B. In this case, following [19], we take

$$V_{up} = \frac{C_{up} |W_0|^2}{\mathcal{V}^{8/3}} \left(1 - \frac{C_{sub}}{\mathcal{V}^{2/3}} \right), \quad \begin{cases} C_{up} &= \frac{9}{16\pi} \alpha^{2/3} \\ C_{sub} &= g_s \frac{|W_0|^2}{18\alpha^{4/3}} \end{cases}. \quad (4.6)$$

Actually, in principle C_{up} and C_{sub} depend on some parameters of the theory [20]; however, this dependence is weak (in the sense that those parameters could take values in small ranges) and we can safely consider them fixed as in (4.6).

We now briefly describe inflation with Kähler moduli, which will be enlighten in the next sections. The idea is to displace the inflaton (one of the blow-ups, τ_2 in our convention) from its minimum while keeping the other moduli in their global minimum; the potential is exponentially flat in this direction (at constant volume) and the inflaton rolls back towards the global minimum driving inflation, as we discussed in 3.1.2. Actually, the displacement of the inflaton affects the other moduli, in the sense that they will be positioned in a new local minimum (the inflationary minimum, which depends on the position of the inflaton); in order to obtain stability, this minima must be very close to the global ones. We stress that for the model to work it is necessary that all the moduli are stable during inflation, in particular the volume modulus.

The blow-ups have a marginal role in inflationary dynamics (except the inflaton of course), but their presence is fundamental to stabilize the volume modulus during inflation. Furthermore, the volume modulus plays a crucial role in the post-inflationary scenario. Depending on the values of the parameters, after the inflaton decays into radiation the universe could enter a period of matter domination due to the small decay rate of the volume. We will analyze in detail this possibility in section 4.3.

4.1.2 Large Volume Limit and constraints

We can now consider a simplified version of the potential taking the large volume limit, including only the leading terms up to $\mathcal{O}(\frac{1}{\mathcal{V}^3})$

$$V_{LARGE} = \sum_{i=2}^n \frac{8(a_i A_i)^2 \sqrt{\tau_i}}{3\alpha\lambda_i \mathcal{V}} e^{-2a_i \tau_i} + \sum_{i=2}^n 4W_0 \frac{a_i A_i}{\mathcal{V}^2} \cos(a_i \theta_i) \tau_i e^{-a_i \tau_i} + \frac{3\xi W_0^2}{4\mathcal{V}^3} + V_{up},$$

where $V_{up} \simeq \frac{C_{up}|W_0|^2}{\mathcal{V}^{8/3}}$. In particular, the volume should take value in the range $10^5 \leq \mathcal{V} \leq 10^7$ (in string length units). Recalling the discussion of section 2.4, we can put the axions in their minima (which satisfy $\cos(a_i \theta_i^{min}) = -1$) as they do not play any active role during inflation, obtaining

$$V_{LARGE} = \sum_{i=2}^n \frac{8(a_i A_i)^2 \sqrt{\tau_i}}{3\alpha\lambda_i \mathcal{V}} e^{-2a_i \tau_i} - \sum_{i=2}^n 4W_0 \frac{a_i A_i}{\mathcal{V}^2} \tau_i e^{-a_i \tau_i} + \frac{3\xi W_0^2}{4\mathcal{V}^3} + \frac{C_{up}|W_0|^2}{\mathcal{V}^3}. \quad (4.7)$$

Now we can find the minima $\frac{\partial V}{\partial \tau_i} = 0$ of the blow-ups τ_i for $i = 2, 3, \dots, n$ keeping the volume \mathcal{V} fixed. For the sake of simplicity, we are using the same notation for the field and its numerical value in the minimum, as the meaning is always clear from the context. In general, τ_i will always indicate the minimum, except when it appears in a potential which explicitly depends on that field, as for instance in V_{LARGE} .

The minimization leads to

$$(a_i A_i) e^{-a_i \tau_i} = \frac{3\alpha\lambda_i W_0}{2\mathcal{V}} \frac{(1 - a_i \tau_i)}{(\frac{1}{2} - 2a_i \tau_i)} \sqrt{\tau_i}. \quad (4.8)$$

It is useful for further calculations to set

$$\epsilon_i = \frac{1}{4a_i \tau_i} \quad (4.9)$$

and to write (4.8) as

$$(a_i A_i) e^{-a_i \tau_i} = \frac{3\alpha \lambda_i W_0 (1 - 4\epsilon_i)}{4\mathcal{V}} \sqrt{\tau_i}. \quad (4.10)$$

Now we can do the same with the volume requiring $\frac{\partial V}{\partial \mathcal{V}}|_{\mathcal{V}_*} = 0$, where \mathcal{V}_* is the post-inflationary minimum for the volume modulus. We can easily find

$$\sum_{i=2}^n \frac{8(a_i A_i)^2 \sqrt{\tau_i}}{3\alpha \lambda_i \mathcal{V}_*} e^{-2a_i \tau_i} - \sum_{i=2}^n 8W_0 \frac{a_i A_i}{\mathcal{V}_*^2} \tau_i e^{-a_i \tau_i} + \frac{9\xi W_0^2}{4\mathcal{V}_*^3} + \frac{8 C_{up} W_0^2}{3 \mathcal{V}_*^{8/3}} = 0.$$

Substituting the minima of the moduli (4.10) into the above relation, with a little algebra (see appendix B for more details) we come to

$$\xi = 2\alpha \sum_{i=2}^n \left[\lambda_i \frac{(1 - 4\epsilon_i)}{(1 - \epsilon_i)^2} \tau_i^{\frac{3}{2}} \right] - \frac{32}{27} C_{up} \mathcal{V}_*^{1/3}. \quad (4.11)$$

The next step is to fix the condition to obtain a Minkowski vacuum. Indeed, after inflation the inflaton relaxes to the global minimum of the potential, whose VEV must correspond to the vacuum energy we measure today. If we substitute the minima (4.10) in the potential (4.7) we are left with

$$V_{LARGE}^{min} = \sum_{i=2}^n \frac{\alpha \lambda_i W_0^2}{\mathcal{V}_*^3} \tau_i^{3/2} \left[\frac{3}{2} \frac{(1 - 4\epsilon_i)^2}{(1 - \epsilon_i)^2} - 3 \frac{(1 - 4\epsilon_i)}{(1 - \epsilon_i)} \right] + \frac{3\xi W_0^2}{4\mathcal{V}_*^3} + \frac{C_{up} W_0^2}{\mathcal{V}_*^{8/3}}; \quad (4.12)$$

using (4.11) and requiring $V_{LARGE}^{min} = 0$ we get

$$\mathcal{V}_*^{1/3} = \frac{27}{C_{up}} \alpha \sum_{i=2}^n \frac{\lambda_i}{(1 - \epsilon_i)^2} \tau_i^{3/2} \epsilon_i (1 - 4\epsilon_i). \quad (4.13)$$

Finally, we can rewrite (4.11) using the equation (4.13) in order to find an expression for ξ which depends only on the parameters of the model and the minima; this will be helpful for the numerical analysis. Furthermore, it is quite instructive to understand its dependence on the important parameters we will focus on. We obtain

$$\xi = 2\alpha \sum_{i=2}^n \frac{\lambda_i}{(1 - \epsilon_i)^2} \tau_i^{3/2} (1 - 16\epsilon_i)(1 - 4\epsilon_i). \quad (4.14)$$

4.1.3 Preliminary considerations on stability

It is now important to make some preliminary considerations about the stability of the moduli minima based on the constraints we found. The stability problem will be discussed further in 4.2.1.

When the inflaton τ_2 is displaced from its minimum, the potential (4.7) no more depends on it; the field minima will be in a slightly different position $\tilde{\tau}_i$ and \mathcal{V}_{in} , where

$$(a_i A_i) e^{-a_i \tilde{\tau}_i} = \frac{3\alpha \lambda_i W_0}{2\mathcal{V}_{in}} \frac{(1 - a_i \tilde{\tau}_i)}{(\frac{1}{2} - 2a_i \tilde{\tau}_i)} \sqrt{\tilde{\tau}_i}. \quad (4.15)$$

Therefore, the minimization condition (4.11) is modified into

$$\xi = 2\alpha \sum_{i=3}^n \left[\lambda_i \frac{(1-4\tilde{\epsilon}_i)}{(1-\tilde{\epsilon}_i)^2} \tilde{\tau}_i^{3/2} \right] - \frac{32}{27} C_{up} \mathcal{V}_{in}^{1/3}. \quad (4.16)$$

Let us now assume that the potential is well stabilized and $\tilde{\tau}_i \simeq \tau_i$. Since ξ is constant, (4.11) and the above relation (4.16) give

$$\mathcal{V}_{in}^{1/3} - \mathcal{V}_*^{1/3} = -\frac{27}{32} \frac{2\alpha}{C_{up}} \left[\lambda_2 \frac{(1-4\epsilon_2)}{(1-\epsilon_2)^2} \tau_2^{3/2} \right]. \quad (4.17)$$

Since we are assuming $\tilde{\tau}_i \simeq \tau_i$, equation (4.15) implies also that $\mathcal{V}_{in} \simeq \mathcal{V}_*$. We underline that (4.17) is not at all correct, as $\mathcal{V}_{in} > \mathcal{V}_*$, but it is significant because it gives us a clue on the parameters we should keep under control in order to obtain a small shift between inflationary and post-inflationary volume minima. Recalling that $C_{up} \sim \alpha^{2/3}$, we gather from the right hand side of (4.17) that we have to require

$$\alpha^{1/3} \left[\lambda_2 \frac{(1-4\epsilon_2)}{(1-\epsilon_2)^2} \tau_2^{3/2} \right] \ll 1. \quad (4.18)$$

Let us now start from a different consideration and assume that the volume is well stabilized, $\mathcal{V}_{in} \simeq \mathcal{V}_*$. Putting together again (4.11) and (4.16) we obtain

$$\sum_{i=3}^n \left[\lambda_i \frac{(1-4\tilde{\epsilon}_i)}{(1-\tilde{\epsilon}_i)^2} \tilde{\tau}_i^{3/2} \right] = \sum_{i=2}^n \left[\lambda_i \frac{(1-4\epsilon_i)}{(1-\epsilon_i)^2} \tau_i^{3/2} \right] = \sum_{i=3}^n \left[\lambda_i \frac{(1-4\epsilon_i)}{(1-\epsilon_i)^2} \tau_i^{3/2} \right] \left(1 + \frac{\lambda_2 \frac{(1-4\epsilon_2)}{(1-\epsilon_2)^2} \tau_2^{3/2}}{\sum_{i=3}^n \left[\lambda_i \frac{(1-4\epsilon_i)}{(1-\epsilon_i)^2} \tau_i^{3/2} \right]} \right).$$

Since, as before, $\mathcal{V}_{in} \simeq \mathcal{V}_*$ implies $\tilde{\tau}_i \simeq \tau_i$, we must require that

$$\frac{\lambda_2 \frac{(1-4\epsilon_2)}{(1-\epsilon_2)^2} \tau_2^{3/2}}{\sum_{i=3}^n \left[\lambda_i \frac{(1-4\epsilon_i)}{(1-\epsilon_i)^2} \tau_i^{3/2} \right]} \ll 1. \quad (4.19)$$

Relations (4.18) and (4.19) must both be true at the same time. Hence, we can imagine at least two ways to achieve stability:

- choosing $\lambda_i \sim \mathcal{O}(1)$ and taking

$$\begin{cases} \frac{(1-4\epsilon_2)}{(1-\epsilon_2)^2} \ll 1 \\ \tau_2 \ll \tau_i, \quad i = 3, 4, \dots, n \end{cases}, \quad (4.20)$$

and thus $\tau_2 \gtrsim \frac{1}{a_2}$;

- choosing $\tau_i \gtrsim 1$ (which gives $\epsilon_i \ll 1$) and using

$$\begin{cases} \lambda_2 \ll 1 \\ \lambda_2 \ll \lambda_i, \quad i = 3, 4, \dots, n \end{cases}. \quad (4.21)$$

The first strategy was adopted for instance in [20]; we will give an example of this method in the example 1 of section 4.4.1. However, in the following discussion we will exploit the second case for reasons that will be clear in a moment.

4.2 Kähler moduli inflation: inflationary analysis

In this kind of model with Swiss-cheese Calabi-Yau manifold we can basically distinguish three kind of fields:

- the inflaton, which in our convention is the modulus τ_2 ;
- the volume modulus τ_1 (or \mathcal{V});
- the spectator fields τ_i , $i = 3, 4, \dots, n$.

In order to study the multi-field dynamics, it is necessary to make some assumptions. Since the spectator fields do not play any active role, it is reasonable to assume that they all behave in the same way. To achieve this, we need to assume that all the parameters are equal, hence

$$\begin{cases} \lambda_i & \rightarrow \lambda_3 \\ a_i & \rightarrow a_3 \\ A_i & \rightarrow A_3 \end{cases}, \quad \forall i = 4, 5, \dots, n. \quad (4.22)$$

In order to wisely choose the parameters not directly constrained by relations in section 4.1.2 (as for example the Calabi-Yau manifold parameters n , α , λ_2 and λ_3) it is important to notice from (4.13) that

$$\mathcal{V}_*^{1/3} \epsilon_i \leq 1 \frac{27}{C_{up}} \alpha \left(\lambda_2 \tau_2^{3/2} \epsilon_2 + (n-2) \lambda_3 \tau_3^{3/2} \epsilon_3 \right). \quad (4.23)$$

From this relation we clearly see that a large number of moduli $n \gg 1$ would lead to an extremely large volume, which is not compatible with the value $\mathcal{V} \leq 10^7$ proposed in [18] and discussed in section 4.2.2. Indeed, with $\tau_2 \sim \tau_3$, $n \gg 1$ and $\lambda_2 \ll \lambda_3$ (as in (4.21)) we have

$$\mathcal{V}_*^{1/3} \simeq \frac{27}{C_{up}} \alpha \left((n-2) \lambda_3 \tau_3^{3/2} \epsilon_3 \right), \quad (4.24)$$

which entails the dependence

$$\mathcal{V}_* \sim \alpha ((n-2) \lambda_3)^3. \quad (4.25)$$

Hence we are forced to choose

$$\lambda_3 = \frac{\lambda'_3}{(n-2)} \quad (4.26)$$

in order to keep the volume under control; for $\tau_3 \gtrsim 1$ and $\alpha \sim \mathcal{O}(1)$, λ'_3 must take values in the range $1 \lesssim \lambda'_3 \lesssim 50$. These conditions could be partially relaxed if the uplift has the form

$$V_{up} = \frac{D}{\mathcal{V}^\gamma}$$

and $\gamma \lesssim 2$, as shown in appendix B.

4.2.1 Single-field potential

We now turn to study the single-field potential for the volume modulus. The goal of this analysis is to understand the physical behavior of the system and to see in particular if there are any connections with the model proposed in [16] and discussed in section 3.2.1.

For the sake of brevity we will indicate V_{LARGE} simply as V . If we consider cases in which $\epsilon_i \ll 1$ (i.e. $\tau_i \gg \frac{1}{4a_i}$, typically $\tau_i \gtrsim 1$), (4.10) can be rewritten as

$$\tau_i \simeq \frac{1}{a_i} \ln \left(\frac{\mathcal{V}}{\mu_i} \right), \quad \mu_i = \frac{3\alpha\lambda_i W_0}{4a_i A_i}. \quad (4.27)$$

To obtain the single-field potential we need to put the moduli in their minima (4.27)

$$V(\mathcal{V}) = \frac{W_0^2}{\mathcal{V}^3} \left[\sum_{i=2}^n \left(-\frac{3\alpha\lambda_i}{2a_i^{3/2}} \right) \ln \left(\frac{\mathcal{V}}{\mu_i} \right)^{3/2} + \frac{3}{4}\xi + C_{up}\mathcal{V}^{1/3} \right]. \quad (4.28)$$

During inflation τ_2 is displaced on the ‘‘plateau’’ of the slow-roll potential, which could be written as

$$\begin{aligned} V(\tau_2) &= \frac{W_0^2}{\mathcal{V}^3} \left[\sum_{i=3}^n \left(-\frac{3\alpha\lambda_i}{2a_i^{3/2}} \right) \ln \left(\frac{\mathcal{V}}{\mu_i} \right)^{3/2} + \frac{3}{4}\xi + C_{up}\mathcal{V}^{1/3} \right] - 4\frac{W_0 a_2 A_2}{\mathcal{V}^2} \tau_2 e^{-a_2 \tau_2} \\ &\equiv V_0 - 4\frac{W_0 a_2 A_2}{\mathcal{V}^2} \tau_2 e^{-a_2 \tau_2}. \end{aligned} \quad (4.29)$$

To obtain the expression for V_0 we should consider the volume in its inflationary minimum \mathcal{V}_{in} (which means its local minimum calculated when the inflaton has a large value). Since the shift between local and global minima is expected to be small, in first approximation we can consider $\mathcal{V}_{in} \simeq \mathcal{V}_*$: from (4.28), using relations (4.13) and (4.14), we find

$$V_0 \simeq \frac{W_0^2}{\mathcal{V}_{in}^3} \frac{3\alpha\lambda_2}{2} \tau_2^{3/2} \simeq \frac{W_0^2}{\mathcal{V}_*^3} \frac{3\alpha\lambda_2}{2} \tau_2^{3/2}. \quad (4.30)$$

It is useful to set $\phi = \ln \mathcal{V}$, as the canonical field for the volume is

$$\phi^c = \sqrt{\frac{2}{3}} \ln \mathcal{V}, \quad \phi = \sqrt{\frac{3}{2}} \phi^c; \quad (4.31)$$

the potential is then

$$V(\phi) = W_0^2 e^{-3\phi} \left[\sum_{i=2}^n \left(-\frac{3\alpha\lambda_i}{2a_i^{3/2}} \right) (\phi - \ln \mu_i)^{3/2} + \frac{3}{4}\xi + C_{up}e^{1/3\phi} \right]. \quad (4.32)$$

During inflation $\tau_2 \gg 1$ and the inflationary potential looks like

$$V_{in}(\phi) = W_0^2 e^{-3\phi} \left[\sum_{i=3}^n \left(-\frac{3\alpha\lambda_i}{2a_i^{3/2}} \right) (\phi - \ln \mu_i)^{3/2} + \frac{3}{4}\xi + C_{up}e^{1/3\phi} \right]. \quad (4.33)$$

As stressed in [18], the volume modulus will be stable during inflation if the ratio

$$R = \frac{\lambda_2 a_2^{3/2}}{\sum_{i=2}^n \lambda_i a_i^{3/2}}, \quad (4.34)$$

is small, as it accounts for the difference between (4.32) and (4.33). The expression of R also shows that we need at least three moduli to achieve stabilization.

If we want to investigate small values of R , the very first idea could be to use lots of moduli with all the parameters of the same order. Actually, this cannot be done: from section 4.1.3 and equation (4.23) it is clear that the only possibility is to choose a small value for the intersection number λ_2 , with $\lambda_3 = \frac{\lambda'_3}{(n-2)}$ and $\lambda'_3 \sim \mathcal{O}(10)$. Setting $a_2 = a_3$ we have

$$R = \frac{\lambda_2}{\lambda_2 + (n-2)\lambda_3} = \frac{\lambda_2}{\lambda_2 + \lambda'_3} \stackrel{\lambda_2 \ll \lambda'_3}{\simeq} \frac{\lambda_2}{\lambda'_3}. \quad (4.35)$$

We can now write the inflationary potential as a contribution of two terms

$$V_{in}(\phi) = V(\phi) + \delta V(\phi), \quad (4.36)$$

where

$$\delta V(\phi) = W_0^2 e^{-3\phi} \frac{3\alpha\lambda_2}{2a_2^{3/2}} (\phi - \ln \mu_2)^{3/2}; \quad (4.37)$$

this last could be an important term only at the beginning of inflation but as we approach to the end of this epoch it has to become less relevant: in fact, we need to recover the full potential $V(\phi)$ with all the moduli in their minima.

In order to estimate the shift of the volume modulus from inflationary and post-inflationary epoch $\delta\phi = \phi_{in} - \phi_*$, we can take the derivatives of (4.36) and expand around ϕ_*

$$V'_{in}(\phi) = V'(\phi) + \delta V'(\phi) \simeq V''(\phi_*)(\phi - \phi_*) + \delta V'(\phi_*) + \delta V''(\phi_*)(\phi - \phi_*), \quad (4.38)$$

where we used $V(\phi_*) = V'(\phi_*) = 0$. The derivatives are

$$\begin{aligned} V''(\phi) &= 3W_0^2 e^{-3\phi} \sum_{i=2}^n \alpha \lambda_i \tau_i^{3/2} \epsilon_i, \\ \delta V'(\phi) &= -\frac{9\alpha\lambda_2}{2} e^{-3\phi} W_0^2 \tau_2^{3/2} (1 - 2\epsilon_2), \\ \delta V''(\phi) &= \frac{27\alpha\lambda_2}{2} e^{-3\phi} W_0^2 \tau_2^{3/2} (1 - 4\epsilon_2), \end{aligned}$$

where after deriving we wrote (4.27) as $\ln \mu_i = \phi - a_i \tau_i$. Evaluating them in ϕ_* , in the limit $R \ll 1$ we obtain

$$\begin{aligned} V''(\phi_*) &\simeq 2W_0^2 e^{-3\phi_*} \frac{3\alpha\lambda_2}{2} \tau_2^{3/2} \epsilon_2 \left(1 + \frac{\sum_{i=3}^n \lambda_i \tau_i^{3/2} \epsilon_i}{\lambda_2 \tau_2^{3/2} \epsilon_2} \right) \\ &\simeq 2V_0 \epsilon_2 \left(1 + \frac{(n-2)\lambda_3}{\lambda_2} \frac{\tau_3^{3/2} \epsilon_3}{\tau_2^{3/2} \epsilon_2} \right) \\ &\simeq 2 \frac{V_0}{R} \frac{\tau_3^{3/2}}{\tau_2^{3/2}} \epsilon_3, \end{aligned} \quad (4.39)$$

and

$$\begin{aligned}\delta V'(\phi_*) &\simeq -3V_0, \\ \delta V''(\phi_*) &\simeq 9V_0.\end{aligned}\tag{4.40}$$

Setting $\phi = \phi_{in}$ in (4.38), which gives $V'_{in}(\phi_{in}) = 0$, and rearranging the terms we get

$$\delta\phi = -\frac{\delta V'(\phi_*)}{V''(\phi_*) + \delta V''(\phi_*)} \simeq \frac{3\lambda_2\tau_2^{3/2}}{9\lambda_2\tau_2^{3/2} + 2\sum_{i=3}^n \lambda_i\tau_i^{3/2}\epsilon_i},\tag{4.41}$$

and with the assumptions (4.22) we finally obtain

$$\delta\phi = \frac{3}{2}R\frac{\tau_2^{3/2}}{\tau_3^{3/2}\epsilon_3}.\tag{4.42}$$

We can now try to analyze the single-field potential in order to reduce it to the simple form of the toy model discussed in 3.2.1 and to gather the expected physical behavior of the model under study. The first task is to understand what are the dominant term during inflation, when $\tau_2 \gg 1$. We start expanding (4.36) around its inflationary minimum ϕ_{in} up to the first relevant order

$$\begin{aligned}V_{in}(\phi) &\simeq V_{in}(\phi_{in}) + V'_{in}(\phi_{in})(\phi - \phi_{in}) + \frac{1}{2}V''_{in}(\phi_*)(\phi - \phi_{in})^2 \\ &\simeq V_0 + \frac{1}{2}V''(\phi_{in})(\phi - \phi_{in})^2 + \frac{1}{2}\delta V''(\phi_{in})(\phi - \phi_{in})^2.\end{aligned}\tag{4.43}$$

Assuming $R \ll 1$ we have $\delta\phi \ll 1$ and in first approximation we can consider $V''(\phi_{in}) \simeq V''(\phi_*)$ and $\delta V''(\phi_{in}) \simeq \delta V''(\phi_*)$; hence we obtain

$$V_{in}(\phi) = \frac{1}{R}V_0\frac{\tau_3^{3/2}}{\tau_2^{3/2}}\epsilon_3(\phi - \phi_{in})^2 + \frac{9}{2}V_0(\phi - \phi_{in})^2 + V_0.\tag{4.44}$$

If we use the canonical field in (4.31), we finally find

$$V_{in}(\phi^c) = \frac{3}{2}R\frac{\tau_3^{3/2}}{\tau_2^{3/2}}\epsilon_3(\phi^c - \phi_{in}^c)^2 + \frac{27}{4}V_0(\phi^c - \phi_{in}^c)^2 + V_0.\tag{4.45}$$

If we now study in the same way the total potential after the end of inflation, when the inflaton reaches its minimum, we get

$$V(\phi^c) = \frac{3}{2}R\frac{\tau_3^{3/2}}{\tau_2^{3/2}}\epsilon_3(\phi - \phi_*^c)^2.\tag{4.46}$$

From these expansions we can read the expression of the mass of the volume modulus, which is

$$m_\phi^2 \equiv 3\frac{V_0}{R}\frac{\tau_3^{3/2}}{\tau_2^{3/2}}\epsilon_3 = \frac{9}{2}\frac{V_0}{\delta\phi},\tag{4.47}$$

where we used (4.42). If we recall (4.30) it is immediate to show that this expression is compatible with (A.48) calculated in appendix, as it should be.

From this analysis we clearly see that the mass of the volume modulus (and hence of all the other moduli) is *always* bigger than the Hubble scale during inflation, which is given by $3H_{inf}^2 = \rho \simeq V_0$, and

$$\frac{m_\phi^2}{H_{inf}^2} = \frac{27}{2} \frac{1}{\delta\phi} \sim \frac{1}{R}. \quad (4.48)$$

This result is actually independent from the specific model, as shown in [21]; however, in our case it is really important to realize that the ratio $\frac{m_\phi}{H_{inf}}$ depends on the R parameter.

In conclusion, in contrast to the standard case discussed in 3.2.1, for $R \ll 1$ the dominant term in the potential is the mass term, and not the Hubble one. We then expect that at the end of inflation the fields never stay pinned in their inflationary minima, as the friction term is sub-dominant, but they continue following their new local minima (as the inflaton evolves), exhibiting at most some small oscillations around them.

4.2.2 Slow-roll parameters

As we have seen from (4.29), the supergravity potential can be really reduced to an exponentially flat function of the form proposed in section 3.1.2. We can now exploit this potential in order to find approximate expressions for some useful parameters of the slow-roll model.

Let us start by introducing the canonically normalized field τ_2^c for the inflaton, which satisfies (since we are dealing with a single field potential)

$$K_{22} \partial_\mu \tau_2 \partial^\mu \tau_2 = \frac{1}{2} \partial_\mu \tau_2^c \partial^\mu \tau_2^c, \quad K_{22} \simeq \frac{3\lambda_2 \alpha}{8\sqrt{\tau_2} \mathcal{V}} \quad (4.49)$$

and whose expression is

$$\tau_2^c = \sqrt{\frac{4\alpha\lambda_2}{3\mathcal{V}}} \tau_2^{3/4}. \quad (4.50)$$

Then, in term of the canonical field the inflationary potential is

$$V = V_0 - \frac{4W_0 a_2 A_2}{\mathcal{V}^2} \left(\frac{3\mathcal{V}}{4\alpha\lambda_2} \right)^{2/3} (\tau_2^c)^{4/3} \exp \left[-a_2 \left(\frac{3\mathcal{V}}{4\alpha\lambda_2} \right)^{2/3} (\tau_2^c)^{4/3} \right]. \quad (4.51)$$

Taking the derivatives respect τ_2^c , the slow-roll parameters (3.29) (rewritten in term of τ_2 for simplicity) are

$$\epsilon_s = \frac{32W_0^2}{3\alpha\lambda_2 V_0^2 \mathcal{V}^3} a_2^2 A_2^2 \sqrt{\tau_2^*} (1 - a_2 \tau_2^*)^2 e^{-2a_2 \tau_2^*}, \quad (4.52)$$

$$\eta = -\frac{4a_2 A_2 W_0}{3\alpha\lambda_2 \sqrt{\tau_2^*} V_0 \mathcal{V}} [(1 - 9a_2 \tau_2^* + 4(a_2 \tau_2^*)^2) e^{-a_2 \tau_2^*}], \quad (4.53)$$

where τ_2^* is the value of the inflaton at the horizon exit. The number of efoldings (3.34) is (see [22] for computational details)

$$N_e^{tot} = \frac{3V_0 \mathcal{V} \alpha \lambda_2}{16W_0 a_2 A_2} \int_{\tau_2^{end}}^{\tau_2^*} \frac{e^{a_2 \tau_2}}{\sqrt{\tau_2} (1 - a_2 \tau_2)} d\tau_2 \simeq \frac{3V_0 \mathcal{V} \alpha \lambda_2}{16W_0 a_2^{3/2} A_2} \frac{e^{a_2 \tau_2^*}}{(a_2 \tau_2^*)^{3/2}}, \quad (4.54)$$

where τ_2^{end} is the point where the slow-roll conditions break down ($\epsilon_s \sim \mathcal{O}(1)$ and $\eta \sim \mathcal{O}(1)$) and $\tau_2^* > \tau_2^{end}$.

We can also calculate the amplitude of scalar perturbations

$$P_s = \frac{e^{K_{cs}} g_s V}{150\pi^2 \epsilon_s} \simeq \frac{e^{K_{cs}} g_s}{150\pi^2} \left(\frac{3\alpha V_0^3 \mathcal{V}^3 \lambda_2 e^{2a_2 \tau_2^*}}{32W_0^2 a_2^2 A_2^2 \sqrt{\tau_2^* (1 - a_2 \tau_2^*)^2}} \right), \quad (4.55)$$

where we have already taken into account the normalization factor necessary to match the COBE normalization. The tensor-to scalar-ratio is as usual

$$r = 16\epsilon_s. \quad (4.56)$$

In particular, in such models ϵ_s is very small and tensor perturbations are unobservable.

Finally, authors of [18] pointed out that for the model to work the internal volume should live within the range

$$10^5 \leq \mathcal{V} \leq 10^7 \quad (4.57)$$

in term of string length unit $l_s = (2\pi)\sqrt{\alpha'}$.

4.3 Post-inflationary scenario

In this section we are going to discuss the scenario after the end of inflation, as was done in [22]. For completeness, in this case we will often use explicitly M_P , as it is important to give the expression of some quantities such as the decay rates.

As we discussed in 3.1, inflation ends when the slow-roll parameter $\epsilon_s = 1$. After this moment the inflaton quickly reaches the global minimum of the potential and starts to oscillate around it. For the other moduli, and in particular for the volume modulus, we can imagine two possibilities:

- the volume stays fixed in its inflationary value as the inflaton reaches the global minimum, and then it starts to oscillate around its minimum with amplitude roughly $\delta\phi = \phi_{in} - \phi_*$;
- the volume follows is local minimum until the global minimum, with some small amplitude oscillations.

As the mass of the volume is smaller than the one of the inflaton, we expect that after the inflaton decays the volume could play an important role, as, depending on the parameters, it could dominate the energy density of the universe.

4.3.1 Inflaton domination

During inflation the Hubble parameter remains constant and its value is given by

$$3H_{inf}^2 M_P^2 = \rho \simeq V_0. \quad (4.58)$$

Soon after the end of inflation at t_{end} , the energy density is dominated by inflaton quanta, $\rho(t_{end}) \simeq \rho_{inf}(t_{end}) \simeq V_0$. Indeed, we can estimate

$$\begin{cases} \rho_{inf}(t_{end}) \simeq V_0 \\ \rho_\phi(t_{end}) \simeq \frac{1}{2} m_\phi^2 (M_P \delta\phi)^2 \end{cases}, \quad \theta^2 \equiv \frac{\rho_\phi(t_{end})}{\rho_{inf}(t_{end})} = \frac{m_\phi^2 \delta\phi^2}{6H_{inf}^2}, \quad (4.59)$$

where $\theta^2 \ll 1$ and $\delta\phi$ is always intended in M_P units for simplicity. Using (4.48) θ^2 can be rewritten as

$$\theta^2 = \frac{9}{4}\delta\phi \sim R, \quad (4.60)$$

and then it can be easily controlled. This period lasts until the inflaton decays; we can assume $H_{inf} > \Gamma_{inf}$ and that when $H(t_1) \simeq \Gamma_{inf}$ all the inflaton quanta are entirely converted into radiation. From this assumption we can calculate the duration of this period, which is

$$N_{mod1} = \ln\left(\frac{a(t_1)}{a(t_{end})}\right) = \frac{2}{3}\ln\left(\frac{H(t_{end})}{H(t_1)}\right) \simeq \frac{2}{3}\ln\left(\frac{H_{inf}}{\Gamma_{inf}}\right), \quad (4.61)$$

where $\Gamma_{inf} \simeq 0.1 \frac{m_{inf}^3}{M_s^2}$, m_{inf} being the mass of the inflaton. We then have

$$\rho_\gamma(t_1) = \rho_{inf}(t_1) = \rho_{inf}(t_{end}) \left(\frac{a(t_{end})}{a(t_1)}\right)^3 = \rho_{inf}(t_{end}) e^{-3N_{mod1}} = 3H_{inf}^2 M_P^2 e^{-3N_{mod1}}. \quad (4.62)$$

Since both the inflaton and the volume redshift as matter ($\rho \propto 1/a^3$), the ratio (4.59) remains constant until this very last moment and

$$\frac{\rho_\phi(t_1)}{\rho_\gamma(t_1)} = \theta^2. \quad (4.63)$$

4.3.2 Modulus domination

At this time $t > t_1$ the energy density of the universe is dominated by radiation. However the energy density associated with radiation dilutes much faster than the energy density associated with the oscillations of the volume modulus, and so the universe may enter a second epoch of matter domination, which lasts until the decay of the volume modulus.

To study this possibility we need to investigate if it does exist t_{eq} such that $\rho_\gamma(t_{eq}) = \rho_\phi(t_{eq})$. In particular, if we consider the volume modulus lifetime $\tau_\phi = 1/\Gamma_\phi$, we can imagine two cases

- $\tau_\phi \gg t_{eq}$, for which we expect a period of matter domination;
- $\tau_\phi \ll t_{eq}$, for which we do not expect a period of matter domination, as the volume decays too quickly and the curves associated with ρ_γ and ρ_ϕ never met.

From the equilibrium condition we find

$$\begin{cases} \rho_\gamma(t_{eq}) = \rho_\gamma(t_1) \left(\frac{a(t_1)}{a(t_{eq})}\right)^4 \\ \rho_\phi(t_{eq}) = \rho_\phi(t_1) \left(\frac{a(t_1)}{a(t_{eq})}\right)^3 \end{cases} \Rightarrow \theta^2 = \frac{\rho_\phi(t_1)}{\rho_\gamma(t_1)} = \frac{a(t_1)}{a(t_{eq})}, \quad (4.64)$$

and

$$\rho(t_{eq}) = \rho_\gamma(t_{eq}) + \rho_\phi(t_{eq}) = 2\rho_\gamma(t_{eq}) = 2\rho_\gamma(t_1)\theta^8. \quad (4.65)$$

We can now calculate $H_{eq} = H(t_{eq})$

$$3H_{eq}^2 M_P^2 = \rho(t_{eq}) \Rightarrow H_{eq}^2 = \frac{2}{3M_P^2} \rho_\gamma(t_1)\theta^8 = 2e^{-3N_{mod1}}\theta^8 H_{inf}^2, \quad (4.66)$$

where we used (4.62). Since the volume decays when $H \simeq \Gamma_\phi$, our prediction for the presence or not of a period of volume modulus domination reduces to

$$\begin{cases} \frac{H_{eq}}{\Gamma_\phi} > 1, & (\text{or } \tau_\phi > t_{eq}) & \Rightarrow \text{volume domination} \\ \frac{H_{eq}}{\Gamma_\phi} < 1, & (\text{or } \tau_\phi < t_{eq}) & \Rightarrow \text{NO volume domination} \end{cases} . \quad (4.67)$$

If we work with (4.66), with the help of (4.59) and (4.48) we can rewrite

$$H_{eq} = \frac{\sqrt{2}e^{-\frac{3}{2}N_{mod1}} m_\phi^4 (\delta\phi)^4}{36 H_{inf}^3} = \frac{9}{8} \sqrt{3} e^{-\frac{3}{2}N_{mod1}} m_\phi (\delta\phi)^{5/2}. \quad (4.68)$$

With $\Gamma_\phi \simeq \frac{1}{16\pi} \frac{m_\phi^3}{M_P^2}$ and H_{inf} in (4.58) we can finally obtain (using again M_P units)

$$\frac{H_{eq}}{\Gamma_\phi} = 4\sqrt{3}\pi e^{-\frac{3}{2}N_{mod1}} \frac{(\delta\phi)^{7/2}}{V_0} = 18\sqrt{3}\pi e^{-\frac{3}{2}N_{mod1}} \frac{(\delta\phi)^{5/2}}{m_\phi^2}. \quad (4.69)$$

Using (4.24), (4.30), (4.42) and (4.61) we can further reduce this expression to obtain

$$\frac{H_{eq}}{\Gamma_\phi} \simeq 5.77 \times 10^{15} \alpha(\lambda_3)^6 \frac{a_2^3}{a_3^4} (\tau_2^6 \tau_3^2) R^2. \quad (4.70)$$

It is important to underline that this last expression is valid only if $\Gamma_{inf} < H_{inf}$. In this case, we can give a real rough estimate of the upper value of R below which the model may not present volume modulus domination. With $\lambda_3' \sim \mathcal{O}(1)$, $a_2 = a_3 = 2\pi$, $\tau_2 \sim \mathcal{O}(1)$ and $\tau_3 \simeq 6$ (in order to obtain at least $\mathcal{V} \sim 10^3$), we expect to be able to avoid matter domination only if $R \lesssim 10^{-8}$.

On the other side, if $\Gamma_{inf} > H_{inf}$ we could still give a prediction setting $N_{mod1} = 0$ (see section 4.4.4 for a brief discussion) in equation (4.69)

$$\frac{H_{eq}}{\Gamma_\phi} = 18\sqrt{3}\pi \frac{(\delta\phi)^{5/2}}{m_\phi^2} \Leftrightarrow \Gamma_{inf} > H_{inf}. \quad (4.71)$$

However, it is more difficult to give an upper bound on R . Indeed, H_{eq}/Γ_ϕ depends on the mass of the volume, which depends on W_0 : the superpotential cannot be freely assigned if we want to obtain the correct power spectrum, and it is difficult to estimate it in advance keeping also in mind the constraints entailed by $\Gamma_{inf} > H_{inf}$. However, once assigned the Calabi-Yau parameters and the minima of the blow-ups, the mass m_ϕ is the same for any value of λ_2 (see section 4.4.4), and it is then clear that there always exists a value of R below which the $H_{eq}/\Gamma_\phi < 1$.

To study this epoch more accurately, we can also use the equations for the energy densities [15]. Energy density of matter particles decreases due to the cosmological expansion, since their number density gets diluted and energy of each particle gets redshifted. However, energy is injected into radiation due to decays of heavy particles. Hence, equations for ρ_ϕ and ρ_γ and have the form

$$\begin{cases} \dot{\rho}_\phi(t) + 3H(t)\rho_\phi(t) = -\Gamma_\phi \rho_\phi(t) \\ \dot{\rho}_\gamma(t) + 4H(t)\rho_\gamma(t) = +\Gamma_\phi \rho_\phi(t) \\ 3H^2(t)M_P^2 = \rho_\phi(t) + \rho_\gamma(t) \end{cases} . \quad (4.72)$$

In case of a period of volume modulus domination, we can estimate its total duration in the same way we did for the inflaton domination epoch, namely

$$N_{mod2} = \frac{2}{3} \ln \left(\frac{H_{eq}}{\Gamma_\phi} \right). \quad (4.73)$$

4.3.3 Number of efoldings

The total number of efoldings between the horizon exit and the end of inflation is really important to make useful predictions in inflationary cosmology. From generic assumptions about the reheating epoch the preferred range in standard cosmological timeline is

$$N_e^{tot} = 55 \pm 5. \quad (4.74)$$

However, post-inflationary cosmology strongly affects the value of N_e^{tot} , which can be predicted (see [22] and [23]) as

$$N_e + \frac{1}{4}N_{mod1} + \frac{1}{4}N_{mod2} \approx 57 + \frac{1}{4} \ln r + \frac{1}{4} \ln \left(\frac{\rho_*}{\rho_{end}} \right), \quad (4.75)$$

where ρ_* is the energy density at horizon exit and ρ_{end} is the energy density at the end of inflation. With generic assumptions, the new preferred range was found to be ([22])

$$N_e^{tot} = \left(55 - \frac{1}{4}N_{mod} \right) \pm 5, \quad (4.76)$$

where $N_{mod} = N_{mod1} + N_{mod2}$.

4.4 Numerical analysis

In this section we present the numerical results, which confirm our predictions. In order to assign the parameters, we used the following strategy:

- we assigned the Calabi-Yau parameters n , α , λ_2 and λ_3 , and hence R ;
- we fixed $a_2 = a_3 = 2\pi$;
- we chose the values of the minima for τ_2 and τ_3 ;
- we assigned the values of A_2 , A_3 and a temporary value \tilde{W}_0 for the superpotential in order to obtain the desired minima and the correct normalized power spectrum $P_s = 3.7 \times 10^{10}$, using (4.10), (4.13) and (4.55);
- we found ξ with the help of (4.14) and a range of values for g_s considering $\xi \equiv \frac{\kappa}{g_s^{3/2}}$, with $\frac{1}{2} \leq \kappa \leq \frac{3}{2}$ (see [24]), and we took $g_s = \frac{1}{\xi^{2/3}}$.

After having assigned these parameters, we cleared the temporary value of W_0 and we look for the minima of the potential using (4.5), keeping W_0 as a running parameter in order match the requirement $V_{min} = 0$. Then we assigned the new value of the tree-level superpotential, which were always found to be $W_0 \simeq \tilde{W}_0$.

Subsequently, in order to fully address the problem we used the full potential (4.5) and we solved the system of differential equations (Einstein-Friedmann equations)

$$\frac{d^2\tau^a}{dN^2} + \Gamma^a_{bc} \frac{d\tau^b}{dN} \frac{d\tau^c}{dN} + \left(3 + \frac{1}{H} \frac{dH}{dN}\right) \frac{d\tau^a}{dN} + \frac{1}{H^2} K^{ab} \partial_b V = 0, \quad (4.77)$$

$$3H^2 = V + \frac{1}{2} H^2 K_{ab} \frac{d\tau^a}{dN} \frac{d\tau^b}{dN}, \quad (4.78)$$

where $\Gamma^a_{bc} = K^{ad} \frac{1}{2} \frac{\partial K_{bd}}{\partial \tau^c}$ are the associated Christoffel symbols and N is the number of efoldings which we are using as “time coordinate” during the evolution via $dN = H dt$. Since the spectator fields all behave in the same way (thanks to the conditions (4.22)), it is sufficient to consider the equations for just three fields $a = 1, 2, 3$. The initial conditions are

$$\tau_a = \{\tau_1^{in}, \tau_2^{in}, \tau_3^{in}\}, \quad \left. \frac{d\tau_a}{dN} \right|_{\tau_a^{in}} = \{0, 0, 0\}, \quad (4.79)$$

where τ_2^{in} is taken to be larger than its value in the minimum, in order to generate enough efoldings, and τ_1^{in} and τ_3^{in} are fixed in their inflationary minimum, i.e. their local minimum calculated fixing $\tau_2 = \tau_2^{in}$ in the potential (4.5).

Using (4.77) and (4.78), the variation of the Hubble rate in terms of the number of efoldings can be expressed as

$$\frac{1}{H} \frac{dH}{dN} = \frac{V}{H^2} - 3. \quad (4.80)$$

Thus the generic expression of the slow-roll parameter ϵ takes the form

$$\epsilon \equiv -\frac{1}{H^2} \frac{dH}{dt} = \frac{1}{H} \frac{dH}{dN} = \frac{1}{2} K_{ab} \frac{d\tau^a}{dN} \frac{d\tau^b}{dN}, \quad (4.81)$$

and in the slow-roll regime it simplifies to

$$\epsilon_s = \frac{K^{ab} \partial_a V \partial_b V}{2V^2}. \quad (4.82)$$

The normalized power spectrum and the spectral index for scalar perturbations are given by

$$P_s = \frac{g_s e^{K_{cs}}}{150\pi^2} \frac{V}{\epsilon}, \quad n_s = 1 + \frac{d \ln(P_s(N))}{dN}. \quad (4.83)$$

The physical observables are evaluated at the horizon exit, which is given by

$$N_e^* = N_e^{end} - N_e^{tot}, \quad (4.84)$$

where N_e^{tot} is the number of efoldings in (4.75) and N_e^{end} is the end of inflation, determined with

$$\epsilon_s(N_e^{end}) = 1. \quad (4.85)$$

4.4.1 Example 1

This first example is meant to discuss the general procedure we used in order to carry on the numerical analysis and to show the general behavior of the solutions of the system of differential equations. Furthermore, it shows that we can achieve stabilization also for large values of R , as long as we keep in mind the constraints we discussed in section 4.1.3; this is very similar to what was done in [20]. In particular, here we use $n = 3$ and we choose $\tau_2 \gtrsim 1/a_2$, generating a hierarchy between the moduli, $\tau_3 \gg \tau_2$, taking

$$\tau_2 = 0.165, \quad \tau_3 = 10. \quad (4.86)$$

The value of τ_3 has been chosen in order to obtain a volume of order $\sim 10^5$. For the Calabi-Yau manifold we choose

Calabi-Yau parameters			
n = 3			
α	λ_2	λ_3	R
1	3	3	0.5

To obtain the desired minima and the correct COBE normalization we find

$$A_2 = 3.89216 \times 10^{-8}, \quad A_3 = 4.4091 \times 10^{21}, \quad W_0 = 0.373231; \quad (4.87)$$

the true values of the minima are given in table 4.1. It can be noticed that in this case the approximation (4.42) is not good, since R is not small enough.

For the other values of the manifold we find

$$\xi = 176.159, \quad 0.0159111 < g_s < 0.0477333, \quad g_s = 0.0318222. \quad (4.88)$$

	τ_2	τ_3	τ_1	vol	ϕ	$\delta\phi$
predicted	0.165	10	3240.24	184349	12.1246	0.235209
calculated	0.165076	10.0019	3257.19	185798	12.1324	0.059741

Table 4.1: Values of minima of example 1. The “predicted” values are the ones given by the approximations in (4.13) and (4.42), whereas the “calculated” ones are those found with the potential (4.5).

Figure 4.1 shows the evolution of all the moduli. In particular, we can see that all of them follow their inflationary minimum until inflation ends at N_e^{end} (represented by the red points). Soon after that, they begin to oscillate around their post-inflationary minimum.

In particular, in this case from figure 4.2 we recognized that our plots seem to be in agreement with the qualitative picture described in 3.2.1 for the standard scenario. In particular, it can be seen that the friction still plays a role, as soon after the end of inflation the volume remains fixed for a few more fractions of efoldings before starting to oscillate around its post-inflationary minimum.

The situation is better represented in the inflationary trajectory in figure 4.3. The green line represents the curve of local minima of ϕ and τ_3 (which change according to the position of the inflaton τ_2), whereas the red line is the trajectory. It is evident that soon after the end of inflation

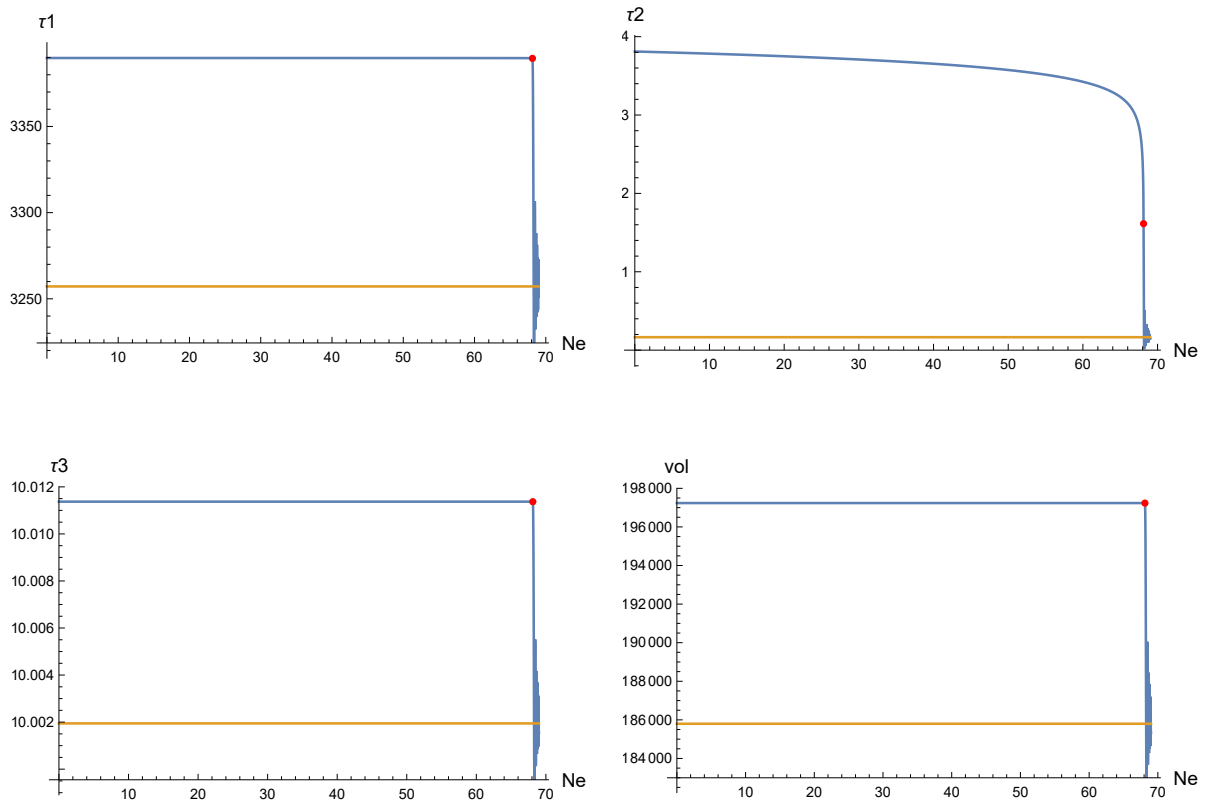


Figure 4.1: Plot for of all the moduli evolution for example 1. The yellow lines represent their value at the global post-inflationary minimum and the red points represent the end of inflation.

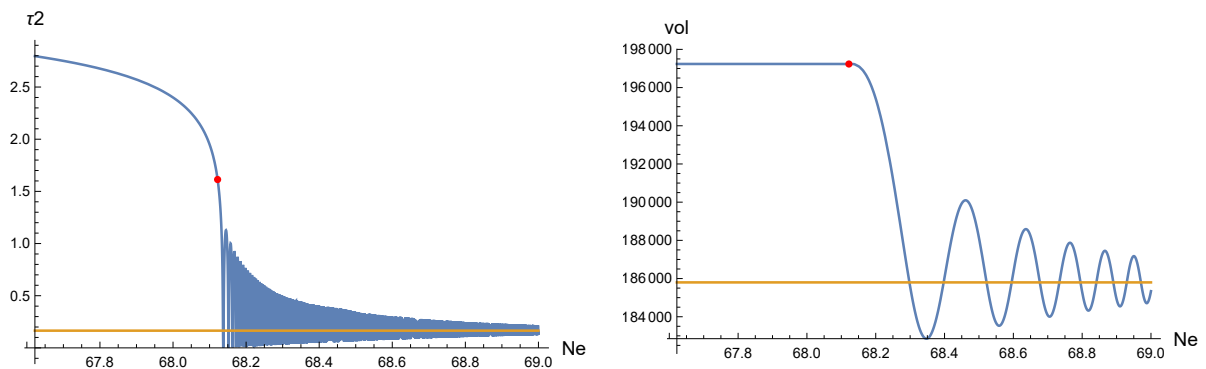


Figure 4.2: Evolution of the inflaton and the volume modulus during the last efoldings for example 1.

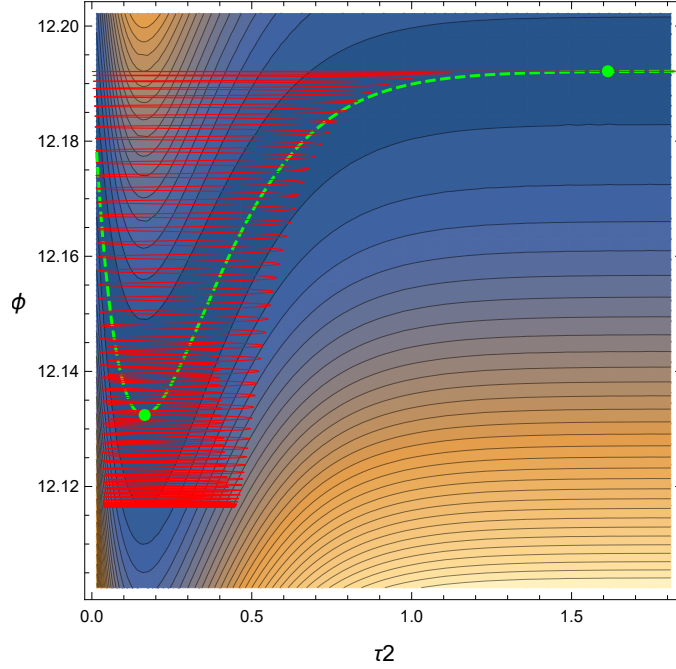


Figure 4.3: Inflationary trajectory in the (τ_2, ϕ) plane for example 1. The green dashed line represents the curve of local minima of ϕ and τ_3 for each value of τ_2 and the green dots represent the end of inflation (the one on the right) and the global minimum (the one on the left).

(green point on the right) the volume remains fixed in its inflationary value before oscillating around the global minimum (green point on the left). If it followed its new minimum, we should expect that the green and the red lines overlap and in particular that the first oscillations of τ_2 should be centered on the green line.

We can now give details of the observables of the model, namely P_s , n_s and r , and discuss the predictions for the post-inflationary scenario and the total duration of inflation. First of all, we give the physical quantities in table 4.2, which are calculated numerically using the full potential and the full metric of section 4.1. The masses are calculated considering $m_\phi \simeq m_1$ and $m_{inf} \simeq m_2$ referring to the appendix A.

\mathbf{H}_{inf}	\mathbf{m}_ϕ	\mathbf{m}_{inf}	$\mathbf{\Gamma}_\phi$	$\mathbf{\Gamma}_{inf}$
1.06177×10^9	1.44896×10^{10}	2.17283×10^{12}	1.02042×10^{-8}	32136.7

Table 4.2: Values of the physical quantities of the model in GeV for example 1.

Given that, we can analyze the post-inflationary scenario. In particular, we expect a period of volume modulus domination as we can estimate $\frac{H_{eq}}{\Gamma_\phi} \simeq 5.46551 \times 10^{10} \gg 1$. Indeed, after the inflaton domination period which lasts

$$N_{mod1} \simeq 6.94,$$

we have a period of modulus domination which extends (if we put $t_1 = 0$) roughly between $t_{eq} \simeq \frac{1}{H_{eq}} \simeq 1.79304 \times 10^{-3} \text{ GeV}^{-1}$ and $t_{\phi,dec} \simeq \frac{1}{\Gamma_\phi} \simeq 9.79989 \times 10^7 \text{ GeV}^{-1}$. More precisely,

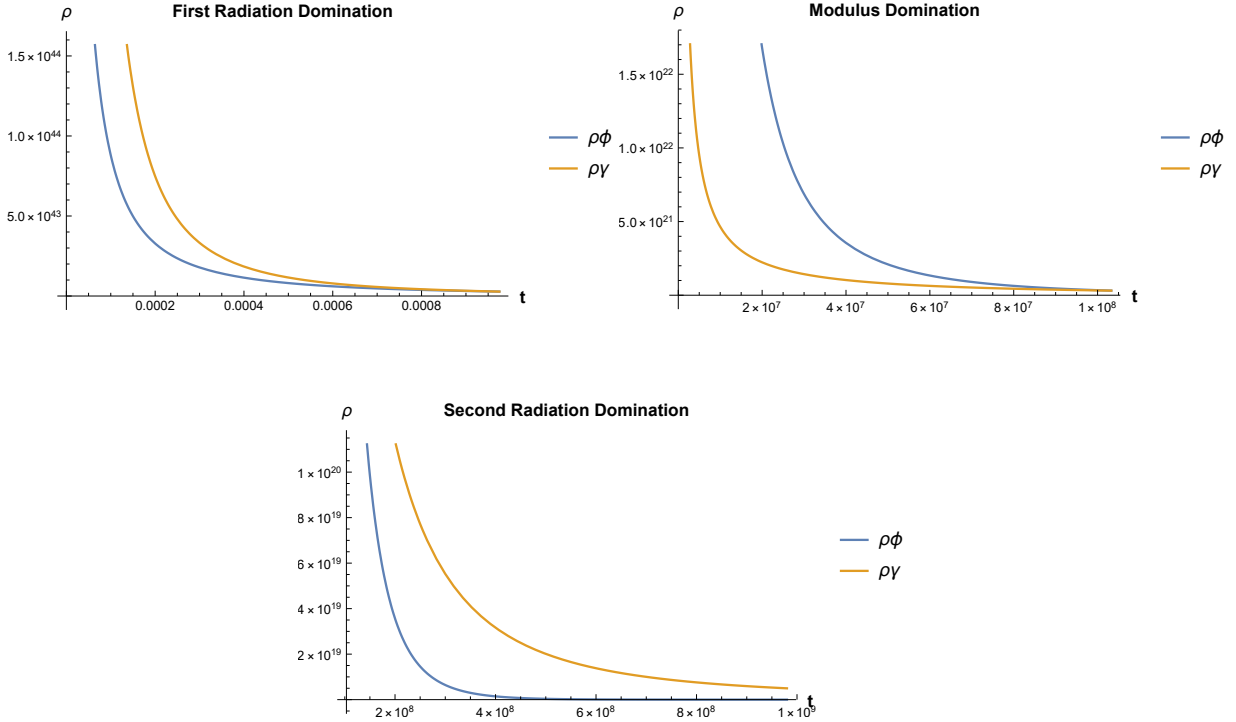


Figure 4.4: Post inflationary scenario for example 1. After a short period of radiation domination, the volume modulus comes to dominate the energy density until it decays and converts mainly into radiation.

numerically solving the equations (4.72), plotted in figure 4.4, we find

$$t_{dom,beg} = 9.75251 \times 10^{-4} \text{ GeV}^{-1}, \quad t_{dom,end} = 1.03271 \times 10^8 \text{ GeV}^{-1},$$

respectively for the beginning and end of this period, and the total duration of the epoch in number of e-folding is

$$N_{mod2} \simeq 16.49.$$

We can then predict the number of e-foldings between horizon exit and end of inflation from (4.75)

$$N_e^{tot} \simeq 45.70,$$

which allows us to predict other observables at horizon exit $N_e^* = N_e^{end} - N_e^{tot}$.

We show the behavior of the power spectrum and the spectral index in figure 4.5 whose values are

$$P_s(K_{cs} = 0) = 5.5745 \times 10^{-13}, \quad n_s = 0.95449.$$

We stress that the parameters (in particular A_2 , A_3 and W_0) could in principle be chosen in order to exactly match the normalization $P_s = 3.7 \times 10^{-10}$, but it is not always easy to precisely assign these values. As already stated, here we used the approximate relation (4.55): in this particular case it did not give a good result (probably because of the small value of τ_2), but in example 2 and example 3 we will see that this strategy always gives the correct order of magnitude.

However, afterwards we could use K_{cs} in order to match the correct normalization; in this case,

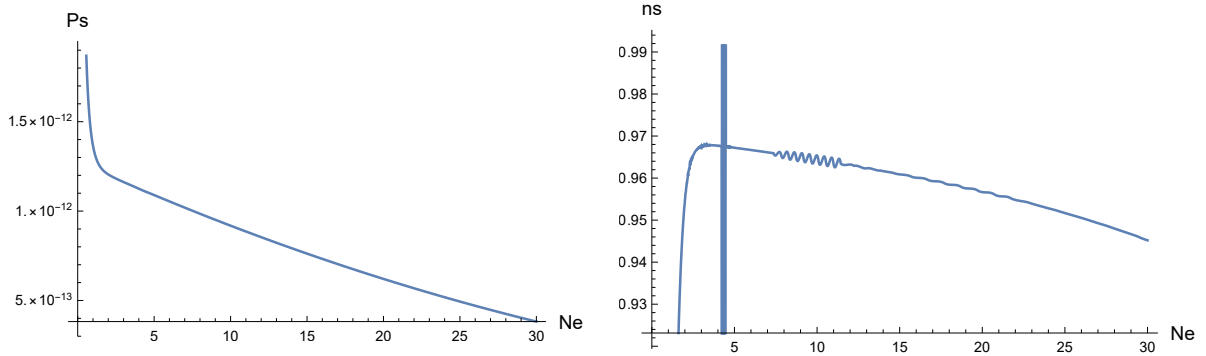


Figure 4.5: Power spectrum and spectral index for example 1 in the first efoldings. Close to $N_e = 0$ the plot is not reliable, as the system is not yet in a slow-roll regime. Fluctuations in n_s are due to computational inaccuracies.

we should take $K_{cs} = 6.49788$.

Finally, the slow-roll parameters ϵ and ϵ_s are plotted in figure 4.6 and the tensor-to-scalar ratio is

$$\epsilon = 2.19883 \times 10^{-11}, \quad r = 16\epsilon = 3.51813 \times 10^{-10}.$$

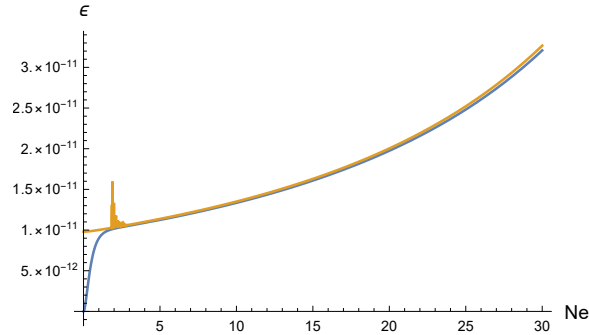


Figure 4.6: Comparison between ϵ (blue line) and ϵ_s (yellow line) in the first efoldings.

4.4.2 Example 2

This second example is meant to verify the expectations we discussed in section 4.2. Actually, here we are not using optimal values (especially for the value of the volume) due to computational reasons: in fact, we find out that the software we used gave better results for small values of the volume, in particular in resolving the final oscillations of the fields. However, it is then very instructive to reason on the output of this example, as the mathematical behavior is the same; we will give a more realistic scenario in example 3.

In particular, here we show how the situation changes when we decrease the value of R , with particular attention to the post-inflationary scenario. Since there is no point in using lots of moduli to stabilize the potential, as we have shown in sections 4.1 and 4.2, for this case we will use $n = 3$ fields. For the minima we choose

$$\tau_2 = 1, \quad \tau_3 = 6,$$

and for the Calabi-Yau manifold we fix

Calabi-Yau parameters		
\mathbf{n}	α	λ_3
3	1	1

We then change the value of $\lambda_2 \ll 1$ in order to decrease $R \simeq \frac{\lambda_2}{\lambda_3}$.

$\mathbf{R} \sim 10^{-2}$

We begin studying the case in which R is still not too small, in order to better enlighten the differences with the next cases. The first stable case we found corresponds to $\lambda_2 \sim 10^{-2}$; we point out that qualitatively this is in agreement with the stability condition we discussed in section 4.1.3 and 4.2. In particular we take

$$\lambda_2 = \frac{1}{100} \quad \Rightarrow \quad R \simeq 0.0099.$$

To obtain the desired minima and the correct COBE normalization we find

$$A_2 = 1.33188 \times 10^{-6}, \quad A_3 = 1.60757 \times 10^{10}, \quad W_0 = 0.00708011;$$

the true values of the minima are given in table 4.3. It can be noticed that also in this case the approximation (4.42) is not too good, since R is not small enough (even if it is already better than in the example 1).

	τ_2	τ_3	τ_1	vol	ϕ	$\delta\phi$
predicted	1	6	212.477	3082.47	8.03349	0.105291
calculated	1.01547	6.01681	222.144	3296.17	8.10052	0.207558

Table 4.3: Values of the minima for the case $R \sim 10^{-2}$ of example 2. The “predicted” values are the ones given by the approximations in (4.13) and (4.42), whereas the “calculated” ones are those found with the potential (4.5).

The other values of the manifold are fixed at

$$\xi = 25.9274, \quad 0.0570774 < g_s < 0.171232, \quad g_s = 0.114155.$$

Figure 4.7 shows the evolution of the volume and the inflaton in the last efoldings. In particular, also in this case we recognized that our plots seem to be in agreement with the qualitative picture described in 3.2.1 for the standard scenario. Indeed, soon after the end of inflation the volume remains pinned for a few more “time” before oscillating around its post-inflationary minimum.

\mathbf{H}_{inf}	\mathbf{m}_ϕ	\mathbf{m}_{inf}	$\mathbf{\Gamma}_\phi$	$\mathbf{\Gamma}_{\text{inf}}$
5.7237×10^9	6.04794×10^{10}	5.99751×10^{13}	7.42048×10^{-7}	1.19895×10^7

Table 4.4: Values of the physical quantities in GeV for the case $R \sim 10^{-2}$ of example 2.

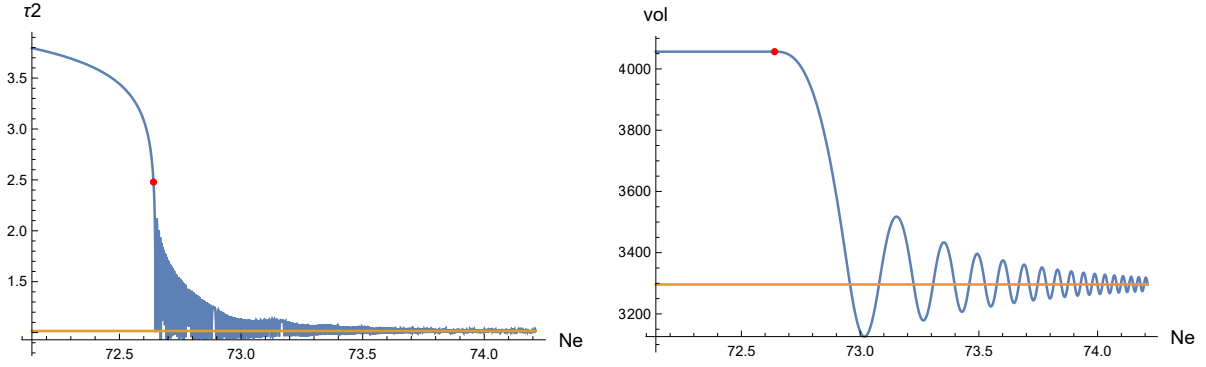


Figure 4.7: Evolution of the inflaton and the volume modulus during the last efoldings in the case $R \sim 10^{-2}$ of example 2.

The situation is better represented in the inflationary trajectory in figure 4.8. As before, it is evident that soon after the end of inflation the volume remains fixed in its inflationary value before oscillating around the global minimum, since the red and the green curves do not overlap. This fact should come as no surprise: from the physical quantities in table 4.4 we see that the ratio $\frac{m_\phi}{H_{inf}} \sim \mathcal{O}(10)$, which implies that the friction term plays an important role.

In this case we are not able to make any predictions for the post-inflationary scenario, as the assumptions made in (4.59) do not hold. However, the case we presented here is extremely useful to appreciate the cases with smaller R .

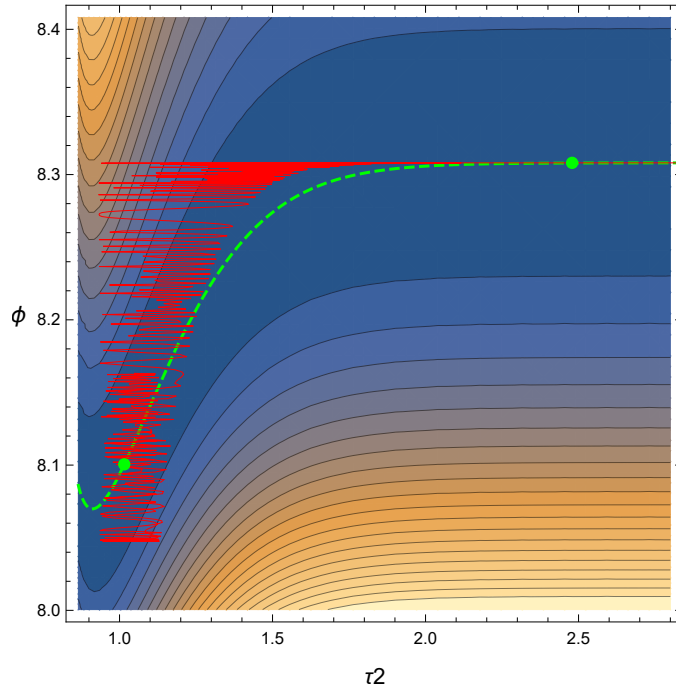


Figure 4.8: Inflationary trajectory in the (τ_2, ϕ) plane in the case $R \sim 10^{-2}$ of example 2. The green dashed line represents the curve of local minima of ϕ and τ_3 for each value of τ_2 and the green dots represent the end of inflation (the one on the right) and the global minimum (the one on the left).

$R \sim 10^{-3}$

We continue our analysis decreasing R about one order of magnitude taking

$$\lambda_2 = \frac{1}{1000} \Rightarrow R \simeq 0.00099.$$

To obtain the chosen minima we find

$$A_2 = 1.30267 \times 10^{-7}, \quad A_3 = 1.57231 \times 10^{10}, \quad W_0 = 0.00685244,$$

which more precisely give the values in table 4.5. With the help of the predicted values of table 4.5 we assign

$$\xi = 25.9214, \quad 0.0570861 < g_s < 0.171258, \quad g_s = 0.114172.$$

	τ_2	τ_3	τ_1	vol	ϕ	$\delta\phi$
predicted	1	6	211.047	3051.29	8.02332	0.0147113
calculated	1.01561	6.01696	220.731	3264.65	8.09091	0.0145412

Table 4.5: Values of the minima for the case $R \sim 10^{-3}$ of example 2. The “predicted” values are the ones given by the approximations in (4.13) and (4.42), whereas the “calculated” ones are those found with the potential (4.5).

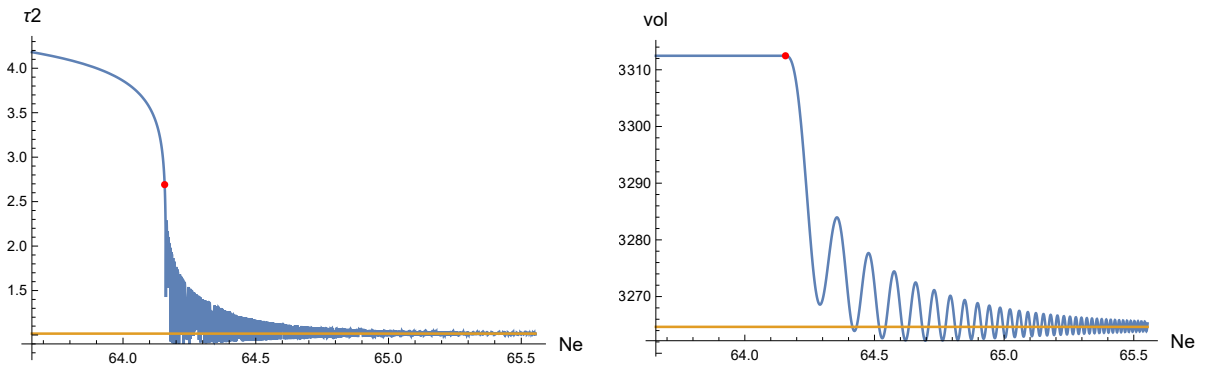


Figure 4.9: Evolution of the inflaton and the volume modulus during the last efoldings for the case $R \sim 10^{-3}$ of example 2.

From figure 4.9 we see that the behavior of the volume is slightly different from the previous case; in fact, the first oscillation is not centered on the post-inflationary minimum, which indicates that the friction is less important and the field is quite free to follow its local minimum. This behavior can also be recognized in figure 4.10, as in this case the green and red curves start to overlap.

We can now turn to analyze the post inflationary scenario. We first give the values of the Hubble parameter, the masses and the decay rates in table 4.6. After the inflaton decays, we can numerically solve equations (4.72) to verify whether a period of volume modulus domination is present or not. We can estimate $\frac{H_{eq}}{\Gamma_\phi} \simeq 2.26161 \times 10^{10} \gg 1$, which tells us that we should expect a period of matter domination.

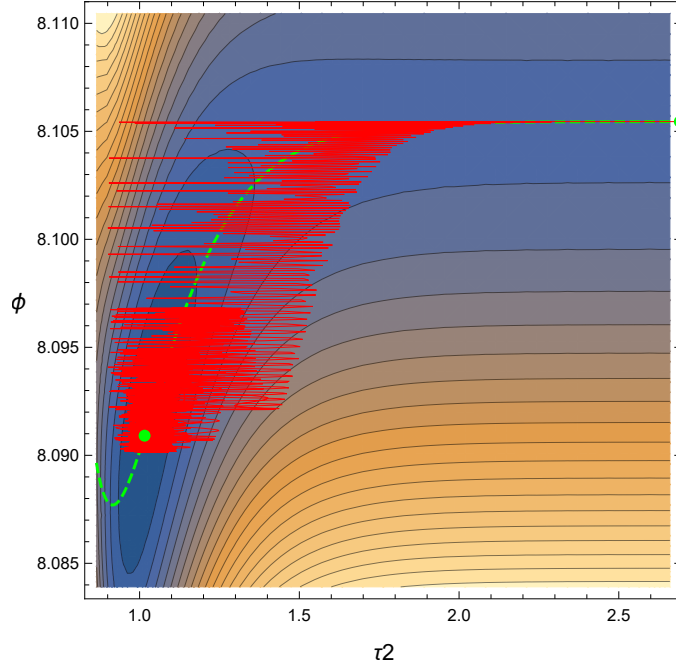


Figure 4.10: Inflationary trajectory in the (τ_2, ϕ) plane for the case $R \sim 10^{-3}$ of example 2. The green dashed line represents the curve of local minima of ϕ and τ_3 for each value of τ_2 and the green dots represent the end of inflation (the one on the right) and the global minimum (the one on the left).

\mathbf{H}_{inf}	\mathbf{m}_ϕ	\mathbf{m}_{inf}	$\mathbf{\Gamma}_\phi$	$\mathbf{\Gamma}_{\text{inf}}$
1.97532×10^9	5.93167×10^{10}	5.86169×10^{13}	7.0007×10^{-7}	1.10863×10^7

Table 4.6: Values of the physical quantities of the model in GeV for the case $R \sim 10^{-3}$ of example 2.

After calculating the duration of the epoch of inflaton domination

$$N_{mod1} \simeq 3.45,$$

we can find the initial conditions for our system of differential equations from (4.62) and (4.63). In this case we find a period of modulus domination which extends (if we consider $t_1 = 0$) roughly between $t_{eq} \simeq \frac{1}{H_{eq}} \simeq 6.31597 \times 10^{-5} \text{ GeV}^{-1}$ and $t_{\phi,dec} = \frac{1}{\Gamma_\phi} \simeq 1.42843 \times 10^6 \text{ GeV}^{-1}$. More precisely, numerically solving the equations, we find

$$t_{dom,beg} = 3.48375 \times 10^{-5} \text{ GeV}^{-1}, \quad t_{dom,end} = 1.50528 \times 10^6 \text{ GeV}^{-1},$$

respectively for the beginning and end of this period, and the total duration of the epoch in number of e-folding is

$$N_{mod2} \simeq 15.90.$$

We can finally give a prediction for the total duration of inflation N_e^{tot} and some of the observables at the horizon exit $N_e^* = N_e^{end} - N_e^{tot}$. From (4.75) we find

$$N_e^{tot} \simeq 45.69,$$

and for the observables

$$\epsilon = 3.57306 \times 10^{-13}, \quad r = 16\epsilon = 5.7169 \times 10^{-12},$$

and

$$P_s(K_{cs} = 0) = 4.25996 \times 10^{-10}, \quad n_s = 0.954692.$$

To exactly match the power spectrum value we could take $K_{cs} = -0.140927$.

$R \sim 10^{-4}$

Now can now continue our study taking

$$\lambda_2 = \frac{1}{10000} \Rightarrow R \simeq 0.000099$$

together with

$$A_2 = 1.27 \times 10^{-8}, \quad A_3 = 1.53288 \times 10^{10}, \quad W_0 = 0.00667356,$$

and

$$\xi = 25.9208, \quad 0.057087 < g_s < 0.171261, \quad g_s = 0.114174,$$

which precisely give the minima in table 4.7.

	τ_2	τ_3	τ_1	vol	ϕ	$\delta\phi$
predicted	1	6	210.905	3048.18	8.0223	0.00153199
calculated	1.01562	6.01697	220.59	3261.51	8.08995	0.00142451

Table 4.7: Values of the minima for the case $R \sim 10^{-4}$ of example 2. The “predicted” values are the ones given by the approximations in (4.13) and (4.42), whereas the “calculated” ones are those found with the potential (4.5).

Figure 4.11 shows the evolution of the inflaton and the volume modulus in the last efoldings, after the end of inflation. In particular, we can see that with a small R the oscillations of the volume modulus seem “damped”. Actually, as we discussed in section 4.2.1, the volume is constantly following its new local minimum (which changes depending on the position of the inflaton) and it oscillates around it. The situation is illustrated also in figure 4.12. We expect that for smaller values of R the oscillations are more and more reduced, and that in the limit $R \rightarrow 0$ they are reduced to zero since the volume is expected to follow adiabatically its minimum.

We can now turn to analyze the post inflationary scenario. We first give the values of the Hubble parameter, the masses and the decay rates in table 4.8.

After the inflaton decays, we can numerically solve equations (4.72). We can estimate the ratio $\frac{H_{eq}}{\Gamma_\phi} \simeq 2.00451 \times 10^8 \gg 1$; we should expect a period of matter domination as in the case $R \sim 10^{-3}$.

After calculating the duration of the epoch of inflaton domination

$$N_{mod1} \simeq 2.73,$$

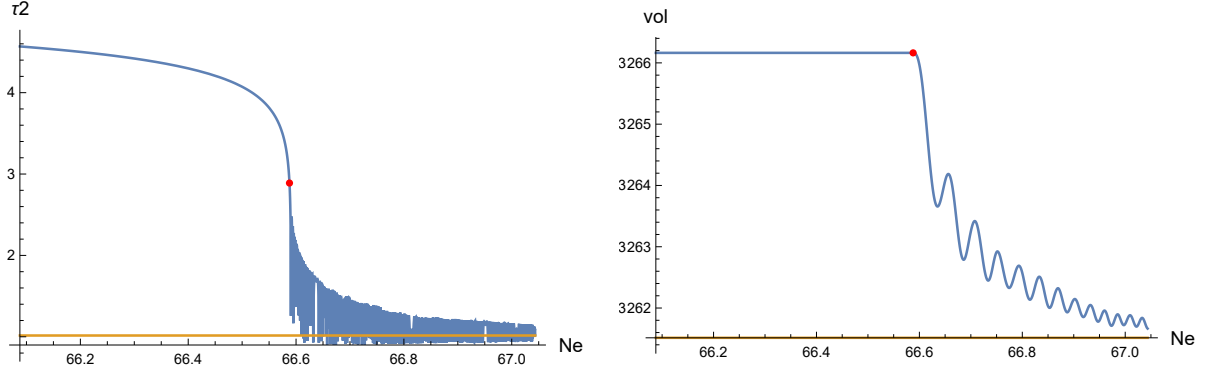


Figure 4.11: Evolution of the inflaton and the volume modulus during the last efoldings for the case $R \sim 10^{-4}$ of example 2.

$\mathbf{H_{inf}}$	$\mathbf{m_\phi}$	$\mathbf{m_{inf}}$	$\mathbf{\Gamma_\phi}$	$\mathbf{\Gamma_{inf}}$
6.14718×10^8	5.78452×10^{10}	5.71427×10^{13}	6.49249×10^{-7}	1.02608×10^7

Table 4.8: Values of the physical quantities of the model in GeV for the case $R \sim 10^{-4}$ of example 2.

we can find the initial conditions for our system of differential equations (4.72) from (4.62) and (4.63). We actually find a period of modulus domination which extends (if we consider $t_1 = 0$) roughly between $t_{eq} \simeq \frac{1}{H_{eq}} \simeq 7.68389 \times 10^{-3} \text{ GeV}^{-1}$ and $t_{\phi dec} = \frac{1}{\Gamma_\phi} \simeq 1.54024 \times 10^6 \text{ GeV}^{-1}$. More precisely, numerically solving the equations, we find

$$t_{dom,beg} = 4.24364 \times 10^{-3} \text{ GeV}^{-1}, \quad t_{dom,end} = 1.6231 \times 10^6 \text{ GeV}^{-1},$$

and the total duration of this epoch in number of efoldings is

$$N_{mod2} \simeq 12.75.$$

We can finally give a prediction for the total duration of inflation N_e^{tot} and some of the observables at the horizon exit $N_e^* = N_e^{end} - N_e^{tot}$. From (4.75) we find

$$N_e^{tot} \simeq 46.05,$$

and for the observables

$$\epsilon = 3.4119 \times 10^{-14}, \quad r = 16\epsilon = 5.45904 \times 10^{-13},$$

and

$$P_s(K_{cs} = 0) = 4.32049 \times 10^{-10}, \quad n_s = 0.955075.$$

In order to exactly match the normalization we need $K_{cs} = -0.155035$.

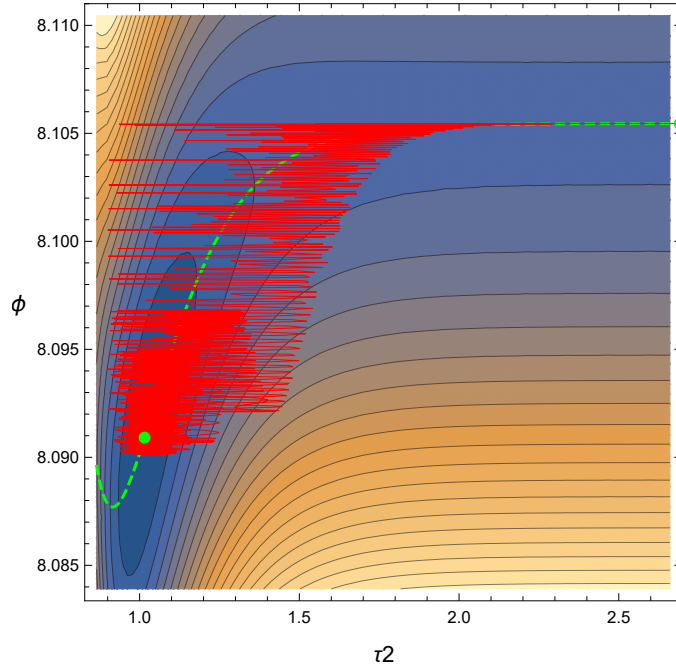


Figure 4.12: Inflationary trajectory in the (τ_2, ϕ) plane for the case $R \sim 10^{-4}$ of example 2. The green dashed line represents the curve of local minima of ϕ and τ_3 for each value of τ_2 and the greens dot represents the end of inflation (the one on the right) and the global minimum (the one on the left).

$R \sim 10^{-8}$

After having shown the different behavior the solutions have for smaller and smaller values of R , we now come to study what is the first value we could find in order to avoid a period of modulus domination. For such small value of R the software we used was not able to solve the oscillations following the end of inflation, and we will not attach the plots in this section; however, we already discuss enough the consequences of small R and there is no reason to worry about that anymore.

For the Calabi-Yau we choose the parameters

$$\lambda_2 = 10^{-8} \quad \Rightarrow \quad R \simeq 10^{-8},$$

and we find

$$\xi = 25.9208, \quad 0.0570871 < g_s < 0.171261, \quad g_s = 0.114174.$$

To obtain the minima in table 4.9, the constraints impose

$$A_2 = 1.14136 \times 10^{-12}, \quad A_3 = 1.37761 \times 10^{10} \quad W_0 = 0.00599684.$$

The physical parameters are given in table 4.10 and from them it can be calculated the ratio

$$\frac{H_{eq}}{\Gamma_\phi} \simeq 1.46972.$$

	τ_2	τ_3	τ_1	vol	ϕ	$\delta\phi$
predicted	1	6	210.889	3047.84	8.02219	1.53906×10^{-7}
calculated	1.01562	6.01697	220.575	3261.17	8.08984	1.42153×10^{-7}

Table 4.9: Values of the minima for the case $R \sim 10^{-8}$ of example 2. The “predicted” values are the ones given by the approximations in (4.13) and (4.42), whereas the “calculated” ones are those found with the potential (4.5).

H_{inf}	m_ϕ	m_{inf}	Γ_ϕ	Γ_{inf}
5.53046×10^6	5.19872×10^{10}	5.13538×10^{13}	4.71301×10^{-7}	7.44682×10^6

Table 4.10: Values of the physical quantities of the model in GeV for the case $R \sim 10^{-8}$ of example 2.

This is the biggest value of R for which $\frac{H_{eq}}{\Gamma_\phi} \sim \mathcal{O}(1)$, and it is hence crucial to study the system (4.72). In particular, as we anticipated this is the first case in which there is no volume domination, as shown in figure 4.13; the hypothetical time of equilibrium was expected to be $t_{eq} \simeq 1.44367 \times 10^6 \text{ GeV}^{-1}$, but the curves never meet, as shown in figure 4.13.

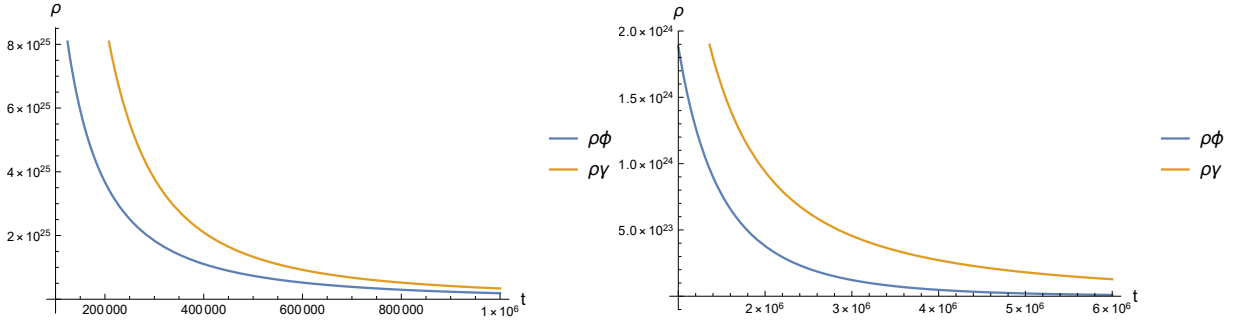


Figure 4.13: Post inflationary scenario for the case $R \sim 10^{-8}$ of example 2. The time of equilibrium was expected to be at $t_{eq} \simeq 1.44367 \times 10^6 \text{ GeV}^{-1}$, but actually radiation always dominates.

Considering that in this case $N_{mod1} \simeq 0$ and $N_{mod2} \simeq 0$ the number of efoldings is

$$N_e^{tot} \simeq 47.58.$$

For what concerns the observables we find

$$\epsilon = 2.76292 \times 10^{-18}, \quad r = 16\epsilon = 4.42068 \times 10^{-17},$$

$$P_s(K_{cs} = 0) = 4.31849 \times 10^{-10};$$

in order to exactly match the normalization we need $K_{cs} = -0.154573$. In this case n_s could not be evaluated due to computational imprecisions.

In conclusion, it is now clear that in this model we can avoid a period of volume modulus domination in the post-inflationary epoch for values $R \lesssim 10^{-8}$.

4.4.3 Example 3

Finally, this last example shows a more realistic scenario for Kähler moduli inflation, as now the volume is of order $\mathcal{V} \sim 10^5$ and we use hundreds of moduli. From a qualitatively point of view, the output is exactly the same of the previous example and this further confirms the predictions we made. For the minima we choose

$$\tau_2 = 1, \quad \tau_3 = 4.5,$$

and for the Calabi-Yau manifold we fix

Calabi-Yau parameters		
n	α	λ_3
100	1	5/98

We recall that $\lambda_3 = \lambda'_3/(n-2)$, and in this case $\lambda'_3 = 5$. This value has been chosen in order to give a larger value of the volume, according to (4.25).

We underline once again that the output of this model is the same as the case of a Calabi-Yau with $n = 3$ and $\lambda_3 = 5$.

$R \sim 10^{-3}$

We start with the case

$$\lambda_2 = \frac{1}{200} \quad \Rightarrow \quad R \simeq 0.00099.$$

To obtain the chosen minima we find

$$A_2 = 1.10139 \times 10^{-6}, \quad A_3 = 94151, \quad W_0 = 0.960163,$$

which more precisely give the values in table 4.11. We assign

$$\xi = 80.4762, \quad 0.0268241 < g_s < 0.0804723, \quad g_s = 0.0536482.$$

	τ_2	τ_3	τ_1	vol	ϕ	$\delta\phi$
predicted	1	4.5	3908.8	244332	12.4063	0.016872
calculated	1.00064	4.5007	3916.12	245019	12.4091	0.0179098

Table 4.11: Values of the minima for the case $R \sim 10^{-3}$ of example 3. The “predicted” values are the ones given by the approximations in (4.13) and (4.42), whereas the “calculated” ones are those found with the potential (4.5).

This case is similar to the case of $R \sim 10^{-3}$ of example 2, as it can be seen in figure 4.14 and 4.15.

For what concerns the post-inflationary scenario, the masses and the other important quantities are given in table 4.12.

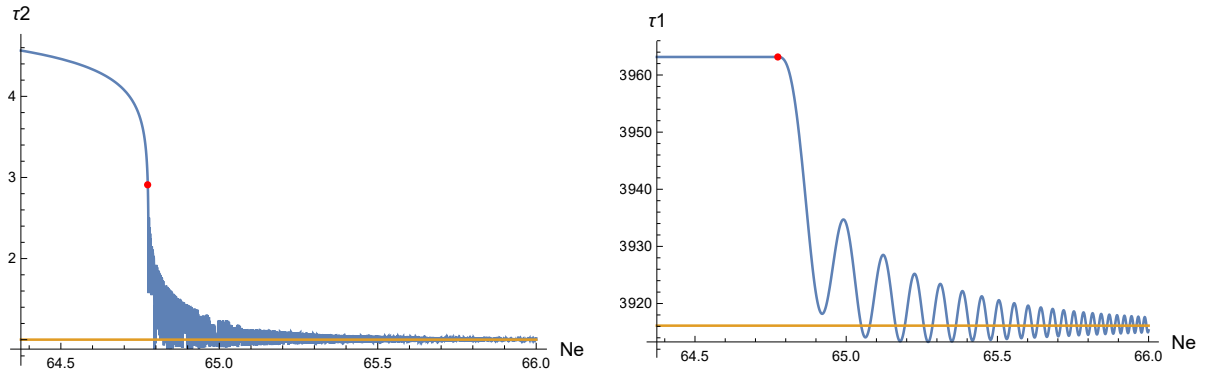


Figure 4.14: Evolution of the inflaton and the volume modulus during the last efoldings for the case $R \sim 10^{-3}$ of example 3.

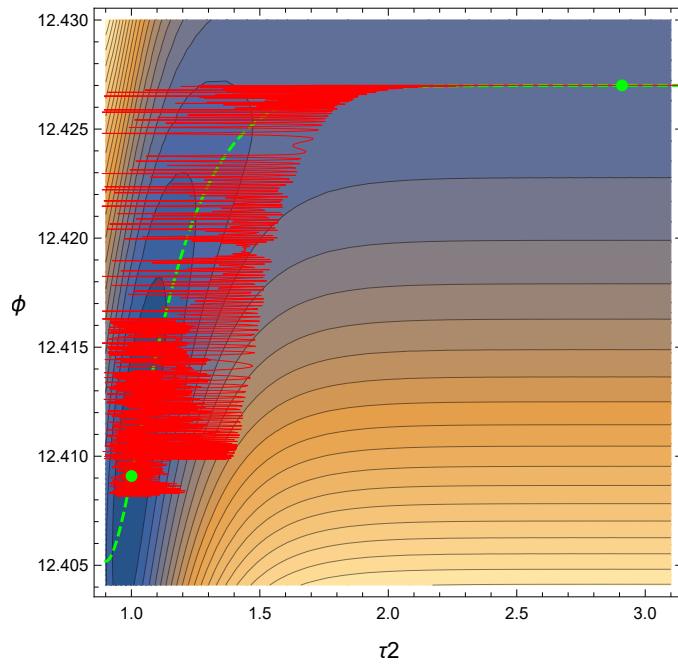


Figure 4.15: Inflationary trajectory in the (τ_2, ϕ) plane for the case $R \sim 10^{-3}$ of example 3. The green dashed line represents the curve of local minima of ϕ and τ_3 for each value of τ_2 and the greens dot represents the end of inflation (the one on the right) and the global minimum (the one on the left).

\mathbf{H}_{inf}	\mathbf{m}_ϕ	\mathbf{m}_{inf}	$\mathbf{\Gamma}_\phi$	$\mathbf{\Gamma}_{\text{inf}}$
9.45042×10^8	2.71433×10^{10}	1.07393×10^{14}	6.70807×10^{-8}	5.1169×10^9

Table 4.12: Values of the physical quantities in GeV for the case $R \sim 10^{-3}$ of example 3.

We expect a period of matter domination as we can calculate $\frac{H_{\text{eq}}}{\Gamma_\phi} \simeq 3.875 \times 10^{13} \gg 1$. Indeed, we find

$$N_{\text{mod}1} \simeq 0, \quad N_{\text{mod}2} \simeq 20.87$$

which give a total number of efoldings of

$$N_e^{\text{tot}} \simeq 44.64. \quad (4.89)$$

For the observables we have

$$\epsilon = 2.37771 \times 10^{-14}, \quad r = 16\epsilon = 3.80434 \times 10^{-13},$$

and

$$P_s(K_{cs} = 0) = 6.88506 \times 10^{-10}, \quad n_s = 0.95368.$$

To exactly match the COBE normalization we find $K_{cs} = -0.621021$.

$\mathbf{R} \sim 10^{-5}$

We now decrease the value of R about two orders of magnitude; we should expect plots of moduli evolution similar to the ones in figure 4.11. We take

$$\lambda_2 = \frac{1}{10000} \Rightarrow R \simeq 0.0000199.$$

To obtain the chosen minima we find

$$A_2 = 2.11389 \times 10^{-8}, \quad A_3 = 90352, \quad W_0 = 0.920233,$$

which more precisely give the values in table 4.13. We assign

$$\xi = 80.473, \quad 0.0268248 < g_s < 0.0804744, \quad g_s = 0.0536496.$$

	τ_2	τ_3	τ_1	vol	ϕ	$\delta\phi$
predicted	1	4.5	3905.45	244018.	12.405	0.000355052
calculated	1.00064	4.5007	3912.77	244705.	12.4078	0.000348543

Table 4.13: Values of the minima for the case $R \sim 10^{-5}$ of example 3. The “predicted” values are the ones given by the approximations in (4.13) and (4.42), whereas the “calculated” ones are those found with the potential (4.5).

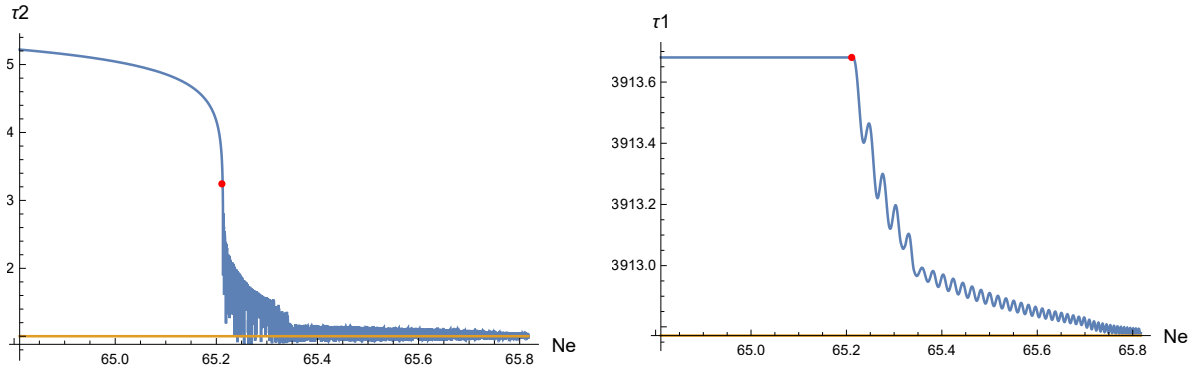


Figure 4.16: Evolution of the inflaton and the volume modulus during the last efoldings for the case $R \sim 10^{-5}$ of example 3.

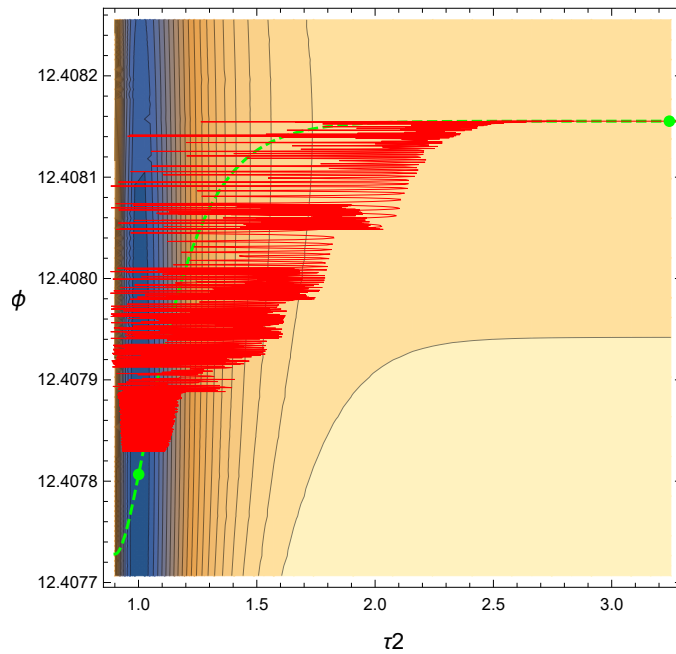


Figure 4.17: Inflationary trajectory in the (τ_2, ϕ) plane for the case $R \sim 10^{-5}$ of example 3. The green dashed line represents the curve of local minima of ϕ and τ_3 for each value of τ_2 and the greens dot represents the end of inflation (the one on the right) and the global minimum (the one on the left).

\mathbf{H}_{inf}	\mathbf{m}_ϕ	\mathbf{m}_{inf}	$\mathbf{\Gamma}_\phi$	$\mathbf{\Gamma}_{\text{inf}}$
1.29891×10^8	2.60646×10^{10}	1.03059×10^{14}	5.9397×10^{-8}	4.51628×10^9

Table 4.14: Values of the physical quantities in GeV for the case $R \sim 10^{-5}$ for example 3.

From figures 4.16 and 4.17 it is evident that the behavior is the same we found in example 2, which confirms again the predictions of section 4.2.

For what concerns the post-inflationary scenario, the masses and the other important quantities are given in table 4.14.

We expect a period of matter domination as we can calculate $\frac{H_{eq}}{\Gamma_\phi} \simeq 2.05562 \times 10^9 \gg 1$. Indeed, we find

$$N_{mod1} \simeq 0, \quad N_{mod2} \simeq 14.30$$

which give a total number of efoldings of

$$N_e^{tot} \simeq 45.28. \quad (4.90)$$

For the observables we have

$$\epsilon = 4.40583 \times 10^{-16}, \quad r = 16\epsilon = 7.04933 \times 10^{-15},$$

and

$$P_s(K_{cs} = 0) = 7.01953 \times 10^{-10}, \quad n_s = 0.954508.$$

To exactly match the COBE normalization we find $K_{cs} = -0.640364$.

$\mathbf{R} \sim 10^{-9}$

Also in this case we explore whether it is possible to avoid a period of volume domination below a certain value of R . We point out that in this case we were not able to compute the complete set of equations due to computational difficulties linked to such a small value of R ; for this reason we did not to predict the observables and the value of W_0 is not optimized to match the COBE normalization, but it as been chosen to be of the same order of the previous cases. However, we could still calculate all the quantities we need in order to analyze the post-inflationary scenario. In this case we have

$$\lambda_2 = \frac{1}{3} \times 10^{-7} \quad \Rightarrow \quad R \simeq 6.66 \times 10^{-9} \quad (4.91)$$

and

$$A_2 = 7.26399 \times 10^{-12}, \quad A_3 = 93143.1, \quad W_0 = 0.948636.$$

The values of the minima are given in table 4.15. We assign

$$\xi = 80.4729, \quad 0.0268248 < g_s < 0.0804745, \quad g_s = 0.0536497.$$

Finally, with the values in table 4.16 we can analyze the post-inflationary scenario. In this case, the inflaton quickly decays ($N_{mod1} \simeq 0$) and from the estimate

	τ_2	τ_3	τ_1	vol	ϕ	$\delta\phi$
predicted	1	4.5	3905.38	244012	12.405	1.18477×10^{-7}
calculated	1.00064	4.5007	3912.71	244698	12.4078	1.16117×10^{-7}

Table 4.15: Values of the minima for the case $R \sim 10^{-9}$ of example 3. The “predicted” values are the ones given by the approximations in (4.13) and (4.42), whereas the “calculated” ones are those found with the potential (4.5).

H_{inf}	m_ϕ	m_{inf}	Γ_ϕ	Γ_{inf}
2.44535×10^6	2.68702×10^{10}	1.06243×10^{14}	6.50761×10^{-8}	4.94777×10^9

Table 4.16: Values of the physical quantities in GeV for the case $R \sim 10^{-9}$ of example 3.

$$\frac{H_{eq}}{\Gamma_\phi} = 3.91237 \sim \mathcal{O}(1)$$

it is clear that we should carefully study the system (4.72) to verify if there is a period of matter domination. In this example there is not, as after the inflaton decay the universe is always radiation dominated. In fact, the hypothetical time of equilibrium was expected to be $t_{eq} \simeq 3.9277 \times 10^6 \text{ GeV}^{-1}$, but the curves never meet, as shown in figure 4.18.

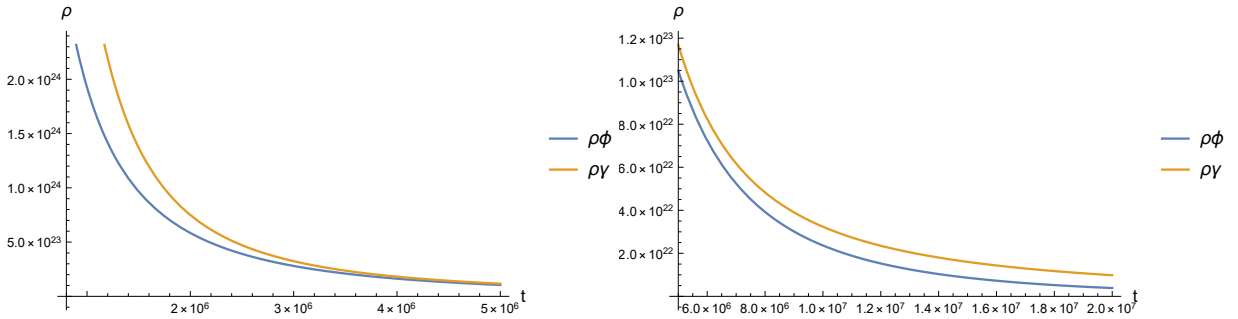


Figure 4.18: Post inflationary scenario for the case $R \sim 10^{-9}$ of example 3. The time of equilibrium was expected to be at $t_{eq} \simeq 3.9277 \times 10^6 \text{ GeV}^{-1}$, but actually radiation always dominates.

Hence, it is now clear that also in this case for values $R \lesssim 10^{-9}$ we can avoid a period of volume modulus domination in the post-inflationary epoch.

4.4.4 Remarks on numerical analysis

We now make some comments about the numerical analysis performed in this section, in order to enlighten some important implications of the study we have carried on.

- The hierarchy between λ_2 and λ_3 and between τ_2 and τ_3 implies a hierarchy also in A_2 and A_3 , typically $A_2 \ll 1$ and $A_3 \gg 1$.
- In every example, W_0 has been assigned numerically: it can be noted that once fixed the fundamental parameters n, α, λ_3 and the minima τ_i , for any choice of λ_2 the value of

W_0 was always found to be of the same order. This fact could be understood looking at equations (4.54) and (4.55): once those parameters are fixed, these quantities depend only on λ_2 , A_2 and W_0 . In particular, also considering the dependence on λ_2 and W_0 of V_0 in (4.30), we have

$$\begin{cases} P_s & \propto \frac{W_0^4 \lambda_2^4}{A_2^2} e^{2a_2 \tau_2^*} \\ e^{a_2 \tau_2^*} & \propto N_e^{tot} \frac{A_2}{\lambda_2^2 W_0} \end{cases} \Rightarrow P_s \propto (N_e^{tot})^2 W_0^2;$$

since N_e^{tot} takes values in a small range (4.76) and $P_s = 3.7 \times 10^{-10}$ it follows that W_0 has roughly the same value for any value of R . Finally, equation (4.15) implies

$$\frac{\lambda_2 W_0}{A_2} = const$$

which entails that with an almost fixed W_0 the value of A_2 changes with λ_2 , and in particular

$$A_2 \propto \lambda_2.$$

- The value of ϵ_s scales with λ_2 : with the same considerations as above and (4.4.4) we realize that

$$\epsilon_s \propto \frac{W_0^2}{V_0^2} A_2^2 \propto \frac{A_2^2}{\lambda_2^3} \propto \frac{1}{\lambda_2}.$$

- Given that W_0 is roughly constant, also the masses are fixed. Thus taking smaller and smaller values of R , the effect is to decrease H_{inf} as it follows from equation (4.48).
- There are cases where there is a large difference between H_{inf} and the masses m_{inf} and m_ϕ . This fact could lead to a ratio $\frac{H_{inf}}{\Gamma_{inf}} < 1$, which, according to (4.61), should give $N_{mod1} < 0$. This is of course not correct, and we need to keep in mind that the inflaton acquires mass at the end of inflation. Hence, in cases with such large masses the inflaton decays soon after the end of inflation and we should set $N_{mod1} \simeq 0$, as was done in example 3.
- Where possible, all the values have been estimated numerically. For example, the masses have been calculated using $m_1^2 \simeq \det(K^{-\tilde{1}} M^2) / m_2^2 m_3^2$ and $m_i^2 = 1/2 K^{ii} V_{ii}$ $i = 2, 3$ (see appendix A), where all the quantities have been evaluated numerically using the full potential and the full metric of section 4.1. These values all agree with our approximations, as it can be readily verified.

CONCLUSIONS

The low energy limit of type IIB string theory compactifications represents a useful source of 4D $\mathcal{N} = 1$ supergravity models which can be used to provide a coherent description of cosmological evolution. In particular, such models are suitable to describe inflation thanks to the Kähler moduli which arise from this procedure.

In this thesis we have studied the multi-field case of a class of inflationary models with Kähler moduli. Indeed, string compactifications usually produce to a lot of fields, easily $n \sim \mathcal{O}(100)$: it is commonly believed that a large value of n is sufficient to build a realistic model and to achieve stabilization between moduli inflationary and post-inflationary minima, making this shift very small.

In this work we have shown that a large value of moduli cannot actually be used to stabilize the minima. Indeed, a large value of n would require an extremely large volume \mathcal{V} in order to reproduce a Minkowskian global minimum, and this is not phenomenologically acceptable. Therefore, we showed that one possibility to achieve stabilization is to act on the intersection numbers λ_i , and in particular on the one associated with the inflaton: while λ_i for the spectator fields ($i = 3, 4, \dots, n$) should be chosen in order to compensate the effect of a large number of particles, the intersection number λ_2 of the inflaton mainly controls the R parameter and it must be made very small. Furthermore, we have shown that this result strictly depends on the specific choice of the uplift term

$$V_{up} = \frac{D}{\mathcal{V}^\gamma}$$

and the considerations we made could be partially relaxed for $\gamma \lesssim 2$.

Studying the case $R \ll 1$ we derived a relation between the mass of the volume modulus and the Hubble constant during inflation, showing that the ratio m_ϕ/H_{inf} is always bigger than 1 and that it depends on R . Thus, we concluded that the friction term of moduli equations never dominates and that during inflation the fields (in particular the volume modulus) are free to follow their local minima until the global minimum, exhibiting at most some small oscillations around them after the end of inflation. We then analyzed the post-inflationary scenario, giving the tools to estimate whether an epoch of volume modulus domination is present or not. In particular, a rough estimate suggests that we could be able to avoid this epoch for $R \lesssim 10^{-8}$ (at least for some specific cases) and that in principle it could be always forbidden for sufficiently small values of R .

Finally, we numerically solved the system of differential equations for the moduli evolution during

inflation and for the energy density evolution after inflation, in order to test our predictions and study whether we could avoid a period of volume domination. In particular, we found that for small R the system really behaves as we expected: at the end of inflation, the volume follows its local minimum until the global one instead of remaining fixed in its inflationary minimum. In addition, we verified that for a given model there exists $R \ll 1$ such that we can avoid a period of volume domination after inflation. In particular, this assures us that the model is free from the cosmological moduli problem and that there is no tension at all with the success of the Big Bang nucleosynthesis.

In this thesis a lot of attention has been given to the study of the post-inflationary dynamics. Indeed, this period is crucial to predict and understand lots of aspect of the cosmological evolution.

First of all, the presence of periods of matter domination after inflation has an important effect on the number of efoldings between horizon exit of the modes relevant for CMB observation and the end of inflation. This value is fundamental to make inflationary predictions for the spectral index n_s and the tensor-to-scalar ratio r . In particular, the preferred number of efoldings was found to be around $N_e^{tot} \approx 45$, which is smaller than the usual estimate $N_e^{tot} \approx 50$; this also causes a reduction at the percent level of the spectral index.

Secondly, the post-inflationary period is necessary to understand how the energy is transferred after the end of inflation via a process of reheating. This is extremely important for model building, as we need to know how the particles of the Standard Model and of the hidden sector are produced: volume modulus domination would imply that they are mainly generated by the volume decay, whereas on the other case they would be generated by the inflaton decay. Consequently, a study of reheating requires also an analysis of all moduli and their decay modes. In particular, it is important to calculate the energy density injected into Standard Model compared to the energy density injected into the hidden sector. Indeed, realistic models have to take into account the correction $\Delta N_{eff} = N_{eff} - N_{eff,SM}$ to the number of neutrino species $N_{eff,SM} = 3$, since observations do not seem to show a clear preference for $\Delta N_{eff} > 0$; excessive branching ratio to the hidden sector would lead to $\Delta N_{eff} \gg 1$ and would spoil the BBN predictions.

In conclusion, it is fundamental to distinguish if there is a period of modulus domination or not in order to be able to correctly predict lots of essential observables and to build suitable models to describe cosmological evolution.

APPENDIX A

COMPUTATIONAL DETAILS

A.1 Preliminar considerations on mass terms

We discuss here how to find the masses of the fields in Kähler moduli inflationary models. Indeed, the moduli we used in our potential (4.5) are not canonically normalized, and we cannot read the mass terms from the Lagrangian.

Let us now label the fields as $\hat{\tau}_i$ and indicate their minimum as τ_i as usual; we can expand them around this point as

$$\hat{\tau}_i = \tau_i + \delta\tau_i.$$

Then we can also expand the Lagrangian about the minimum and find

$$\begin{aligned}\mathcal{L}_{kin} &= K_{ij}\partial_\mu(\delta\tau_i)\partial^\mu(\delta\tau_j), \\ \mathcal{L}_{mass} &= -(M^2)_{ij}(\delta\tau_i)(\delta\tau_j),\end{aligned}$$

where

$$(M^2)_{ij} = \frac{1}{2}V_{ij} = \frac{1}{2}\frac{\partial^2 V}{\partial\hat{\tau}_i\partial\hat{\tau}_j}\Big|_{\tau_i,\tau_j} \equiv \frac{1}{2}\frac{\partial^2 V}{\partial\tau_i\partial\tau_j}.$$

In order to find the canonically normalized fields we must look for τ_i^c such that

$$\mathcal{L}_{kin} = \frac{1}{2}\partial_\mu(\delta\tau_i^c)\partial^\mu(\delta\tau_i^c).$$

In particular, we have to look for a transformation for the vector $\delta\tau$

$$\delta\tau \equiv \begin{pmatrix} \delta\tau_1 \\ \delta\tau_2 \\ \vdots \\ \delta\tau_n \end{pmatrix} = \frac{1}{\sqrt{2}}U\delta\tau^c = \frac{1}{\sqrt{2}}(u_1 \quad u_2 \quad \dots \quad u_n) \begin{pmatrix} \delta\tau_1^c \\ \delta\tau_2^c \\ \vdots \\ \delta\tau_n^c \end{pmatrix} \quad (\text{A.1})$$

where U is the $n \times n$ matrix of the mass eigenvectors u_i , and $\delta\tau^c$ is the column vector of the canonically normalized fields.

Applying this transformation to the kinetic Lagrangian written in a compact form (\tilde{K} is now the metric, not to be confused with the Kähler potential) we find

$$\partial_\mu(\delta\tau)^\dagger \tilde{K} \partial^\mu(\delta\tau) = \frac{1}{2} \partial_\mu(\delta\tau^c)^\dagger U^\dagger \tilde{K} U \partial^\mu(\delta\tau^c)$$

and if we want to obtain the canonical form we need

$$U^\dagger \tilde{K} U = \begin{pmatrix} u_1^\dagger \\ u_2^\dagger \\ \dots \\ u_3^\dagger \end{pmatrix} \tilde{K} (u_1 \quad u_2 \quad \dots \quad u_3) = \begin{pmatrix} u_1^\dagger \tilde{K} u_1 & u_1^\dagger \tilde{K} u_2 & \dots & u_1^\dagger \tilde{K} u_n \\ u_2^\dagger \tilde{K} u_1 & \ddots & & \vdots \\ \vdots & & \ddots & \vdots \\ u_n^\dagger \tilde{K} u_1 & u_n^\dagger \tilde{K} u_2 & \dots & u_n^\dagger \tilde{K} u_n \end{pmatrix} = I_{n \times n} \quad (\text{A.2})$$

which implies $u_i^\dagger \tilde{K} u_j = \delta_{ij}$, which is finally the normalization relation for the eigenvectors. For the mass terms we have

$$(\delta\tau)^\dagger M^2(\delta\tau) = \frac{1}{2} (\delta\tau^c)^\dagger U^\dagger M^2 U (\delta\tau^c);$$

if $\delta\tau^c$ represents the correct mass eigenstates $U^\dagger M^2 U$ must be diagonal and its entries (i.e. its eigenvalues) are the squared masses of the fields. From explicit calculations we get

$$U^\dagger M^2 U = \begin{pmatrix} u_1^\dagger \\ u_2^\dagger \\ \dots \\ u_3^\dagger \end{pmatrix} M^2 (u_1 \quad u_2 \quad \dots \quad u_3) = \begin{pmatrix} u_1^\dagger M^2 u_1 & u_1^\dagger M^2 u_2 & \dots & u_1^\dagger M^2 u_n \\ u_2^\dagger M^2 u_1 & \ddots & & \vdots \\ \vdots & & \ddots & \vdots \\ u_n^\dagger M^2 u_1 & u_n^\dagger M^2 u_2 & \dots & u_n^\dagger M^2 u_n \end{pmatrix} \quad (\text{A.3})$$

with $u_i^\dagger M^2 u_j = m_i^2 \delta_{ij}$. Therefore, if we want to calculate the masses, we need to diagonalize

$$\tilde{K}^{-1} M^2,$$

which satisfies

$$\tilde{K}^{-1} M^2 u_i = m_i^2 u_i \quad (\text{A.4})$$

as it can be readily shown from

$$u_i^\dagger M^2 u_j = u_i^\dagger \tilde{K} (\tilde{K}^{-1} M^2) u_j = m_j^2 u_i^\dagger \tilde{K} u_j = m_j^2 \delta_{ij}.$$

A.2 Kähler metric

We now give explicit computation for the Kähler metric K_{ij} in the large volume limit. Recalling that $\frac{\partial}{\partial T_i} = \frac{1}{2} \frac{\partial}{\partial \tau_i}$

$$K_1 = \frac{1}{2} \frac{\partial K}{\partial \tau_1} = -\frac{\frac{3}{2} \alpha \sqrt{\tau_1}}{(\mathcal{V} + \frac{\xi}{2})} \simeq -\frac{3 \alpha \sqrt{\tau_1}}{2 \mathcal{V}},$$

$$K_i \stackrel{i \neq 1}{=} \frac{1}{2} \frac{\partial K}{\partial \tau_i} = \frac{\frac{3}{2} \alpha \lambda_i \sqrt{\tau_i}}{(\mathcal{V} + \frac{\xi}{2})} \simeq \frac{3 \alpha \lambda_i \sqrt{\tau_i}}{2 \mathcal{V}}$$

and

$$K_{11} = \frac{1}{2} \frac{\partial}{\partial \tau_1} K_1 \simeq -\frac{3}{4} \alpha \left(\frac{1}{2} \frac{1}{\mathcal{V} \sqrt{\tau_1}} - \frac{3}{2} \frac{\alpha \tau_1}{\mathcal{V}^2} \right) \simeq \frac{3}{4} \frac{1}{\tau_1^2}, \quad (\text{A.5})$$

$$K_{1j} \stackrel{j \neq 1}{=} \frac{1}{2} \frac{\partial}{\partial \tau_j} K_1 \simeq \frac{3}{4} \frac{\alpha \sqrt{\tau_1}}{\mathcal{V}^2} \left(-\frac{3}{2} \alpha \lambda_j \sqrt{\tau_j} \right) \simeq -\frac{9}{8} \frac{\lambda_j \sqrt{\tau_j}}{\tau_1^{5/2}}, \quad (\text{A.6})$$

$$K_{ij} \stackrel{i, j \neq 1}{=} \frac{1}{2} \frac{\partial}{\partial \tau_j} K_i \simeq \frac{3}{4} \alpha \left(\frac{1}{2} \frac{\lambda_i}{\sqrt{\tau_i} \mathcal{V}} \delta_{ij} - \frac{\lambda_i \sqrt{\tau_i}}{\mathcal{V}^2} \left(-\frac{3}{2} \alpha \lambda_j \sqrt{\tau_j} \right) \right) \quad (\text{A.7})$$

where we approximated $\mathcal{V} \simeq \alpha \tau_1^{3/2}$ and more precisely for $i, j > 1$

$$K_{ii} \simeq \frac{3}{8} \frac{\lambda_i}{\tau_1^{3/2} \sqrt{\tau_i}}, \quad (\text{A.8})$$

$$K_{ij} \stackrel{i \neq j}{\simeq} \frac{9}{8} \frac{\lambda_i \lambda_j \sqrt{\tau_i} \sqrt{\tau_j}}{\tau_1^3}. \quad (\text{A.9})$$

From now on, we will always implicitly consider $i, j > 1$. The full matrix has the form

$$\tilde{K} = \begin{pmatrix} \frac{3}{4} \frac{1}{\tau_1^2} & -\frac{9}{8} \frac{\lambda_2 \sqrt{\tau_2}}{\tau_1^{5/2}} & -\frac{9}{8} \frac{\lambda_3 \sqrt{\tau_3}}{\tau_1^{5/2}} & \cdots & -\frac{9}{8} \frac{\lambda_n \sqrt{\tau_n}}{\tau_1^{5/2}} \\ -\frac{9}{8} \frac{\lambda_2 \sqrt{\tau_2}}{\tau_1^{5/2}} & \frac{3}{8} \frac{\lambda_2}{\tau_1^{3/2} \sqrt{\tau_2}} & \frac{9}{8} \frac{\lambda_3 \lambda_2 \sqrt{\tau_3} \sqrt{\tau_2}}{\tau_1^3} & \cdots & \frac{9}{8} \frac{\lambda_n \lambda_2 \sqrt{\tau_n} \sqrt{\tau_2}}{\tau_1^3} \\ -\frac{9}{8} \frac{\lambda_3 \sqrt{\tau_3}}{\tau_1^{5/2}} & \frac{9}{8} \frac{\lambda_3 \lambda_2 \sqrt{\tau_3} \sqrt{\tau_2}}{\tau_1^3} & \frac{3}{8} \frac{\lambda_3}{\tau_1^{3/2} \sqrt{\tau_3}} & \ddots & \vdots \\ \vdots & \vdots & \ddots & \ddots & \vdots \\ -\frac{9}{8} \frac{\lambda_n \sqrt{\tau_n}}{\tau_1^{5/2}} & \frac{9}{8} \frac{\lambda_n \lambda_2 \sqrt{\tau_n} \sqrt{\tau_2}}{\tau_1^3} & \cdots & \frac{9}{8} \frac{\lambda_n \lambda_{n-1} \sqrt{\tau_n} \sqrt{\tau_{n-1}}}{\tau_1^3} & \frac{3}{8} \frac{\lambda_n}{\tau_1^{3/2} \sqrt{\tau_n}} \end{pmatrix}. \quad (\text{A.10})$$

From these calculations, with $\tau_1 \gg 1$ we can readily find its inverse

$$K^{11} \simeq \frac{4}{3} \tau_1^2, \quad (\text{A.11})$$

$$K^{ii} \simeq \frac{8}{3} \frac{\tau_1^{3/2} \sqrt{\tau_i}}{\lambda_i}, \quad (\text{A.12})$$

$$K^{1i} \simeq 4 \tau_1 \tau_i, \quad (\text{A.13})$$

$$K^{ij} \simeq 4 \tau_i \tau_j. \quad (\text{A.14})$$

In particular the first two terms can be found simply by taking $K^{ii} \simeq \frac{1}{K_{ii}}$, which ensure that $(K^{-1}K)_{ii} \simeq 1$ (at leading order in $\frac{1}{\mathcal{V}}$), whereas the last ones are chosen in order to obtain exactly $(K^{-1}K)_{ij} = 0$ for $i \neq j$. Actually, in the latter we could have also taken $K^{ij} \simeq 0$, since the product $(K^{-1}K)_{ij}$ would have been close enough to zero (order $\mathcal{O}(\frac{1}{\tau_1})$) and these terms would have been much smaller than all the other entries of the inverse matrix. However, we prefer to keep these terms in order to obtain more precise results.

The complete inverse matrix is then

$$\tilde{K}^{-1} = \begin{pmatrix} \frac{4}{3}\tau_1^2 & 4\tau_1\tau_2 & 4\tau_1\tau_3 & \dots & 4\tau_1\tau_n \\ 4\tau_1\tau_2 & \frac{8}{3}\frac{\tau_1^{3/2}\sqrt{\tau_2}}{\lambda_2} & 4\tau_2\tau_3 & \dots & 4\tau_2\tau_n \\ 4\tau_1\tau_3 & 4\tau_2\tau_3 & \frac{8}{3}\frac{\tau_1^{3/2}\sqrt{\tau_3}}{\lambda_3} & \ddots & \vdots \\ \vdots & \vdots & \ddots & \ddots & 4\tau_n\tau_{n-1} \\ 4\tau_1\tau_n & 4\tau_2\tau_n & \dots & 4\tau_n\tau_{n-1} & \frac{8}{3}\frac{\tau_1^{3/2}\sqrt{\tau_n}}{\lambda_n} \end{pmatrix}. \quad (\text{A.15})$$

To test these approximations, we can check the large volume limit of the expression (4.2) and (4.3) and see that the calculations of this section agree with them.

A.3 Potential calculations

We now turn to calculate the second derivatives of the large volume limit potential (4.7), essential to calculate the mass matrix. It is useful to rewrite the potential with $\mathcal{V} \simeq \alpha\tau_1^{3/2}$

$$V = \sum_{i=2}^n \mu_i \frac{\sqrt{\hat{\tau}_i}}{\hat{\tau}_1^{3/2}} e^{-2a_i\hat{\tau}_i} - \sum_{i=2}^n \nu_i \frac{\hat{\tau}_i}{\hat{\tau}_1^3} e^{-a_i\hat{\tau}_i} + \frac{\zeta}{\hat{\tau}_1^{9/2}} + \frac{\beta}{\hat{\tau}_1^4} \quad (\text{A.16})$$

where we assigned for brevity

$$\begin{aligned} \mu_i &= \frac{8(a_i A_i)^2}{3\alpha^2 \lambda_i}, & \nu_i &= \frac{4W_0 a_i A_i}{\alpha^2}, \\ \zeta &= \frac{3\xi W_0^2}{4\alpha^3}, & \beta &= \frac{C_{up} W_0^2}{\alpha^{8/3}}. \end{aligned}$$

As before, for the derivatives we use the notation $V_i = \left. \frac{\partial V}{\partial \hat{\tau}_i} \right|_{\tau_i} = \frac{\partial V}{\partial \tau_i}$.

For the first derivatives we have

$$\begin{aligned} \frac{\partial V}{\partial \hat{\tau}_1} &= -\sum_{i=2}^n \frac{3}{2} \mu_i \frac{\sqrt{\hat{\tau}_i}}{\hat{\tau}_1^{5/2}} e^{-2a_i\hat{\tau}_i} + \sum_{i=2}^n 3\nu_i \frac{\hat{\tau}_i}{\hat{\tau}_1^4} e^{-a_i\hat{\tau}_i} - \frac{9}{2} \frac{\zeta}{\hat{\tau}_1^{11/2}} - 4 \frac{\beta}{\hat{\tau}_1^5}, \\ \frac{\partial V}{\partial \hat{\tau}_i} &= \frac{\mu_i}{\hat{\tau}_1^{3/2}} \left[\frac{1}{2\sqrt{\hat{\tau}_i}} - 2a_i\sqrt{\hat{\tau}_i} \right] e^{-2a_i\hat{\tau}_i} - \frac{\nu_i}{\hat{\tau}_1^3} [1 - a_i\hat{\tau}_i] e^{-a_i\hat{\tau}_i}. \end{aligned}$$

Then, the second derivatives are

$$\frac{\partial^2 V}{\partial \hat{\tau}_1^2} = \sum_{i=2}^n \frac{15}{4} \mu_i \frac{\sqrt{\hat{\tau}_i}}{\hat{\tau}_1^{7/2}} e^{-2a_i\hat{\tau}_i} - \sum_{i=2}^n 12\nu_i \frac{\hat{\tau}_i}{\hat{\tau}_1^5} e^{-a_i\hat{\tau}_i} + \frac{99}{4} \frac{\zeta}{\hat{\tau}_1^{13/2}} + 20 \frac{\beta}{\hat{\tau}_1^6} \quad (\text{A.17})$$

$$\frac{\partial^2 V}{\partial \hat{\tau}_1 \partial \hat{\tau}_i} = -3 \frac{\mu_i}{\hat{\tau}_1^{5/2}} a_i \sqrt{\hat{\tau}_i} \left[-1 + \frac{1}{4a_i\hat{\tau}_i} \right] e^{-2a_i\hat{\tau}_i} + 3 \frac{\nu_i}{\hat{\tau}_1^4} a_i \hat{\tau}_i \left[-1 + \frac{1}{a_i\hat{\tau}_i} \right] e^{-a_i\hat{\tau}_i}, \quad (\text{A.18})$$

$$\frac{\partial^2 V}{\partial \hat{\tau}_i^2} = \frac{\mu_i}{\hat{\tau}_1^{3/2}} 4a_i^2 \sqrt{\hat{\tau}_i} \left[1 - \frac{1}{2a_i\hat{\tau}_i} - \frac{1}{16a_i^2\hat{\tau}_i^2} \right] e^{-2a_i\hat{\tau}_i} - \frac{\nu_i}{\hat{\tau}_1^3} a_i^2 \hat{\tau}_i \left[1 - \frac{2}{a_i\hat{\tau}_i} \right] e^{-a_i\hat{\tau}_i}, \quad (\text{A.19})$$

$$\frac{\partial^2 V}{\partial \hat{\tau}_i \partial \hat{\tau}_j} = \delta_{ij} \frac{\partial^2 V}{\partial \hat{\tau}_i^2}. \quad (\text{A.20})$$

Using $\epsilon_i = \frac{1}{4a_i\tau_i}$ and the relations (4.10), that we can rewrite as

$$e^{-a_i\tau_i} = \frac{m_i}{\tau_1^{3/2}} \frac{(1-4\epsilon_i)}{(1-\epsilon_i)} \sqrt{\tau_i}, \quad m_i = \frac{3\lambda_i W_0}{4a_i A_i},$$

and noting that $\nu_i = 2m_i\mu_i$, we can easily evaluate the derivatives in the minima τ_i

$$V_{1i} = \frac{\partial^2 V}{\partial \tau_1 \partial \tau_i} = -3 \frac{\mu_i m_i^2}{\tau_1^{11/2}} a_i \tau_i^{3/2} \frac{(1-4\epsilon_i)^2}{(1-\epsilon_i)}, \quad (\text{A.21})$$

$$V_{ii} = \frac{\partial^2 V}{\partial \tau_i \partial \tau_i} = 2 \frac{\mu_i m_i^2}{\tau_1^{9/2}} a_i^2 \tau_i^{3/2} \frac{(1-4\epsilon_i)}{(1-\epsilon_i)} (1-2\epsilon_i). \quad (\text{A.22})$$

For V_{11} , using the equivalent of (4.11)

$$4 \frac{\beta}{\tau_1^4} = -\frac{9}{2} \frac{\zeta}{\tau_1^{9/2}} + \sum_{i=2}^n \frac{9}{2} \mu_i m_i^2 \frac{\tau_i^{3/2}}{\tau_1^{9/2}} \frac{(1-4\epsilon_i)}{(1-\epsilon_i)^2} \quad (\text{A.23})$$

we have

$$V_{11} = \frac{\partial^2 V}{\partial \tau_1 \partial \tau_1} = \frac{9}{4} \frac{1}{\tau_1^{13/2}} \left[\sum_{i=2}^n \tau_i^{3/2} \mu_i m_i^2 \frac{(1-4\epsilon_i)(1+4\epsilon_i)}{(1-\epsilon_i)^2} + \zeta \right];$$

this expression can be manipulated a little bit more using the full expression for ζ and (4.14) for $\epsilon_i \ll 1$

$$\zeta \stackrel{\epsilon_i \ll 1}{\simeq} 2\alpha \sum_{i=2}^n \lambda_i \tau_i^{3/2} (1-18\epsilon_i)$$

together with the assumptions (4.22) and $\mu_i m_i^2 = \frac{3W_0^2 \lambda_i}{2\alpha^2}$

$$\begin{aligned} V_{11} &\stackrel{\epsilon_i \ll 1}{\simeq} \frac{27}{8} \frac{W_0^2}{\alpha^2 \tau_1^{13/2}} \left[\sum_{i=2}^n \tau_i^{3/2} (1+2\epsilon_i) + \frac{\xi}{2\alpha} \right] \\ &= \frac{27}{4} \frac{W_0^2}{\alpha^2 \tau_1^{13/2}} \left[\sum_{i=2}^n \tau_i^{3/2} (1-8\epsilon_i) \right] \\ &= \frac{27}{4} \frac{W_0^2}{\alpha^2 \tau_1^{13/2}} \left\{ \lambda_2 \tau_2^{3/2} (1-8\epsilon_2) \left[1 + (n-2) \frac{\lambda_3 \tau_3^{3/2} (1-8\epsilon_3)}{\lambda_2 \tau_2^{3/2} (1-8\epsilon_2)} \right] \right\} \\ &\simeq \frac{27}{4} \frac{W_0^2}{\alpha^2 \tau_1^{13/2}} \left\{ \lambda_2 \tau_2^{3/2} (1-8\epsilon_2) \left[1 + \frac{1}{R} \frac{\tau_3^{3/2} (1-8\epsilon_3)}{\tau_2^{3/2} (1-8\epsilon_2)} \right] \right\} \\ &\simeq \frac{27}{4} \frac{W_0^2}{\alpha^2 \tau_1^{13/2}} \lambda_3 (n-2) \tau_3^{3/2} (1-8\epsilon_3) \end{aligned} \quad (\text{A.24})$$

where we used $R \simeq \frac{\lambda_2}{(n-2)\lambda_3} \ll 1$.

Finally, for the second derivatives at the first order in ϵ_i we obtain

$$V_{11} = \frac{\partial^2 V}{\partial \tau_1 \partial \tau_1} = \frac{27}{4} \frac{W_0^2}{\alpha^2 \tau_1^{13/2}} \lambda_3 (n-2) \tau_3^{3/2} (1 - 8\epsilon_3), \quad (\text{A.25})$$

$$V_{1i} = \frac{\partial^2 V}{\partial \tau_1 \partial \tau_i} = -\frac{9}{2} \frac{W_0^2}{\alpha^2} \lambda_i \frac{a_i \tau_i^{3/2}}{\tau_1^{11/2}} (1 - 7\epsilon_i), \quad (\text{A.26})$$

$$V_{ii} = \frac{\partial^2 V}{\partial \tau_i \partial \tau_i} = 3 \frac{W_0^2}{\alpha^2} \lambda_i \frac{a_i^2 \tau_i^{3/2}}{\tau_1^{9/2}} (1 - 5\epsilon_i). \quad (\text{A.27})$$

A.4 Masses computation

Now that we have all the elements we need, we can proceed with the calculation of the eigenvalues of $\tilde{K}^{-1}M^2$. Before addressing the general case for an arbitrary value of n , it is useful to study the case $n = 3$ and $n = 4$; the first allows us to find the dominant terms in the matrix, whereas the second helps us to generalize the calculation to a generic n .

To find the squared masses we simply consider that

$$\det(\tilde{K}^{-1}M^2) = m_1^2 m_2^2 \dots m_n^2, \quad (\text{A.28})$$

$$\text{Tr}[\tilde{K}^{-1}M^2] = m_1^2 + m_2^2 + \dots + m_n^2. \quad (\text{A.29})$$

Since $m_1 \ll m_i$ as τ_1 mainly corresponds to the volume modulus, as we will see in a moment, and $m_i \simeq m_j$, $\forall i \neq j$, the values for the masses are

$$m_i^2 \simeq \frac{\text{Tr}[\tilde{K}^{-1}M^2]}{n-1}, \quad (\text{A.30})$$

$$m_1^2 \simeq \frac{\det(\tilde{K}^{-1}M^2)}{\left(\frac{\text{Tr}[\tilde{K}^{-1}M^2]}{n-1}\right)^{n-1}}. \quad (\text{A.31})$$

In particular, to be more precise, $m_i = m_j$ only if the minima are all equal and if $a_i = a_j$, as it will be clear in the following section.

A.4.1 n=3

Let us write down the matrix

$$\begin{aligned}
\tilde{K}^{-1}M^2 &= \begin{pmatrix} (\tilde{K}^{-1}M^2)_{11} & (\tilde{K}^{-1}M^2)_{12} & (\tilde{K}^{-1}M^2)_{13} \\ (\tilde{K}^{-1}M^2)_{21} & (\tilde{K}^{-1}M^2)_{22} & (\tilde{K}^{-1}M^2)_{23} \\ (\tilde{K}^{-1}M^2)_{31} & (\tilde{K}^{-1}M^2)_{32} & (\tilde{K}^{-1}M^2)_{33} \end{pmatrix} \\
&= \frac{1}{2} \begin{pmatrix} K^{11}V_{11} + K^{12}V_{21} + K^{13}V_{31} & K^{11}V_{12} + K^{12}V_{22} & K^{11}V_{13} + K^{13}V_{33} \\ K^{21}V_{11} + K^{22}V_{21} + K^{23}V_{31} & K^{21}V_{12} + K^{22}V_{22} & K^{21}V_{13} + K^{23}V_{33} \\ K^{31}V_{11} + K^{32}V_{21} + K^{33}V_{31} & K^{31}V_{12} + K^{32}V_{22} & K^{31}V_{13} + K^{33}V_{33} \end{pmatrix} \\
&\simeq \frac{1}{2} \begin{pmatrix} K^{11}V_{11} + K^{13}V_{31} & K^{11}V_{12} + K^{12}V_{22} & K^{11}V_{13} + K^{13}V_{33} \\ K^{22}V_{21} & K^{22}V_{22} & K^{21}V_{13} + K^{23}V_{33} \\ K^{33}V_{31} & K^{31}V_{12} + K^{32}V_{22} & K^{33}V_{33} \end{pmatrix}
\end{aligned}$$

where we used $\tau_1 \gg 1$ and $R \simeq \frac{\lambda_2}{\lambda_3} \ll 1$. In particular, we can explicit the order in $\frac{1}{\tau_1}$ of the matrix entries as

$$\tilde{K}^{-1}M^2 \sim \begin{pmatrix} \mathcal{O}(\frac{1}{\tau_1^{9/2}}) & \mathcal{O}(\frac{\lambda_2}{\tau_1^{7/2}}) & \mathcal{O}(\frac{1}{\tau_1^{7/2}}) \\ \mathcal{O}(\frac{1}{\tau_1^4}) & \mathcal{O}(\frac{1}{\tau_1^3}) & \mathcal{O}(\frac{1}{\tau_1^{9/2}}) \\ \mathcal{O}(\frac{1}{\tau_1^4}) & \mathcal{O}(\frac{\lambda_2}{\tau_1^{9/2}}) & \mathcal{O}(\frac{1}{\tau_1^3}) \end{pmatrix} \quad (\text{A.32})$$

It is now clear that the trace is

$$\text{Tr}[\tilde{K}^{-1}M^2] \simeq \frac{1}{2} (K^{22}V_{22} + K^{33}V_{33}), \quad (\text{A.33})$$

and that the masses of the blow-ups are roughly

$$m_2^2 \simeq \frac{1}{2}K^{22}V_{22} \simeq \frac{4W_0^2}{\alpha^2} \frac{1}{\tau_1^3} a_2^2 \tau_2^2 (1 - 5\epsilon_2), \quad (\text{A.34})$$

$$m_3^2 \simeq \frac{1}{2}K^{33}V_{33} \simeq \frac{4W_0^2}{\alpha^2} \frac{1}{\tau_1^3} a_3^2 \tau_3^2 (1 - 5\epsilon_3). \quad (\text{A.35})$$

We now turn to calculate the determinant: from (A.32) we see that the relevant terms are

$$\begin{aligned}
\det(\tilde{K}^{-1}M^2) &= + (\tilde{K}^{-1}M^2)_{11}(\tilde{K}^{-1}M^2)_{22}(\tilde{K}^{-1}M^2)_{33} \\
&\quad - (\tilde{K}^{-1}M^2)_{13}(\tilde{K}^{-1}M^2)_{22}(\tilde{K}^{-1}M^2)_{31} \\
&\quad - (\tilde{K}^{-1}M^2)_{12}(\tilde{K}^{-1}M^2)_{21}(\tilde{K}^{-1}M^2)_{33}, \quad (\text{A.36})
\end{aligned}$$

and $\det(\tilde{K}^{-1}M^2) \sim \mathcal{O}(\frac{1}{\tau_1^{21/2}})$. We could be tempted to keep only the first term of this expression in order to estimate the mass simply as $m_1^2 \simeq \frac{1}{2}K^{11}V_{11}$; this is actually not a good estimate, as explicit calculations show that the first two terms cancel up to the second order in ϵ_i .

With a lot of patience we can calculate these three terms, obtaining

$$\begin{aligned} (\tilde{K}^{-1}M^2)_{11}(\tilde{K}^{-1}M^2)_{22}(\tilde{K}^{-1}M^2)_{33} &= -144 \frac{W_0^6}{\alpha^6 \tau_1^{21/2}} \lambda_3 (a_3^3 \tau_3^{9/2}) (a_2^2 \tau_2^2) [(1 - 14\epsilon_3 + 61\epsilon_3^2)(1 - 5\epsilon_2)] , \\ (\tilde{K}^{-1}M^2)_{13}(\tilde{K}^{-1}M^2)_{22}(\tilde{K}^{-1}M^2)_{31} &= -144 \frac{W_0^6}{\alpha^6 \tau_1^{21/2}} \lambda_3 (a_3^3 \tau_3^{9/2}) (a_2^2 \tau_2^2) [(1 - 14\epsilon_3 + 63\epsilon_3^2)(1 - 5\epsilon_2)] , \\ (\tilde{K}^{-1}M^2)_{12}(\tilde{K}^{-1}M^2)_{21}(\tilde{K}^{-1}M^2)_{33} &= -144 \frac{W_0^6}{\alpha^6 \tau_1^{21/2}} \lambda_2 (a_3^2 \tau_3^2) (a_2^3 \tau_2^{9/2}) [(1 - 14\epsilon_2 + 63\epsilon_2^2)(1 - 5\epsilon_3)] . \end{aligned}$$

Hence, the determinant is

$$\begin{aligned} \det(\tilde{K}^{-1}M^2) &\simeq 144 \frac{W_0^6}{\alpha^6 \tau_1^{21/2}} \lambda_3 (a_3^3 \tau_3^{9/2}) (a_2^2 \tau_2^2) (1 - 5\epsilon_2) \times \\ &\quad \times \left[2\epsilon_3^2 + \frac{\lambda_2 a_2 \tau_2^{5/2}}{\lambda_3 a_3 \tau_3^{5/2}} (1 - 14\epsilon_2 + 63\epsilon_2^2) \frac{(1 - 5\epsilon_3)}{(1 - 5\epsilon_2)} \right] \\ &\simeq 144 \frac{W_0^6}{\alpha^6 \tau_1^{21/2}} \lambda_3 (a_3^3 \tau_3^{9/2}) (a_2^2 \tau_2^2) (1 - 5\epsilon_2) \times \\ &\quad \times \left[2\epsilon_3^2 + R \frac{a_2 \tau_2^{5/2}}{a_3 \tau_3^{5/2}} (1 - 9\epsilon_2)(1 - 5\epsilon_3) \right] \\ &\simeq 288 \frac{W_0^6}{\alpha^6 \tau_1^{21/2}} \lambda_3 (a_3^3 \tau_3^{9/2}) (a_2^2 \tau_2^2) (1 - 5\epsilon_2) \epsilon_3^2 \\ &\simeq 18 \frac{W_0^6}{\alpha^6 \tau_1^{21/2}} \lambda_3 (a_3 \tau_3^{5/2}) (a_2^2 \tau_2^2) (1 - 5\epsilon_2) , \end{aligned} \tag{A.37}$$

where the R term can be neglected if $R \ll \frac{a_2^{3/2} \epsilon_2^{5/2}}{a_3^{3/2} \epsilon_3^{1/2}}$, which can be easily achieved.

Finally, the mass term is

$$m_1^2 \simeq \frac{\det(\tilde{K}^{-1}M^2)}{m_2^2 m_3^2} \simeq \frac{9}{8} \frac{W_0^2}{\alpha^2 \tau_1^{9/2}} \lambda_3 \frac{\tau_3^{1/2}}{a_3} (1 + 5\epsilon_3) . \tag{A.38}$$

Solving $\tilde{K}^{-1}M^2 u_i = m_i^2 u_i$ we can find the eigenvectors

$$u_i = \begin{pmatrix} (u_i)_1 \\ (u_i)_2 \\ (u_i)_3 \end{pmatrix}$$

and we can then write the original fields in term of the canonically normalized ones

$$\begin{aligned} \delta\tau &= \begin{pmatrix} \delta\tau_1 \\ \delta\tau_2 \\ \delta\tau_3 \end{pmatrix} = \frac{1}{\sqrt{2}} \begin{pmatrix} u_1 \\ u_2 \\ u_3 \end{pmatrix} \delta\tau_1^c + \frac{1}{\sqrt{2}} \begin{pmatrix} u_2 \\ u_3 \end{pmatrix} \delta\tau_2^c + \frac{1}{\sqrt{2}} \begin{pmatrix} u_3 \end{pmatrix} \delta\tau_3^c \\ &= \frac{1}{\sqrt{2}} \begin{pmatrix} (u_1)_1 \delta\tau_1^c + (u_2)_1 \delta\tau_2^c + (u_3)_1 \delta\tau_3^c \\ (u_1)_2 \delta\tau_1^c + (u_2)_2 \delta\tau_2^c + (u_3)_2 \delta\tau_3^c \\ (u_1)_3 \delta\tau_1^c + (u_2)_3 \delta\tau_2^c + (u_3)_3 \delta\tau_3^c \end{pmatrix} . \end{aligned} \tag{A.39}$$

We sketch here the main dependence of the fields on the big modulus τ_1 , in order understand the connection of fields we are using with the canonical ones. Referring to [25], considering $\tau_2 = \tau_3 = \tau_s$ the results are

$$\begin{aligned}\delta\tau_1 &\sim (\tau_1) \frac{\delta\tau_1^c}{\sqrt{2}} + \left(\tau_1^{1/4}\tau_s^{3/4}\right) \frac{\delta\tau_2^c}{\sqrt{2}} + \left(\tau_1^{1/4}\tau_s^{3/4}\right) \frac{\delta\tau_3^c}{\sqrt{2}}, \\ \delta\tau_2 &\sim (a_2^{-1}) \frac{\delta\tau_1^c}{\sqrt{2}} + \left(\tau_1^{3/4}\tau_s^{1/4}\right) \frac{\delta\tau_2^c}{\sqrt{2}} + \left(\tau_1^{-3/4}\tau_s^{7/4}\right) \frac{\delta\tau_3^c}{\sqrt{2}}, \\ \delta\tau_3 &\sim (a_3^{-1}) \frac{\delta\tau_1^c}{\sqrt{2}} + \left(\tau_1^{-3/4}\tau_s^{7/4}\right) \frac{\delta\tau_2^c}{\sqrt{2}} + \left(\tau_1^{3/4}\tau_s^{1/4}\right) \frac{\delta\tau_3^c}{\sqrt{2}}.\end{aligned}\tag{A.40}$$

In particular, from these relations we can see that the volume modulus $\mathcal{V} \sim \tau_1^{3/2}$ is mostly τ_1^c and the inflaton τ_2 is mostly τ_2^c and consequently the masses are

$$\begin{aligned}m_\phi^2 &\simeq m_1^2, \\ m_{inf}^2 &\simeq m_2^2.\end{aligned}$$

A.4.2 n=4

Following the reasoning of the previous section, in this case the matrix $\tilde{K}^{-1}M^2$ is readily found to be

$$\tilde{K}^{-1}M^2 \simeq \frac{1}{2} \begin{pmatrix} K^{11}V_{11} + 2K^{13}V_{31} & K^{11}V_{12} + K^{12}V_{22} & K^{11}V_{13} + K^{13}V_{33} & K^{11}V_{13} + K^{13}V_{33} \\ K^{22}V_{21} & K^{22}V_{22} & K^{21}V_{13} + K^{23}V_{33} & K^{21}V_{13} + K^{23}V_{33} \\ K^{33}V_{31} & K^{31}V_{12} + K^{32}V_{22} & K^{33}V_{33} & K^{31}V_{13} + \tilde{K}^{33}V_{33} \\ K^{33}V_{31} & K^{31}V_{12} + K^{32}V_{22} & K^{31}V_{13} + \tilde{K}^{33}V_{33} & K^{33}V_{33} \end{pmatrix},$$

where we used (4.22), which also implies $\tau_4 \rightarrow \tau_3$, and $\tilde{K}^{33} \equiv K^{34}$, not to be confused with K^{33} . It is useful to rename the matrix elements in order to find a well defined structure that could be easily extended to the general case; we define

$$\tilde{K}^{-1}M^2 \equiv \begin{pmatrix} a_4 & h & i & i \\ d & b & l & l \\ e & f & c & g \\ e & f & g & c \end{pmatrix}.\tag{A.41}$$

The order in $\frac{1}{\tau_1}$ of these terms can be gathered from (A.32) and the new term is $g \sim \mathcal{O}(\frac{1}{\tau_1^{9/2}})$. The determinant is

$$\det(\tilde{K}^{-1}M^2) = a_4 \begin{vmatrix} b & l & l \\ f & c & g \\ f & g & c \end{vmatrix} - h \begin{vmatrix} d & l & l \\ e & c & g \\ e & g & c \end{vmatrix} + i \begin{vmatrix} d & b & l \\ e & f & g \\ e & f & c \end{vmatrix} - i \begin{vmatrix} d & b & l \\ e & f & c \\ e & f & g \end{vmatrix}\tag{A.42}$$

$$= a_4 \begin{vmatrix} b & l & l \\ f & c & g \\ f & g & c \end{vmatrix} - h \begin{vmatrix} d & l & l \\ e & c & g \\ e & g & c \end{vmatrix} + 2i \begin{vmatrix} d & b & l \\ e & f & g \\ e & f & c \end{vmatrix};\tag{A.43}$$

keeping the dominant terms ($\mathcal{O}(\frac{1}{\tau_1^{27/2}})$) we are left with

$$\det(\tilde{K}^{-1}M^2) = a_4bcc - hdcc - 2ibec \simeq a_4bcc - 2ibec,\tag{A.44}$$

where the last step is justified by the fact that $h \sim \mathcal{O}(\frac{\lambda_2}{\tau_1^{7/2}})$ and that we are interested in the case $R \ll 1$, which implies $\lambda_2 \ll 1$, as we discussed in 4.2. This is equivalent to discard the term $(\tilde{K}^{-1}M^2)_{12}(\tilde{K}^{-1}M^2)_{21}(\tilde{K}^{-1}M^2)_{33}$ in (A.36), which is precisely what we did in (A.37).

With this notation

$$\begin{aligned} m_2^2 &\simeq b, \\ m_3^2 &\simeq c, \\ m_1^2 &\simeq \frac{\det(\tilde{K}^{-1}M^2)}{bcc} \simeq a_4 - 2\frac{ie}{c}. \end{aligned}$$

A.4.3 Generic n

We are now ready to generalize what we have done until now to the most generic case. The matrix (A.41) is extended to

$$\tilde{K}^{-1}M^2 \equiv \begin{pmatrix} a_n & h & i & i & \dots & i \\ d & b & l & l & \dots & l \\ e & f & c & g & \dots & g \\ e & f & g & c & \ddots & \vdots \\ \vdots & \vdots & \vdots & \ddots & \ddots & g \\ e & f & g & \dots & g & c \end{pmatrix}, \quad (\text{A.45})$$

where $a_n = \frac{1}{2}(K^{11}V_{11} + (n-2)K^{13}V_{31})$.

The determinant is

$$\det(\tilde{K}^{-1}M^2) \simeq a_n bc^{n-2} - (n-2)ibec^{n-3} \quad (\text{A.46})$$

and the masses

$$\begin{aligned} m_2^2 &\simeq b, \\ m_3^2 &\simeq c, \\ m_1^2 &\simeq \frac{\det(\tilde{K}^{-1}M^2)}{bc^{n-2}} \simeq a_n - (n-2)\frac{ie}{c}. \end{aligned}$$

Recalling that

$$\begin{aligned} a_n &= \frac{1}{2}(K^{11}V_{11} + (n-2)K^{13}V_{31}), \\ i &= \frac{1}{2}(K^{11}V_{13} + K^{13}V_{33}), \\ e &= \frac{1}{2}K^{33}V_{31}, \\ c &= \frac{1}{2}K^{33}V_{33} \end{aligned}$$

we find

$$\begin{aligned}
a_n &= -9 \frac{W_0^2}{\alpha^2} \frac{1}{\tau_1^{9/2}} \lambda_3 (n-2) a_3 \tau_3^{5/2} (1 - 9\epsilon_3 + 16\epsilon_3^2), \\
i &= 6 \frac{W_0^2}{\alpha^2} \frac{1}{\tau_1^{7/2}} \lambda_3 a_3^2 \tau_3^{5/2} (1 - 7\epsilon_3 + 14\epsilon_3^2), \\
e &= -6 \frac{W_0^2}{\alpha^2} \frac{1}{\tau_1^4} a_3 \tau_3^2 (1 - 7\epsilon_3), \\
c &= 4 \frac{W_0^2}{\alpha^2} \frac{1}{\tau_1^3} a_3^2 \tau_3^2 (1 - 5\epsilon_3),
\end{aligned}$$

from which we can explicitly evaluate the mass term

$$m_1^2 \simeq \frac{9}{8} \frac{W_0^2}{\alpha^2} \frac{1}{\tau_1^{9/2}} \lambda_3 (n-2) \frac{\tau_3^{1/2}}{a_3} (1 + 5\epsilon_3). \quad (\text{A.47})$$

From this expression the mass of the volume seems to depend on the number of moduli; however, if we recall the discussion of section 4.2, we immediately realize that

$$\lambda_3(n-2) = \lambda'_3 \simeq \mathcal{O}(10).$$

Hence, we conclude that in principle the volume modulus mass increases with the number of moduli, but in practice the constraints of the model force it to be independent from n ,

$$m_\phi^2 \simeq m_1^2 \simeq \frac{9}{8} \frac{W_0^2}{\alpha^2} \frac{1}{\tau_1^{9/2}} \lambda'_3 \frac{\tau_3^{1/2}}{a_3} (1 + 5\epsilon_3). \quad (\text{A.48})$$

B.1 Constraints for a generic uplift

In this section we will explicitly calculate some constraints of the model used in section 4.1.2 using a generic uplift

$$V_{up} = W_0^2 \frac{C_{up}}{\mathcal{V}^\gamma}, \quad 1 \leq \gamma < 3 \quad (\text{B.1})$$

and referring to the potential (4.7). The goal is to understand the link between the specific uplift choice and the number of moduli n .

We start requiring

$$\left. \frac{\partial V_{LARGE}}{\partial \mathcal{V}} \right|_{\mathcal{V}_*} = 0$$

which gives

$$\sum_{i=2}^n \frac{8(a_i A_i)^2 \sqrt{\tau_i}}{3\mathcal{V}_* \lambda_i \alpha} e^{-2a_i \tau_i} - \sum_{i=2}^n 8W_0 \frac{a_i A_i}{\mathcal{V}_*^2} \tau_i e^{-a_i \tau_i} + \frac{9\xi W_0^2}{4\mathcal{V}_*^3} + \gamma \frac{C_{up} W_0^2}{\mathcal{V}_*^\gamma} = 0. \quad (\text{B.2})$$

Substituting the minima (4.10) and multiplying by \mathcal{V}_*^3 we obtain

$$\sum_{i=2}^n \alpha \lambda_i W_0^2 \tau_i^{3/2} \left[\frac{3(1-4\epsilon_i)^2}{2(1-\epsilon_i)^2} - 6 \frac{(1-4\epsilon_i)}{(1-\epsilon_i)} \right] + \frac{9\xi W_0^2}{4} + \gamma C_{up} W_0^2 \mathcal{V}_*^{3-\gamma} = 0,$$

and after a little algebra

$$\xi = 2\alpha \sum_{i=2}^n \left[\lambda_i \frac{(1-4\epsilon_i)}{(1-\epsilon_i)^2} \tau_i^{\frac{3}{2}} \right] - \frac{4}{9} \gamma C_{up} \mathcal{V}_*^{3-\gamma}. \quad (\text{B.3})$$

Calculating V_{LARGE}^{min} , substituting again the minima (4.10) and $\mathcal{V} = \mathcal{V}_*$ and using the relation

(B.3)

$$\begin{aligned}
V_{LARGE}^{min} &= \sum_{i=2}^n \frac{\alpha \lambda_i W_0^2}{\mathcal{V}_*^3} \tau_i^{3/2} \left[\frac{3(1-4\epsilon_i)^2}{2(1-\epsilon_i)^2} - 3 \frac{(1-4\epsilon_i)}{(1-\epsilon_i)} \right] + \frac{3\xi W_0^2}{4\mathcal{V}_*^3} + \frac{C_{up} W_0^2}{\mathcal{V}_*^\gamma} \\
&= \frac{W_0^2}{\mathcal{V}_*^3} \left\{ \sum_{i=2}^n \frac{\alpha \lambda_i}{(1-\epsilon_i)^2} \tau_i^{3/2} \left(-\frac{3}{2} + 3\epsilon_i + 12\epsilon_i^2 \right) + C_{up} \mathcal{V}_*^{3-\gamma} \right. \\
&\quad \left. + \sum_{i=2}^n \alpha \lambda_i \tau_i^{3/2} \frac{3(1-4\epsilon_i)}{2(1-\epsilon_i)^2} - \frac{1}{3} \gamma C_{up} \mathcal{V}_*^{3-\gamma} \right\} \\
&= \frac{W_0^2}{\mathcal{V}_*^3} \left\{ -3 \sum_{i=2}^n \frac{\alpha \lambda_i}{(1-\epsilon_i)^2} \tau_i^{3/2} \epsilon_i (1-4\epsilon_i) + \left(1 - \frac{1}{3} \gamma \right) C_{up} \mathcal{V}_*^{3-\gamma} \right\},
\end{aligned}$$

and requiring a Minkowskian minimum $V_{LARGE}^{min} = 0$ we finally obtain

$$\mathcal{V}_*^{3-\gamma} = \frac{3}{C_{up} \left(1 - \frac{1}{3} \gamma \right)} \sum_{i=2}^n \frac{\alpha \lambda_i}{(1-\epsilon_i)^2} \tau_i^{3/2} \epsilon_i (1-4\epsilon_i). \quad (\text{B.4})$$

B.2 Multi-field consequences

Let us now turn to the multi-field case and see how the value of γ affects the choice of the number of moduli of the model. If we use the assumptions (4.22) and consider the case $\epsilon_i \ll 1$, from (B.4) we obtain

$$\mathcal{V}_*^{3-\gamma} = \frac{3\alpha}{C_{up} \left(1 - \frac{1}{3} \gamma \right)} \left(\lambda_2 \tau_2^{3/2} \epsilon_2 + (n-2) \lambda_3 \tau_3^{3/2} \epsilon_3 \right). \quad (\text{B.5})$$

Hence, we see that with $\tau_i \sim \mathcal{O}(1)$, the volume depends on the number of moduli as

$$\mathcal{V}_* \sim (n-2)^{\frac{1}{3-\gamma}}; \quad (\text{B.6})$$

for $\gamma \rightarrow 1$ it weakly depends on n , whereas for $\gamma \rightarrow 3$ the number of moduli strongly affects the value of the minimum of the volume.

BIBLIOGRAPHY

- [1] A. Nijenhuis and R. W. Richardson Jr, “Cohomology and deformations in graded lie algebras,” *Bulletin of The American Mathematical Society - BULL AMER MATH SOC*, vol. 72, 01 1966.
- [2] F. Quevedo, S. Krippendorff, and O. Schlotterer, “Cambridge Lectures on Supersymmetry and Extra Dimensions,” 2010.
- [3] S. P. Martin, “A Supersymmetry primer,” 1997. [Adv. Ser. Direct. High Energy Phys.21,1(2010)].
- [4] J. Wess and J. Bagger, *Supersymmetry and supergravity*. Princeton, NJ, USA: Princeton University Press, 1992.
- [5] D. G. Cerdeno and C. Munoz, “An introduction to supergravity,” 1998. [PoScorfu98,011(1998)].
- [6] D. Baumann and L. McAllister, *Inflation and String Theory*. Cambridge Monographs on Mathematical Physics, Cambridge University Press, 2015.
- [7] M. Cicoli, “String Loop Moduli Stabilisation and Cosmology in IIB Flux Compactifications,” *Fortsch. Phys.*, vol. 58, pp. 115–338, 2010.
- [8] J. P. Conlon, “Moduli Stabilisation and Applications in IIB String Theory,” *Fortsch. Phys.*, vol. 55, pp. 287–422, 2007.
- [9] D. Lust and T. R. Taylor, “Limits on Stringy Signals at the LHC,” *Mod. Phys. Lett.*, vol. A30, no. 15, p. 1540015, 2015.
- [10] M. Berg, M. Haack, and B. Kors, “String loop corrections to Kahler potentials in orientifolds,” *JHEP*, vol. 11, p. 030, 2005.
- [11] M. Berg, M. Haack, and B. Kors, “On volume stabilization by quantum corrections,” *Phys. Rev. Lett.*, vol. 96, p. 021601, 2006.
- [12] V. Balasubramanian, P. Berglund, J. P. Conlon, and F. Quevedo, “Systematics of moduli stabilisation in Calabi-Yau flux compactifications,” *JHEP*, vol. 03, p. 007, 2005.

- [13] R. Allahverdi, M. Cicoli, and F. Muia, “Affleck-Dine Baryogenesis in Type IIB String Models,” *JHEP*, vol. 06, p. 153, 2016.
- [14] M. Cicoli, J. P. Conlon, and F. Quevedo, “General Analysis of LARGE Volume Scenarios with String Loop Moduli Stabilisation,” *JHEP*, vol. 10, p. 105, 2008.
- [15] D. S. Gorbunov and V. A. Rubakov, *Introduction to the Theory of the Early Universe: Hot Big Bang Theory*. Singapore: World Scientific, 2017.
- [16] A. D. Linde, “Relaxing the cosmological moduli problem,” *Phys. Rev.*, vol. D53, pp. R4129–R4132, 1996.
- [17] D. H. Lyth and E. D. Stewart, “Thermal inflation and the moduli problem,” *Phys. Rev.*, vol. D53, pp. 1784–1798, 1996.
- [18] J. P. Conlon and F. Quevedo, “Kahler moduli inflation,” *JHEP*, vol. 01, p. 146, 2006.
- [19] M. Cicoli, F. Quevedo, and R. Valandro, “De Sitter from T-branes,” *JHEP*, vol. 03, p. 141, 2016.
- [20] M. Cicoli, I. García-Etxebarria, C. Mayrhofer, F. Quevedo, P. Shukla, and R. Valandro, “Global Orientifolded Quivers with Inflation,” *JHEP*, vol. 11, p. 134, 2017.
- [21] G. R. Dvali, “Inflation versus the cosmological moduli problem,” 1995.
- [22] M. Cicoli, K. Dutta, A. Maharana, and F. Quevedo, “Moduli Vacuum Misalignment and Precise Predictions in String Inflation,” *JCAP*, vol. 1608, no. 08, p. 006, 2016.
- [23] K. Dutta and A. Maharana, “Inflationary constraints on modulus dominated cosmology,” *Phys. Rev.*, vol. D91, no. 4, p. 043503, 2015.
- [24] M. Kreuzer and H. Skarke, “Complete classification of reflexive polyhedra in four-dimensions,” *Adv. Theor. Math. Phys.*, vol. 4, pp. 1209–1230, 2002.
- [25] M. Cicoli and A. Mazumdar, “Reheating for Closed String Inflation,” *JCAP*, vol. 1009, no. 09, p. 025, 2010.
- [26] M. F. Sohnius, “Introducing Supersymmetry,” *Phys. Rept.*, vol. 128, pp. 39–204, 1985.
- [27] M. Dine, *Supersymmetry and String Theory*. Cambridge University Press, 2016.
- [28] D. S. Gorbunov and V. A. Rubakov, *Introduction to the theory of the early universe: Cosmological perturbations and inflationary theory*. 2011.
- [29] J. P. Conlon and F. Quevedo, “Astrophysical and cosmological implications of large volume string compactifications,” *JCAP*, vol. 0708, p. 019, 2007.
- [30] J. J. Blanco-Pillado, D. Buck, E. J. Copeland, M. Gomez-Reino, and N. J. Nunes, “Kahler Moduli Inflation Revisited,” *JHEP*, vol. 01, p. 081, 2010.
- [31] C. P. Burgess, M. Cicoli, M. Gomez-Reino, F. Quevedo, G. Tasinato, and I. Zavala, “Non-standard primordial fluctuations and nongaussianity in string inflation,” *JHEP*, vol. 08, p. 045, 2010.
- [32] J. R. Bond, L. Kofman, S. Prokushkin, and P. M. Vaudrevange, “Roulette inflation with Kahler moduli and their axions,” *Phys. Rev.*, vol. D75, p. 123511, 2007.

- [33] L. Randall and S. D. Thomas, “Solving the cosmological moduli problem with weak scale inflation,” *Nucl. Phys.*, vol. B449, pp. 229–247, 1995.
- [34] S. Bhattacharya, K. Dutta, M. R. Gangopadhyay, and A. Maharana, “Confronting Kähler moduli inflation with CMB data,” *Phys. Rev.*, vol. D97, no. 12, p. 123533, 2018.
- [35] M. Cicoli, D. Ciupke, C. Mayrhofer, and P. Shukla, “A Geometrical Upper Bound on the Inflaton Range,” *JHEP*, vol. 05, p. 001, 2018.
- [36] M. Cicoli, J. P. Conlon, and F. Quevedo, “Dark radiation in LARGE volume models,” *Phys. Rev.*, vol. D87, no. 4, p. 043520, 2013.

LIST OF FIGURES

2.1	Typical behavior of the potential after LVS stabilization.	24
2.2	Plot of the potential with inclusion of the uplift term V_{up} and with a nearly Minkowskian minimum.	24
3.1	Illustration of the horizon problem in comoving coordinates. All the events that we observe (we are the central dotted wordline) are in our past light cone. At time of CMB formation it can be seen that photons coming from opposite regions were never in causal contact, as their light cones (shaded in gray) never cross. . .	27
3.2	Example of an exponentially flat potential. Inflation occurs in the “plateau” region, and ends at the vertical red line, which represents the point where the slow-roll regime ends. After that the field rolls down towards the minimum, oscillating around it.	30
3.3	Numerical solution with $C = 1$, $m_\phi = 1$, $\phi_* = 0$ and $\phi_{in} = 1$. The yellow line represents the line of the mean value of the field at each time.	32
3.4	Numerical solution with $C = 3$, $m_\phi = 1$, $\phi_* = 0$ and $\phi_{in} = 1$. The yellow line represents the line of the mean value of the field each time.	33
4.1	Plot for of all the moduli evolution for example 1. The yellow lines represent their value at the global post-inflationary minimum and the red points represent the end of inflation.	51
4.2	Evolution of the inflaton and the volume modulus during the last efoldings for example 1.	51
4.3	Inflationary trajectory in the (τ_2, ϕ) plane for example 1. The green dashed line represents the curve of local minima of ϕ and τ_3 for each value of τ_2 and the green dots represent the end of inflation (the one on the right) and the global minimum (the one on the left).	52
4.4	Post inflationary scenario for example 1. After a short period of radiation domination, the volume modulus comes to dominate the energy density until it decays and converts mainly into radiation.	53

4.5	Power spectrum and spectral index for example 1 in the first efoldings. Close to $N_e = 0$ the plot is not reliable, as the system is not yet in a slow-roll regime. Fluctuations in n_s are due to computational inaccuracies.	54
4.6	Comparison between ϵ (blue line) and ϵ_s (yellow line) in the first efoldings.	54
4.7	Evolution of the inflaton and the volume modulus during the last efoldings in the case $R \sim 10^{-2}$ of example 2.	56
4.8	Inflationary trajectory in the (τ_2, ϕ) plane in the case $R \sim 10^{-2}$ of example 2. The green dashed line represents the curve of local minima of ϕ and τ_3 for each value of τ_2 and the green dots represent the end of inflation (the one on the right) and the global minimum (the one on the left).	56
4.9	Evolution of the inflaton and the volume modulus during the last efoldings for the case $R \sim 10^{-3}$ of example 2.	57
4.10	Inflationary trajectory in the (τ_2, ϕ) plane for the case $R \sim 10^{-3}$ of example 2. The green dashed line represents the curve of local minima of ϕ and τ_3 for each value of τ_2 and the green dots represent the end of inflation (the one on the right) and the global minimum (the one on the left).	58
4.11	Evolution of the inflaton and the volume modulus during the last efoldings for the case $R \sim 10^{-4}$ of example 2.	60
4.12	Inflationary trajectory in the (τ_2, ϕ) plane for the case $R \sim 10^{-4}$ of example 2. The green dashed line represents the curve of local minima of ϕ and τ_3 for each value of τ_2 and the greens dot represents the end of inflation (the one on the right) and the global minimum (the one on the left).	61
4.13	Post inflationary scenario for the case $R \sim 10^{-8}$ of example 2. The time of equilibrium was expected to be at $t_{eq} \simeq 1.44367 \times 10^6 \text{ GeV}^{-1}$, but actually radiation always dominates.	62
4.14	Evolution of the inflaton and the volume modulus during the last efoldings for the case $R \sim 10^{-3}$ of example 3.	64
4.15	Inflationary trajectory in the (τ_2, ϕ) plane for the case $R \sim 10^{-3}$ of example 3. The green dashed line represents the curve of local minima of ϕ and τ_3 for each value of τ_2 and the greens dot represents the end of inflation (the one on the right) and the global minimum (the one on the left).	64
4.16	Evolution of the inflaton and the volume modulus during the last efoldings for the case $R \sim 10^{-5}$ of example 3.	66
4.17	Inflationary trajectory in the (τ_2, ϕ) plane for the case $R \sim 10^{-5}$ of example 3. The green dashed line represents the curve of local minima of ϕ and τ_3 for each value of τ_2 and the greens dot represents the end of inflation (the one on the right) and the global minimum (the one on the left).	66
4.18	Post inflationary scenario for the case $R \sim 10^{-9}$ of example 3. The time of equilibrium was expected to be at $t_{eq} \simeq 3.9277 \times 10^6 \text{ GeV}^{-1}$, but actually radiation always dominates.	68

LIST OF TABLES

4.1	Values of minima of example 1. The “predicted” values are the ones given by the approximations in (4.13) and (4.42), whereas the “calculated” ones are those found with the potential (4.5).	50
4.2	Values of the physical quantities of the model in GeV for example 1.	52
4.3	Values of the minima for the case $R \sim 10^{-2}$ of example 2. The “predicted” values are the ones given by the approximations in (4.13) and (4.42), whereas the “calculated” ones are those found with the potential (4.5).	55
4.4	Values of the physical quantities in GeV for the case $R \sim 10^{-2}$ of example 2. . .	55
4.5	Values of the minima for the case $R \sim 10^{-3}$ of example 2. The “predicted” values are the ones given by the approximations in (4.13) and (4.42), whereas the “calculated” ones are those found with the potential (4.5).	57
4.6	Values of the physical quantities of the model in GeV for the case $R \sim 10^{-3}$ of example 2.	58
4.7	Values of the minima for the case $R \sim 10^{-4}$ of example 2. The “predicted” values are the ones given by the approximations in (4.13) and (4.42), whereas the “calculated” ones are those found with the potential (4.5).	59
4.8	Values of the physical quantities of the model in GeV for the case $R \sim 10^{-4}$ of example 2.	60
4.9	Values of the minima for the case $R \sim 10^{-8}$ of example 2. The “predicted” values are the ones given by the approximations in (4.13) and (4.42), whereas the “calculated” ones are those found with the potential (4.5).	62
4.10	Values of the physical quantities of the model in GeV for the case $R \sim 10^{-8}$ of example 2.	62
4.11	Values of the minima for the case $R \sim 10^{-3}$ of example 3. The “predicted” values are the ones given by the approximations in (4.13) and (4.42), whereas the “calculated” ones are those found with the potential (4.5).	63
4.12	Values of the physical quantities in GeV for the case $R \sim 10^{-3}$ of example 3. . .	65

4.13	Values of the minima for the case $R \sim 10^{-5}$ of example 3. The “predicted” values are the ones given by the approximations in (4.13) and (4.42), whereas the “calculated” ones are those found with the potential (4.5).	65
4.14	Values of the physical quantities in GeV for the case $R \sim 10^{-5}$ for example 3. . .	67
4.15	Values of the minima for the case $R \sim 10^{-9}$ of example 3. The “predicted” values are the ones given by the approximations in (4.13) and (4.42), whereas the “calculated” ones are those found with the potential (4.5).	68
4.16	Values of the physical quantities in GeV for the case $R \sim 10^{-9}$ of example 3. . .	68